Fraunhofer ISE

FRAUNHOFER INSTITUTE FOR SOLAR ENERGY SYSTEMS ISE

COST FORECAST FOR LOW TEMPERATURE ELECTROLYSIS – TECHNOLOGY DRIVEN BOTTOM-UP PROGNOSIS FOR PEM AND ALKALINE WATER ELECTROLYSIS SYSTEMS

A cost analysis study on behalf of Clean Air Task Force

COST FORECAST FOR LOW-TEMPERATURE ELECTROLYSIS – TECHNOLOGY DRIVEN BOTTOM-UP PROGNOSIS FOR PEM AND ALKALINE WATER ELECTROLYSIS SYSTEMS

Marius Holst
Stefan Aschbrenner
Tom Smolinka
Christopher Voglstätter
Gunter Grimm

Fraunhofer Institute for Solar Energy Systems ISE

October 2021

Disclaimer

This study was prepared by Fraunhofer Institute for Solar Energy Systems ISE on behalf of Clean Energy Task Force. Neither Fraunhofer ISE, Clean Air Task Force, nor any person acting on behalf of them:

a. Makes any warranty or representation, express or implied with respect to the accuracy, completeness, or usefulness of the information contained in this report, or that the use of any information, technology, method, or process disclosed in this report may not infringe privately-owned rights. The results, conclusions, or analysis of the results by Fraunhofer ISE represent Fraunhofer ISE's opinion based on gathered technical data, empirical relationships, and values, which inferences, and assumptions are not infallible.
b. Assumes any liability with respect to the use of, or for any and all damages resulting from the use of, any information, results, or conclusions in this report; any other use of, or reliance on, this report by any third party is at the third party's sole risk.

Commissioned by

Clean Air Task Force
114 State Street, 6th Floor
Boston, MA 02109, U.S.A.

Project lead: Mike Fowler
Contact: mfowler@catf.us

Study by

Fraunhofer-Institute for Solar Energy Systems ISE
Heidenhofstraße 2
79110 Freiburg, Germany

Corresponding author: Dr. Tom Smolinka
Contact: tom.smolinka@ise.fraunhofer.de

Acknowledgements

Fraunhofer ISE thanks Asahi Kasei Corp., Burkhardt Compression, Enapter, Grünbeck Wasseraufbereitung, ITM Power, Plug Power (GINER ELX), Silica Verfahrenstechnik and thyssenkrupp, for the courtesy of using their pictures for illustration purposes. Furthermore, we would like to thank all experts who were interviewed for their valuable contribution to this study.

Table of Contents

List of Abbreviations

Abbreviation	Explanation
AC	Alternating Current
AEL	Alkaline Water Electrolysis
AEMEL	Alkaline Electrolyte Membrane Water Electrolysis
BPP	Bipolar Plate
CAPEX	Capital Expenditure
CCM	Catalyst Coated Membranes
CEPCI	Chemical Engineering Plant Cost Index
CO_2	Carbon Dioxide
DEA	Diaphragm Electrode Assembly
DC	Direct Current
FF	Flow Field
H_2	Hydrogen
HTEL	High Temperature Electrolysis
GDL	Gas Diffusion Layer
$LCOH_2$	Levelized Cost of Hydrogen Production
MEA	Membrane Electrode Assembly
O&M	Operation and Maintenance
PAES	Polyarylether Sulfone
PEM	Polymer Electrolyte Membrane
PEMEL	PEM Water Electrolysis
PGM	Platin Group Metal
PNEC	Predicted No Effect Concentration
PREN	Pitting Resistance Equivalent Numbers
PTE	Porous Transport Electrode
PTFE	Polytetrafluorethylene
PTSA	Perfluotinated Sulfonic Acid
PFSI	Perfluorosulfonated Ionomer
PTL	Porous Transport Layer
PVD	Physical Vapor Deposition
TRL	Technology Readiness Level

Executive Summary

Fossil-free hydrogen production by water electrolysis is a key technology for a future sustainable energy system since hydrogen enables sector coupling and thus simplifies decarbonization of sectors with high carbon dioxide emissions while supporting the implementation of intermittent renewable energy sources. Supported by the recent realization that necessary measures in climate protection must be implemented more quickly and consistently, considerable efforts are currently being started worldwide to make electrolysis technology mature and economically competitive for large-scale use. In this context, a precise understanding of the cost structures of the most promising electrolysis technologies is important to take the correct measures and to further advance the technology in a targeted manner.

This study is intended to provide a comprehensive understanding of the cost structures of alkaline and proton exchange membrane (PEM) electrolysis systems and the individual cost reduction potentials for these electrolysis technologies. Therefore, two system sizes are considered for each technology at two different time scales. The chosen matrix of scenarios can be seen in Table 1.
The scenarios for 2020 consider today's available technology, components, and existing solutions. Thereby, the scenarios for 2030 are based on "next-generation" developments for future low-temperature electrolysis systems as far as they can be estimated from today's perspective.
The system capacities were chosen to represent decentralized (5 MW) and centralized (100 MW) applications. In accordance with the set scenarios, typical layouts of the electrolysis systems were designed, and technical parameters derived by solving all energy and mass balance equations of these systems in a stationary simulation. The most relevant parameters of this analysis are listed in Table 1.

Technical specifications of the analyzed systems

The steadily growing numbers and capacities of current and future electrolysis projects over the coming years is consistent with the fact that manufacturers are upscaling their electrolysis stack and system designs and at the same time building up large manufacturing capacities. These development trends were taken into account in the scenario determination and cost analysis.

Table 1: Overview of key performance indicators and system design parameter depending on the scenarios

		AEL				**PEMEL**			
	Unit	**2020**		**2030**		**2020**		**2030**	
System Power	MW_{AC}	**5**	**100**	**5**	**100**	**5**	**100**	**5**	**100**
Rated Stack Input Power	MW_{DC}	2.5	2.5	10	10	1	1	5	5
Number of stacks		2	40	1	10	5	100	1	20
Cell Area	dm²	200	200	300	300	10	10	30	30
Rated Current Density	A/cm²	0.6	0.6	1	1	2	2	3	3

Rated Cell Voltage (BoL)	V	1.8	1.8	1.7	1.7	1.9	1.9	1.7	1.7
Pressure Cathode	bar	1	1	1	1	30	30	30	30
Temperature	°C	80	80	80	80	60	60	70	70
Number of compressors		1	2	1	2	0	0	0	0
Specific Energy Demand System	kWh_{AC} /kg	52.8	53.4	48.9	49.4	54.5	55.1	47.6	48.1

The PEMEL cell, stack and system components are designed for an operating pressure of 30 bar. The AEL cell and stack design is oriented on well-proven and advanced chlor-alkali electrolysis designs including operation at atmospheric pressure, which makes additional mechanical compressors on the system side necessary to ensure a comparability between both technologies. The focus of "next-generation" PEMEL technology is assumed to be on the development of new electrolysis block concepts and MEA's, while in AEL technology it is on incremental improvement of the diaphragm-electrode assembly. In both cases, these developments result in larger and more efficient stacks with higher power density.

Main result of the cost analysis

The cost analysis is performed with the help of a bottom-up cost model, which was developed by Fraunhofer ISE in recent years and already applied in other studies. The cost model is structured into cell, stack and system-level and implements compiled cost data from manufacturers for the main stack components and materials, staggered by quantity, as well as target prices for system components, stakeholder information and available literature. For this study the cost model has been updated with current data and extended to enable the cost modeling of AEL systems. Cost-breakdowns of the next-generation stacks for the 2030 scenarios are shown in Figure 0-1. Cost-breakdowns of the according system design in the 2030 scenarios are given in Figure 0-2.

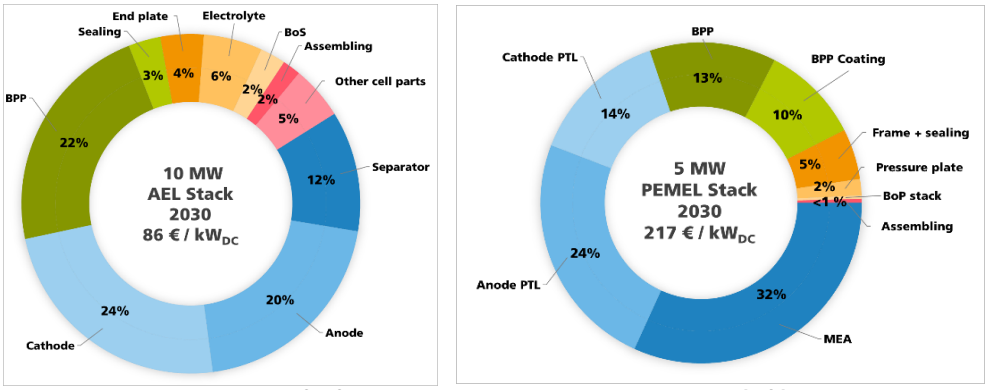

Figure 0-1: Cost breakdowns of a future 10 MW alkaline electrolysis stack (left) and a 5 MW PEMEL stack (right) in 2030

For 10 MW AEL stacks it is estimated that almost half of the stack costs are associated to the electrodes alone, followed by 22 % for the bipolar plates. Looking on the system level, the largest cost share in AEL systems is not the stack but the combined balance of plant components. However, the three main single cost drivers on AEL system level are the stacks, the power electronics, and the compression unit. As expected, the results

show a strong decrease in the total specific system costs with increasing system size. Main reasons for the cost reduction are the equipment savings by scaling-up and numbering-up of the required balance of plant components, such as the compression unit, instrumentation and minimizing the overall engineering effort per installed capacity. On top of this trend a further cost reduction towards 2030 of around 25-30 % compared to 2020 is expected due to the estimated technology development on the stack level.

The largest share on the total stack costs of a next generation 5 MW PEMEL stack is the membrane electrode assembly (MEA) with 32 %, followed by the anode and cathode porous transport layers (PTL) with 24 % and 14 % share, as depicted in Figure 0-1. In comparison to today's stack technology the share of the MEA on the total stack costs will be reduced significantly towards 2030, due to progress in technology development and manufacturing processes. As illustrated in Figure 0-2 the stack presents the dominant cost component for a PEM electrolysis system with 30 %, followed by the power electronics. The larger the system the smaller the specific costs for peripheral components (gas purification and BoP) become. This can be explained by optimized and centralized balance of plant (BoP) components and is a general trend for all larger electrolysis systems. Further system cost reduction from 2020 towards 2030 is mainly caused by cost reductions of the stack, due to the assumed technological progress.

By comparing the results for both technologies, it can be observed that the specific costs for alkaline electrolysis are lower compared to PEM systems. The cost benefit mostly results from lower stack costs for the alkaline technology. However, depending on the system size, this cost benefit for the AEL systems is almost negated by the need for an additional mechanical compressor. Smaller, decentralized, 5 MW systems show almost the same specific system costs, thereby in large, 100 MW centralized installations, AEL systems provide the highest cost benefit. Furthermore, specific costs for power electronics for both technologies are high compared to other components and justify the need for adapted and cost optimized solutions in the field of water electrolysis.
The compression unit contributes a large part to the AEL system cost as well but offers strong cost reduction potential by sizing-up to larger capacities, halving the share on the overall costs from 5 MW to 100 MW system size. Thereby, a single compressor unit is more cost-effective than several smaller compressors. However, for large systems it is beneficial to use several smaller compressors in parallel to have a reasonable trade-off between part-load operation capability and providing a minimum of redundancy.

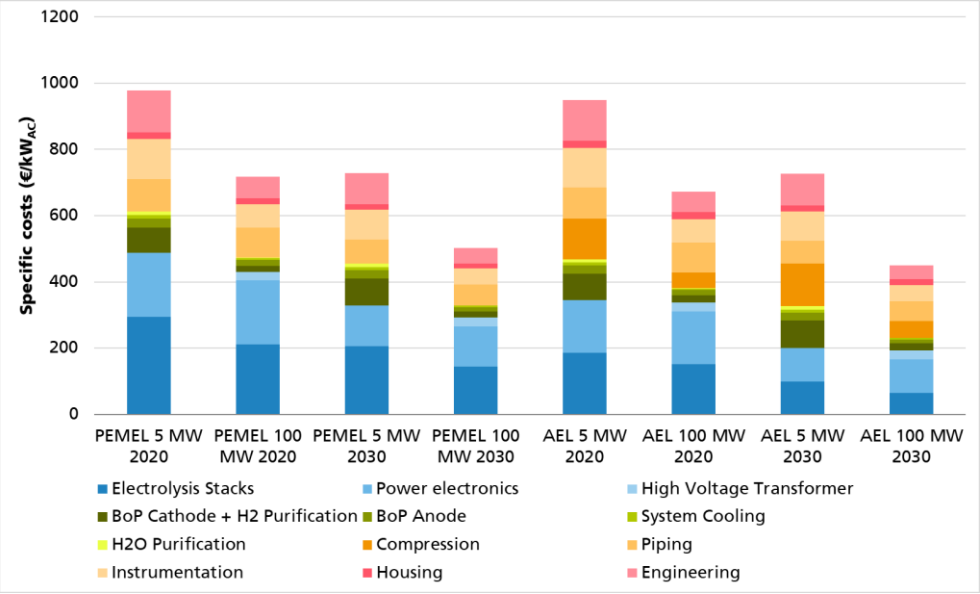

Figure 0-2: Alkaline and PEM electrolysis system cost for different system capacities in 2020 and 2030

Regarding the limitations of the applied bottom-up cost calculation, it needs to be mentioned, that data quality and quantity are crucial for the generated results because data inaccuracies could be propagated from the bottom to the top of the cost model. In general, reliable cost data is very scarce, in particular for estimations of GW-scale manufacturing volumes. Moreover, even well-founded data for the developed costs models quickly can lose their relevance due to the dynamic developments in the current electrolysis market. Finally, the bottom-up approach in this study does not include certain overhead (rent, insurance etc.) and markup costs of installed electrolysis systems, because these are highly manufacturer and project dependent and can result in almost doubling the final installed system cost.

Comparison of the results with other cost models

A direct comparison of the results with specific cost values of other studies is often difficult due to large differences in the respective system boundaries, underlying assumptions, and used cost model methods, which can influence the results drastically. What all analyzed studies have in common is the prediction of significant cost reductions within a certain corridor in the next 10 years mostly due to anticipated technological progress and economies of scale in production. However, the individual figures of resulting specific system costs can differ greatly. However, cost results from some recent studies, focusing on similar capacities present comparable results. The overall picture shows that in this study the cost results are rather somewhat conservative, especially for PEM electrolysis. This might be based on the usage of a bottom-up approach, while in comparison, several other studies use projections and learning curves for the forecasts only. However, to estimate the costs for concrete system setups, as it was the scope of this study, a bottom-up cost model provides more accurate results.

Cost-reduction potentials

Four different paths for cost reductions on stack level are discussed in this study: scaling-up (sizing-up) of stack components, technological advancements, increasing production volumes (numbering-up) and improvements in production technologies (e.g. automatization). The technological development of the AEL stack towards 2030 gives the highest leverage in cost reduction (~50 %), followed by scaling-up in size (15 % by quadrupling the capacity) and increasing manufacturing volume (20 % from one stack to 40 stacks).
The assumed technological advancements on PEMEL stack level towards 2030 results in a lower cost-reduction potential (20 % for 5 MW stack, 11% for 1 MW stack) compared to the AEL technology. Although, the AEL technology is technically established, efforts for further development of this technology can provide cost-effective solutions. A fivefold scaling-up in capacity of AEL systems based on the year 2020 can reduce the costs by 20 % and an increase in manufacturing volume from one stack to 100 stacks by even 40 %. Power supply and electronics are major cost drivers in all scenarios and show only a very limited cost-reduction potential so far. In case the stack cost can be decreased as estimated, the power electronics in large electrolysis systems will become the largest single cost factor. It can be assumed that there is still a high potential for improvement in power supply and electronics, that are tailored to water electrolysis, but that this is currently not yet taken into account in the cost models.
Apparently, based on these results, efforts to improve the rated current density and rated cell voltage of the already mature AEL stack technology as well as a ramp-up in the manufacturing volumes of PEMEL stacks could present the most promising pathways for cost-reductions. The latter is conditioned by the development of more automated production processes as well. The announcements of several PEMEL and AEL manufacturers to timely increase their production to at least 1 GW/year, is backing up this trend.

Hydrogen production costs

The economic viability of electrolysis systems is not only dependent on the investment costs of an installed system, but on the electricity costs (variable costs) and the annual full-load hours as well. In general, the hydrogen production costs decrease strongly with rising, annual full-load hours. Only for annual full load hours below the threshold of approximately 3,000 h do the investment costs of an electrolysis system dominate the total hydrogen production costs. At higher full load hours, the electricity cost and overall system efficiencies become the main cost drivers rather than the investment costs. In consequence, a substantial cost-reduction for hydrogen production from electrolysis can also be achieved by decreasing electricity prices, increasing the system efficiency and maximizing the annual full-load hours of the electrolysis system.

This study presents a unique cost analysis for AEL and PEMEL systems based on detailed bottom-up cost models. The findings here provide an insight in the potential cost structures of AEL and PEMEL systems with different capacities, meant for decentralized and centralized applications. The evaluated cost-reduction potentials on stacks level can give a clue, which paths to exploit on the way to reach the set cost targets. It needs to be mentioned that only other water electrolysis technologies such anion exchange membrane electrolysis (AEMEL) or high-temperature electrolysis (HTEL) exist, which were not part of the scope in this study. Overall, the water electrolysis market is highly dynamic, so that data and results may quickly become outdated and therefore the context on which the study is based must always be critically considered.

1 Introduction

1.1 Hydrogen as a Solution for a Carbon Free Economy

Climate change is one of the greatest challenges for the upcoming decades. In particular, the greenhouse gas, carbon dioxide (CO_2) promotes the development of climate change and the resulting rise in global temperature. To limit the temperature rise to well below two degrees, the international community decided with the *Paris Agreement* to reduce their greenhouse gas emissions by 2050 in order to establish a climate-neutral society as far as is possible [1,2].
The reduction of greenhouse gas emissions affects all sectors (power generation, transportation, building heat, agriculture, etc.). A conversion of the sectors to low-carbon electricity or electricity-based energy carriers will be a key issue for the reduction of greenhouse gas emission. This results in a higher demand of low-carbon energy sources. Especially, due to the fluctuating energy generation from renewable energy sources, such as wind and solar, and the currently limited electric storage capacities, flexible chemical energy storage in form of hydrogen can represent a central pillar in the future [3]. Hydrogen offers a wide range of applications. It can be directly used for mobility, as feedstock in the chemical industry, or as energy storage for conversation back into electricity at a later time. Furthermore, it is possible to produce liquids like methanol or ammonia from hydrogen and carbon dioxide or nitrogen, respectively. Figure 1-1 shows a selection of discussed pathways for hydrogen.

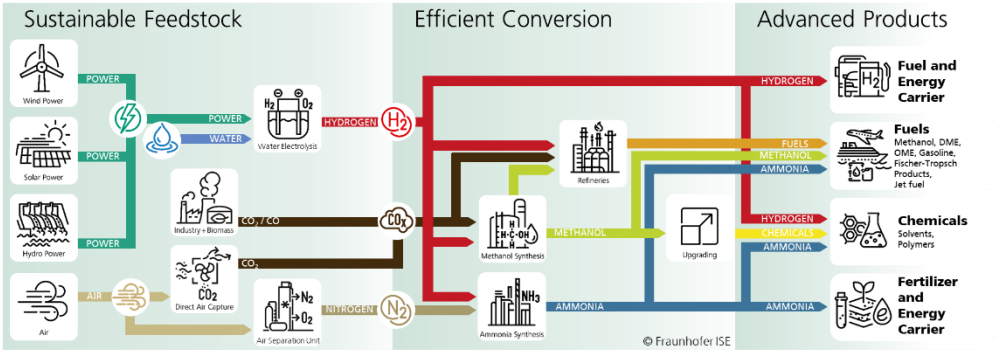

Figure 1-1: Pathways for hydrogen in a carbon free society

Although hydrogen is the most abundant molecule on earth, it occurs only in bound form, e.g. water or hydrocarbons. Also, hydrogen is not new. Currently, the global hydrogen production and consumption is more than 70 Mt annually, which is mostly produced by reforming hydrocarbons like methane, lignite, and oils [3,4]. These processes allow for the production of large quantities of hydrogen at comparably low costs. However, large amounts of carbon dioxide are emitted.
At this point water electrolysis comes into play. Next to water, electric energy is required to split the water into hydrogen and oxygen. When using renewable energy carriers like wind and solar, hydrogen is produced with low carbon dioxide emissions and can be considered as fossil-free or "green" hydrogen". Provided that governments stick to the goals of the Paris Climate Agreement, the demand for low-carbon hydrogen, and thus the need for electrolysis capacities, will increase significantly in the coming years and decades. Several countries already presented national hydrogen roadmaps and targets to promote the market entry of electrolysis technologies to produce fossil-free hydrogen. At this stage, 13 countries and the European Union presented hydrogen strategies that, among other things, include targets for the expansion of electrolysis technologies [5]. The European union, for example, wants to install 6 GW of electrolysis capacity before

2024 and 40 GW of electrolysis capacity before 2030. To achieve these goals, the production capacities for electrolyzers must be expanded enormously. For comparison, a few years ago the annual electrolyzer production capacity was in the range of 100 MW [6].

Figure 1-2 shows an excerpt of low-temperature water electrolysis projects and installations worldwide starting from the year 2020 till 2030. The presented data here is based on a combination of own research and available information concerning electrolysis projects from the International Energy Agency IEA [7]. The projects are sorted according to electrolysis technology, planned capacity, and planned year of commissioning. Thereby, the category "Unknown Electrolysis Technology" labels projects, where the applied electrolyzer technology is not disclosed or known at the point of time of this study.
It is already obvious that besides the mentioned capacity targets, many electrolysis systems with capacities below 10 MW are presently or will soon be commissioned. For the years 2021 and 2022, even a few electrolysis systems in the multi-100 MW range are planned to start operating.

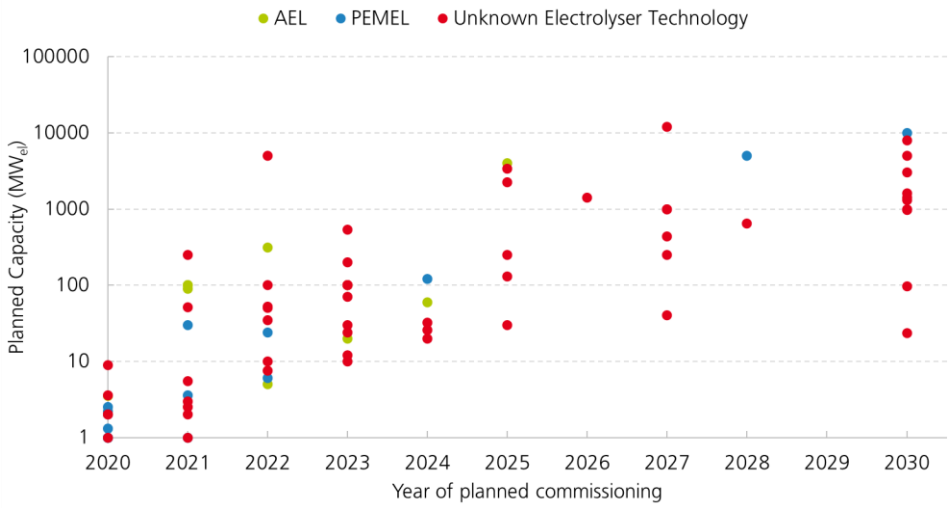

Figure 1-2: Overview of planned electrolyzer installations worldwide till the year 2030 (based on [7])

1.2 Scope of this Study

Electrolysis technologies for hydrogen production are currently gaining rapid momentum. The production capacities need to be increased significantly in the upcoming years. Hydrogen production costs will have a high influence on the economic operation of electrolysis plants. Currently, the energy generation costs have the highest share of hydrogen production costs, followed by the capital expenditure for the electrolysis system itself.
In this study, a bottom-up cost analysis for state-of-the-art PEM water electrolysis (PEMEL) and Alkaline electrolysis (AEL) systems has been performed. To represent a future electrolysis market in a comprehensive way, this analysis distinguishes between decentralized, small capacity, and centralized, large-scale systems for each technology. This approach enables the creation of a profound data basis for a detailed analysis of the CAPEX structures of both low-temperature electrolysis systems, down to the cell-component level of the system's electrolysis stacks. Furthermore, the cost data is extended by a cost forecast for 2030, which considers commercial development trends and academic research activities. Thereby, the cost data itself is generated and structured by existing, inhouse, stack costs models, which are updated or completely newly-developed. The stack cost models are connected with associated self-developed system cost models on a higher level. All cost models include component costs from

manufacturers for a wide range of quantities, expert information, and own expert assumptions. For the different time scales, improvements in the technology, as well as new materials are considered on the stack level.
The resulting cost of the different scenarios and technologies are analyzed downstream with the aim of identifying the main investment cost drivers. This is followed by an evaluation of the future cost-reduction potential with respect to classic approaches in emerging industry sector, such as scaling-up, increasing production volumes, and more efficient production technologies.

2
Low-Temperature Electrolysis System Characterization

Hydrogen is one of the most abundant elements on Earth's surface, mostly chemically bonded in hydrocarbons and water. As a result, gaseous, molecular hydrogen is very rare in the atmosphere. The electrochemical decomposition of water to produce hydrogen and oxygen is a quite simple process, involving two electrodes in an electrolyte, that are connected to a direct current (DC) supply. It is an endothermic reaction which requires the supply of energy and once a sufficiently high cell voltage is applied, the redox reaction takes place, producing hydrogen at the cathode (negative electrode) and oxygen at the anode (positive electrode). A semipermeable separator is used to separate both half-cells to prevent mixing of the product gases, while at the same time enabling an ion transport. The overall reaction of the water decomposition is given by the following equation

$$H_2O_{(l/g)} + \Delta H_R \Leftrightarrow H_{2(g)} + \frac{1}{2}O_{2(g)}$$

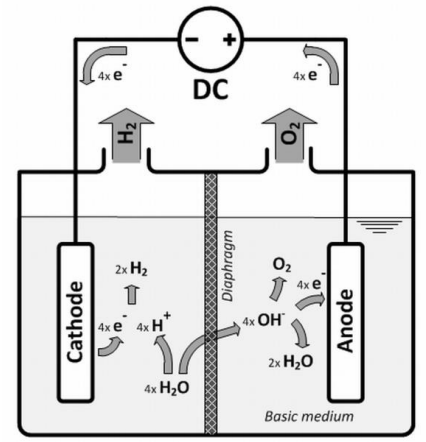

Figure 2-1: Basic principle of an electrolysis cell in basic medium with a semi-permeable diaphragm between the two half-cells to separate hydrogen and oxygen from mixing.

This fundamental operating principle is valid for all types of water electrolysis cells, they only differ in the utilized electrolyte. The most relevant technologies are alkaline electrolysis cells (AEL cell), which work with a basic liquid electrolyte, polymer electrolyte membrane electrolysis (PEMEL) cells, where an acidic ionomer is used, and high-temperature or solid oxide electrolysis cells (SOEC), which have a solid oxide as electrolyte. The latter technology is not in the scope of this study and therefore will not be discussed in more detail here.

In alkaline water electrolysis, the water is usually supplied to the cathode side, where hydrogen and hydroxide-ions (OH^-) are formed. The OH^--ions pass through the microporous diaphragm or an anion conducting membrane and are converted to oxygen and water on the anode side. The general structure and operation of an alkaline cell can be seen in Figure 2-1.

In acidic electrolytes (PEMEL), the water is normally supplied at the anode side of the electrolytic cell where it is split into oxygen and protons (H^+). For each water molecule half an oxygen molecule is produced, which is discharged on the anode side, and two protons, which are transported through a proton-conducting membrane to the cathode side where they are reduced to a hydrogen molecule by accepting two electrons.

To ensure a sufficiently high ionic conductivity a minimum temperature is required for the respective electrolytes. The upper temperature limit is determined mostly by the stability of the cell materials and components.

For the technical exploitation of the above fundamental electrochemical principles, conventional electrolysis systems are subdivided into three levels:

- The cell is where the electrochemical reactions are taking place and therefore it is the most basic element of the electrolyzer.
- At the stack level several cells are stacked together and connected in series, which includes the integration of additionally required structural components.
- The system level comprises all auxiliary process equipment to run an electrolysis system.

Due to the fact, that the focus of this study is on low-temperature water electrolysis with the potential of prompt large scale deployment, only the AEL and PEMEL technologies are described in more detail here. However, an overview of main aspects of the emerging anion exchange membrane electrolysis (AEMEL) technology are presented as well. Table 2-1 summarizes typical technical features.

Table 2-1: Characteristics of the main low temperature water electrolysis technologies

	Alkaline electrolysis	**PEM electrolysis**	**AEM electrolysis**
Cathode (HER)	$2H_2O + 2e^- \rightarrow H_2 + 2OH^-$	$2H^+ + 2e^- \rightarrow H_2$	$2H_2O + 2e^- \rightarrow H_2 + 2OH^-$
Anode (OER)	$2OH^- \rightarrow ½\ O_2 + H_2O + 2e^-$	$H_2O \rightarrow ½\ O_2 + 2H^+ + 2e^-$	$2OH^- \rightarrow ½\ O_2 + H_2O + 2e^-$
Charge carrier	OH^-	H^+	OH^-
Electrolyte	Liquid electrolyte KOH	Acidic polymer membrane	Polymer membrane with diluted KOH
Temperature range	60 - 90 °C	RT - 80 °C	50-70 °C
Electrodes / Catalyst	Catalyst coated nickel substrates -	Noble metals (platinum, iridium)	PGM and non-PGM catalyst, nickel substrates
Typical current density	0.2 – 0.6 A/cm²	1.0 – 2.5 A/cm²	0.5 – 1.5 A/cm² (at lab scale)
Technology Readiness Level (TRL)	8-9 (industrial mature)	7-8 (commercially available)	6-7 (field tests)
Typical pressure	atm. - 30 bar	atm. - 50 bar (350 bar)	atm. - 35 bar
Stack / module size	< 1,000 Nm³/h 0.5 – 2.5 MW_{el}	x-fold 100 Nm³/h 0.1 – 1.5 MW_{el}	Up to 0.5 Nm³/h < 2.5 kW_{el}
Specific electrical energy demand	4.2 – 5.8 kWh/Nm³ H_2	4.5 – 6.8 kWh/Nm³ H_2	4.8 – 6.9 kWh/Nm³ H_2

Each technology has its own advantages and disadvantages. General technical properties are summarized in the following Table 2-2. The characteristics that are relevant in terms of investment cost will be discussed in more detail in the next chapters as well.

Table 2-2: Advantages and Disadvantages of AEL and PEMEL electrolysis technologies

	AEL	PEMEL	AEMEL
Advantages	• Mature, robust, and therefore, proven technology • Multi-MW stacks enable systems with large capacities already today • Potential to use earth abundant and inexpensive materials	• Very high-power densities • Compact designs and small footprint • Fast cold start-up time, fast load changing capabilities • Suitable for high pressure operation • Stacks in MW range available • High intrinsic product gas purity	• Potential to use cheap and abundant materials -> High cost-reduction potential • Compact designs and small footprint • Suitable for high pressure operation
Disadvantages	• High material effort on system level by using highly alkaline liquid as electrolyte • Low power densities and large footprint • Additional effort for gas purity required • Slow cold start-up time	• Use of expensive materials as titanium and critical platinum group metals (PGM) on cell level • long-term stability needs to be proven at MW-scale	• Low technology readiness level, only few commercial systems available • Limited long-term stability

2.1 Alkaline Water Electrolysis

Alkaline water electrolysis is with a history of more than 120 years the oldest and most widely used water electrolysis technology. Thereby, typical applications included already MW-scale hydrogen production in industrial applications, such as the ammonia synthesis. Historically, AEL was therefore aimed for stationary applications. Predominantly, AEL was used where electricity is very cheaply available, the production from fossil sources is not favorable, and the transport of hydrogen in the required quantities to the consumer is too expensive. Until today the AEL technology dominates the niche market of water electrolysis, but also for new upcoming applications in the capacity range of over 100 MW, such as the interconnection of the energy consuming sectors (sector coupling), especially AEL systems are discussed at the moment. In order to meet new requirements for this emerging market, the AEL sector is also seeing a rise in research and development activities to adapt the classic designs to meet new requirements, such as flexibility, high efficiency, and cost reductions.

2.1.1 General Cell Design

The design of an **AEL cell** basically consists of two half-cell compartments separated by a porous diaphragm, which is permeable for the charge carrier, the Hydroxide ions, but at the same time largely prevents a mixing of the product gases but can never completely prevent some gas crossover.
A schematic of a typical alkaline electrolysis cell design is depicted in Figure 2-2.

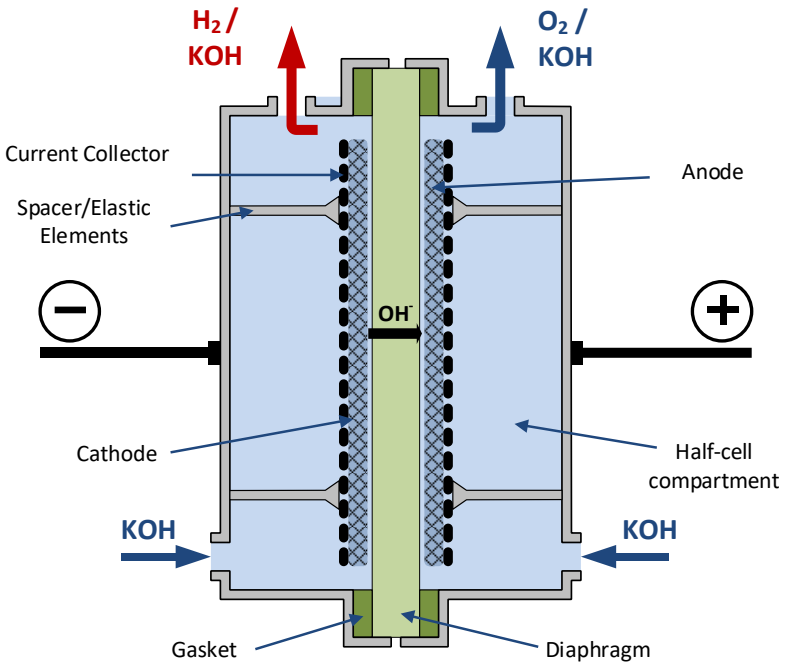

Figure 2-2:Typical structure of a current alkaline electrolysis cell [8]

In the area of commercial AEL systems alone, many different cell designs and material combinations exist today, not including approaches coming from the research sector. The most common electrode substrates can be shaped as perforated metal sheets with a porous surface, woven metal meshes, or expanded metal sheets.
The electrode substrates usually get a porous and electrochemically activated surface by coating of an electrocatalyst, which improves the respective half-cell reaction.
The electrodes are placed as close as possible towards the diaphragm from both sides in a sandwich-like manner, which on the one hand minimizes the distance between both electrodes and thus decreases the ionic resistance, but on the other hand the generated gas bubbles evolve mostly at the back of the electrodes, which leads to reduced overpotentials as well. This results in an improved cell efficiency. Nowadays, the next generation alkaline electrolyzers are already built following this "close-to" or so-called 'zero-gap' design. This kind of arrangement of separator and electrodes is often named Diaphragm Electrode Assembly (DEA), following the terminology from the PEMEL technology.
The positioning of the electrodes can be achieved by pressing the cell components together and adjusting the contact pressure via elastic elements or spacers placed between the electrodes and the cell housings (or bipolar plates). In some cell designs additional fore/pre-electrodes (e.g. perforated plates) are also integrated, which act as current distributors and are useful for positioning purposes. These cell housings can be made as flat, bipolar plates or as metal-folded compartments and they function as cell frames, which in combination with gaskets prevent the leakage of the alkaline electrolyte. The alkaline electrolyte flows in parallel through the two half-cells, thereby immersing the electrodes in the electrolyte. Generally, potassium hydroxide solution (KOH) with a concentration of 20-40 % is used. Furthermore, electrical contact is established via the bipolar plates.
The operating pressure of cells used in today's large-scale, commercial systems can vary from atmospheric pressure up to pressures of 30 bar. Alkaline electrolytic cells generally operate at an operating temperature of 65 to max. 90 °C.
The size, shape, and deployed materials of AEL cells are often dependent on the targeted pressure level of the whole system. In current systems running at atmospheric pressure, the active area of a cell can reach up to 3 m² and the cells mostly have a rectangular

shape, with the exception of the current design from NEL. Round shape cell designs are mainly used for higher pressure levels to facilitate an even distribution of the pressure along the whole area of the cell and therefore prevent leakages. However, from a manufacturing perspective, circular cells, compared to rectangular ones, are causing higher material cutting losses of up to 20%.

On the **material side**, state-of-the-art diaphragms for AEL need to show a high thermal, chemical, and electrochemical resistance besides sufficient gas tightness and ion permeability. The most common diaphragm in next generation AEL designs today is marketed under the name Zirfon Perl UTP from the company AGFA. Nowadays, it is available in different configurations, but the base material always is ZrO_2 supported by a polymer fabric with lattice structure. Besides these, other diaphragms made from fiberglass-reinforced polyphenylene sulfides or from polysulfones with inorganic oxides such as antimony oxide are still manufactured today, but only a few manufacturers integrate them into their cells. Also, other innovative approaches have been recently investigated, such as woven, stainless-steel meshes as separators, which promise a tenfold decrease in separator cost [9]. However, many innovative developments often lack adequate testing under industrial conditions and there are often other unsolved issues, such as gas purity.
The electrode requirements are also challenging; they need to be long-term resistant against corrosion in a high pH environment, as well as have good electrical conductivity and high electrochemical activity. Therefore, the base materials of choice are pure nickel (200 or 201), stainless steel (316L), or even mild steel (Grade St37) substrates, where the last two need to be additionally electroplated with a thin nickel layer in order to prevent corrosion and increase of the surface area.
In most commercial AEL cell designs, different electrocatalysts are applied onto these base substrates to enhance the electrochemical activity and increase the corrosion resistance. Some of them have been adapted from the chlor-alkali (C/A) electrolysis industry, where the electrolyte on the cathode side is NaOH solution, which has similar characteristics to KOH solution, and these commercial coatings proved to have stable operation with lifetimes of several years [10]. Catalyst materials are specifically tailored to the half-cell reaction and can therefore differ between cathode and anode. Although, only little specific information or performance data of the commercially used catalyst has been published. It can be stated that the cathode side is often coated with a layer of highly porous Raney-nickel, Rutheniumdioxid (RuO_2), or other Mixed Metal Oxides (MMO's) and Molybdenum (Mo). Raney-nickel also gets utilized for increasing the surface area of the anode. Furthermore, nickel oxides and nickel and cobalt-based, mixed oxides can also be used to further improve the electrochemical activity of the anode [11–13].
The half-cell compartments/bipolar plates, as well as spacers or elastic elements, are mainly fabricated from nickel or nickel-coated steel, again to provide suitable corrosion protection from the KOH. In general, the materials need to be rather soft and flexible so that they can be lightly pressed onto the membrane from the backside with elastic elements.
The gasket material is made of PTFE or EPDM and thus seals the half-cells from the outside.

2.1.2 General Stack Design

The hydrogen production capacity per cell is given by its current density and cell size. To obtain larger production capacities, several cells can be electrically connected in series to form a cell stack. The back side of the cathode of one cell is the anode of the neighboring cell and only the end plates need to be electrically contacted. The electrolyte flows in parallel through each of the half-cells. This bipolar stack construction is also state-of-the-art in commercial AEL stack designs. The electrical connection between the bipolar cells is provided by pressing them together in a so-called filter press arrangement. The filter press concept implies that the individual electrolysis cells of a stack are clamped between two end-plates and pressed together with threaded rods, as is depicted in Figure 2-3. A

drawback of this design can be that if one cell is defective, the entire stack fails. In some stack designs, however, the defective cell can be electrically bypassed.
In most pressurized commercial AEL stacks, long, massive rods are used, which usually run along the whole length of a stack, while some atmospheric designs offer solutions with smaller rods only for fixation purposes of the endplates or pressing systems with hydraulic or pneumatic support.
Stacks operating at higher pressures can take advantage of an improved product gas evacuation out of the cells due to smaller gas bubbles evolving at the electrodes. This means, for a given current density, a pressurized stack can be designed to be more compact than a stack operating at atmospheric pressure.

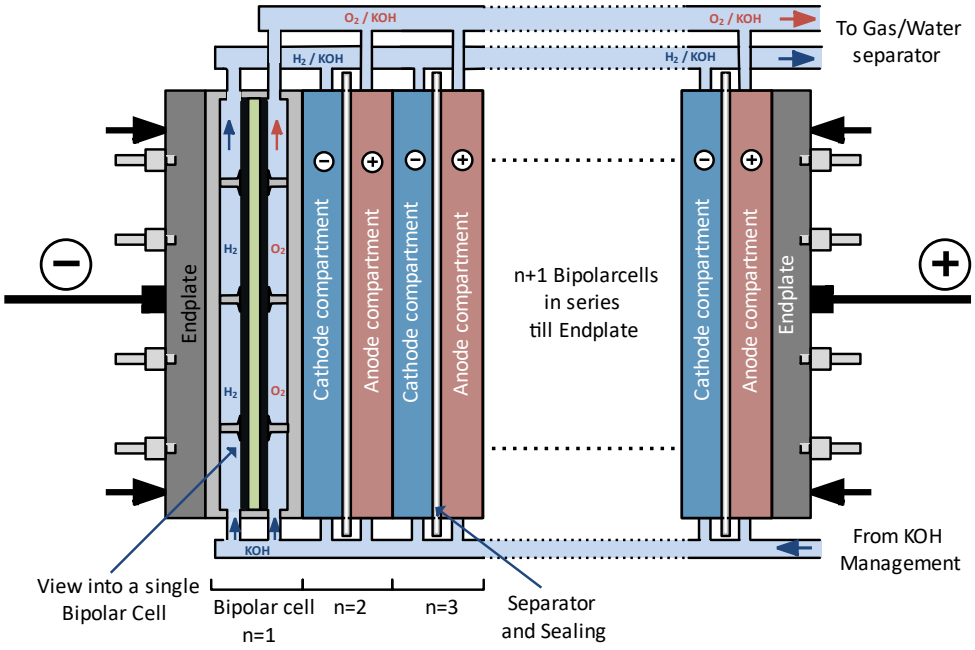

Figure 2-3: General schematic of an AEL stack design

2.1.3 Typical Plant Layout

Although the stack is the main component of an electrolyzer, the complete system consists of several additional process components, instrumentation, and control devices. A principal system layout for an alkaline electrolyzer operating with one stack at (nearly) atmospheric conditions is given in Figure 2-4. In the following, the functionalities and interactions between the different components are shortly explained.

The power electronics consist of a transformer and rectifier and convert the incoming AC power, usually from the electricity grid, into a regulated DC current, which is applied to the contacts of the stack.
The gases evolve from the electrodes and drag the electrolyte in a two-phase flow towards the gas/water separators which are spatially positioned above the stack. Depending on the system design inside the gas/water separators, heat-exchangers and baffles are installed to cool down the electrolyte and to reduce the aerosol content of hydrogen and oxygen, respectively. In the majority of the conventional stack designs, a two-phase mixture of product gas and KOH exits the cells towards the liquid/gas separator. Some atmospheric cell designs offer the possibility of liquid (KOH)/gas separation already inside the cells, saving an additional separator on the system side.
Subsequently, the gases flow through demisters (coalescent filters) in order to retain fine droplets of liquid KOH in the electrolyte circulation. Control valves after the demister

regulate the pressure inside the system. At least on the hydrogen side, the remaining KOH is washed out in a gas scrubber. Due to the fact that water is consumed on the cathode side while it is produced on the anode side, the electrolyte streams get mixed after the separators to prevent a dilution or concentration gradients of KOH between the respective cells. This results in a contamination of product gases due to the electrolyte-carrying, dissolved gases, as the separators can only remove the gas bubbles. This effect increases with slower KOH circulation and higher system pressure. A critical contamination of the gas streams, especially in part-load, must be avoided by a proper control of the KOH circulation, which in conventional AEL systems is automatically done via natural convection. This potential contamination also limits part-load operation to less than 20% of the nominal hydrogen production rate in most AEL systems. However, newer AEL systems can be operated down to approximately 10% of the nominal production capacity, and with modern AEL systems reaching higher current densities, a forced circulation is required for fast gas evacuation and heat dissipation purposes.
The product gas quality after drying is typically in the range of 99.5–99.9% for H_2 and 99–99.8% for O_2 which can be increased to above 99.999% by catalytic gas purification via a deoxidizer.

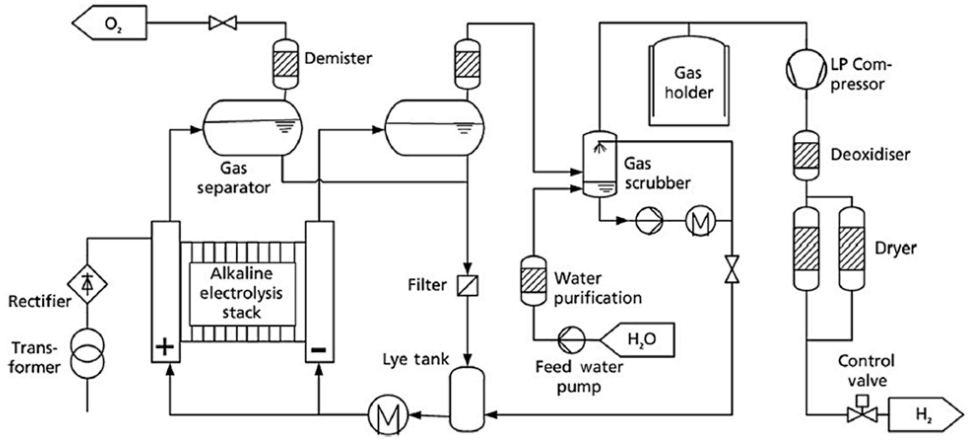

Figure 2-4: Conventional plant layout of an alkaline water electrolysis system

Pressurized operation requires a cell design and a common lye system with a pressure balanced operation of the anode and cathode, which means that the pressure difference between the anode and cathode is only a few millibars. A control valve on the hydrogen side regulates the pre-pressure in the system and a second pressure valve on the oxygen side follows the hydrogen pressure.

A feed water system with a pump is necessary to maintain the concentration of the alkaline solution at a constant level. The quality of the feed water is guaranteed by deionization to prevent fouling in the system. Most systems have additional heat-exchangers for electrolyte and gas cooling. Often a (low-pressure) gas reservoir for hydrogen is installed to decouple electrolysis from mechanical compression to compensate pressure fluctuations.

2.1.4 Commercial Examples and Developments

Nowadays, many manufacturers worldwide offer alkaline water electrolysis systems, and the number is still rising with new players entering the market. Most of them follow a classic, pressurized, round-shaped system design and they usually operate at temperatures of 60 to max. 90 °C with current densities varying between 200-400 mA/cm². However, some manufacturers are developing next generation alkaline electrolysis systems that are capable of at least double the current density of classic systems at comparable energy efficiencies. Table 2-3 lists some examples of commercially

available systems. Even maximum current densities of up to 1200 mA/cm² have been reported and/or demonstrated already today; although the corresponding energy efficiencies are not always published [14–16]. As examples of large-scale atmospheric demonstrator systems adapted from chlor-alkali electrolysis, the designs from thyssenkrupp Uhde Chlorine Engineers GmbH and from Asahi Kasei Corporation are shown in Figure 2-5 and Figure 2-6.

Table 2-3: Examples of current commercial alkaline single stack electrolysis systems based on manufacturer information

Type	A485 [17]	HyProvide A90 [18]	HySTAT®-15-10 [19]	McLyzer 100-30 [15,20,21]	"Aqualyzer™" [22–24]	"Demo unit" [16,25]
Manufacturer	NEL (NOR)	GreenHydrogen (DK)	Cummins (CA, BE)	McPhy (FR, GER, IT)	Asahi Kasei (JP)	ThyssenKrupp (GER)
Rated Stack Input Power (MW)	~2.13	0.39	0.08	0.5	Max. 10	2 (demonstrated)
Hydrogen Production Capacity	485 m³/h 43.6 kg/h	90 m³/h 8.1 kg/h	16.7 m³/h 1.5 kg/h	100 m³/h 9 kg/h	Max. 2000 m³/h 180 kg/h	440 m³/h
Cell Area (cm²)	~21,000	~3,000	1,000	n/a	~ 25,000	~ 27,000
Current Density (mA/cm²)	300	600	~400	Up to 900	up to ~ 1000	up to ~ 1000
Pressure (bar)	atm	35	10	30	atm	atm
Additional information					CAEL-Design	CAEL-Design

Figure 2-5: Current 2 MW atmospheric AEL Demo-plant Carbon2Chem® in Duisburg, Germany (left) and a developed 20 MW AEL standard module (2x10 MW) from thyssenkrupp (right) (courtesy of thyssenkrupp)

Figure 2-6: Large size atmospheric demo system 2017 (left) and upscaled 10 MW demo plant in Fukushima 2020 (right) (courtesy of Asahi Kasei Corporation)

Furthermore, Hydrogen Europe published targets of 1000 mA/cm² in current density without the use of critical raw materials as catalyst for AEL systems by 2030 [26]. The necessary reduction of platinum group metals as part of the catalyst is one of the challenges for future developments. On the other side, the latest long-term tests at the lab scale showed that industrially relevant, current densities (700 mA/cm²) can be reached with PGM-free electrodes even today [27]. Furthermore, even some commercial systems exist today that already claim not to use them. Based on these points, current densities of up to 1,000 mA/cm² are likely to become the standard in next generation commercial products in the next few years. Another noteworthy aspect is that, in the recent years, many stack prototypes show a significantly lower energy consumption than commercial stacks. This can be interpreted in a way that:

1. For commercial applications, stack lifetime is more important than energy efficiency; and therefore, commercial stack designs are generally built under more conservative premises.
2. By making sure low energy consumption at higher current densities can also be delivered with high durability, a certain development potential in alkaline technology exists.

Besides changes in the materials used to improve performance or cost efficiency, it does not seem likely that the AEL market will see revolutionary other cell or stack designs in the coming years. NEL shows, for example, a potential future 20 MW stack concept with rectangular shaped and larger cells in comparison to the current commercial system [28]. Most manufacturers are rather developing stacks with larger dimensions and improved materials. Furthermore, they invest massively in building factories to ramp up production. As can be seen in the Figure 2-5 and Figure 2-6, the upscaling of stack dimensions and an improved standardized system integration is a general trend, both resulting in larger modules with higher power. Here, the challenge remains to produce the advanced electrodes in the required large dimensions, consistent quality, and comparable longevity to conventional electrodes. Another aspect is that the required, special-purpose machinery in the new factories might be limited to only handle current electrode dimensions and parts.
The aim to increase the system pressures exceeding 30 bar is also mentioned in literature and by some manufacturers [6]. A direct correlation would be the saving of operational costs through power savings of approximately 5% [29] for compression compared to atmospheric systems with downstream compressors. This is offset by the need of superalloys and seals on the cell and stack level, which can withstand the high temperatures, high pressures, and the caustic environment. These materials are 3 to 4-times more expensive than standard stainless steel, which is usually sufficient for the requirements in atmospheric systems. According to other analysis, the specific

investment costs of a pressurized alkaline systems can be ~ 20-30% higher than for an ambient system, depending on system size [30,31]. From an operational point of view, less maintenance due to there not being a need to comply with pressure equipment directives is another benefit. Furthermore, compressor efficiency is rising in line with size, which results in less cost added to the hydrogen produced for larger systems. Therefore, elevating the pressure limit might not present the most cost-effective solution for large plants at multi-MW scale.
Furthermore, atmospheric systems have the potential to reach high current densities without the need for high temperature, while pressurized systems require increased temperatures to compensate the increase in reversible cell voltage due to increased pressure in the cells. An increase of stack temperatures will affect the separators as well, which implies the need to develop more temperature resistant separator materials.
There is a wide variety of commercial AEL systems available, which will probably become even more diversified by further developments in the following years. There are many trade-offs associated with one development path or another, which leads to a high risk of uncertainties in predictions as far as 2030. However, in this study, on the alkaline side, the focus is on advanced atmospheric systems. The main reasons are maturity of the basic technology used, existing plants and experience in large multi-MW scale applications, and therefore existing supply chains for a ramp-up of production.

2.2 PEM Water Electrolysis

The development of PEM water electrolysis started in the 1960s with the Gemini space program, but the decisive breakthrough came in the early 1970s with the developments by General Electric using DuPont's Nafion® membrane, which had been commercialized a few years earlier [32]. For the first 20 years, R&D efforts focused almost exclusively on military or aerospace applications, although General Electrics also developed concepts for large-scale use [33]. BBC then took the first steps in Europe toward opening up other markets with the 100 kW Membrel PEM system in the 1980s [34]. However, a commercial breakthrough did not occur until the 2000s, when Proton OnSite placed its HoGen series on the market for industrial applications. Since then, a strong increase in R&D activities by many companies has been observed over the last 20 years. An overview of PEM stack and system manufacturers can be found in Table 2-4.

2.2.1 General Cell Design

The design of a PEM water electrolysis cell is quite similar to that of a PEM fuel cell. Figure 2-7 shows the typical structure of a PEM electrolysis cell. The two half-cell reactions occur in distinct chambers (anode and cathode half-cells), which are separated from each other by the membrane. As membranes, perfluorinated sulfonic acid (PFSA) membranes are usually used such as Nafion® from Chermours (formerly DuPont) or fumapem® from FuMA-Tech. Typically, the membranes have a thickness of 100-200 µm. Next to a high proton-conductivity, the membranes need to prevent a mixing of the product gases. However, during operation, permeation of oxygen and hydrogen through the membrane cannot be completely suppressed. Especially during differential pressure operation with a several bar difference from the cathode to the anode, PFSA membranes exhibit relatively high gas permeability, which is much smaller than in an AEL cell, but nonetheless requires countermeasures. The safety issue especially becomes important with thinner membranes and high differential pressures. In order to reduce the hydrogen crossover to the anode site, membranes with Pt nanoparticles as a recombination catalyst are applied [35,36]. Another challenge of PFSA membranes is their swelling behavior during water absorption. This leads to undesirable wrinkling, especially with large surface areas, and the membrane can be mechanically damaged in the compressed cell. This can be remedied by using internal fabric structures as reinforcement, which counteract the swelling but also reduce the conductivity. For these reasons, alternative ionomers are also being developed for PEM electrolysis, such as so-called hydrocarbon membranes.

However, these materials have not yet been able to establish themselves technologically [37].

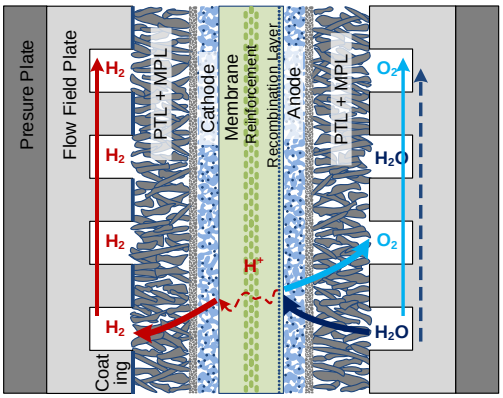

Figure 2-7: Schematic design of a PEM electrolysis cell

The membrane and the electrodes, which are directly coated on the membrane, form the membrane electrode assembly (MEA). An efficient hydrogen production on the cathode requires platinum as a catalyst, usually supported on carbon for a more efficient material use. For oxygen production, the metals iridium (preferred), ruthenium, and their oxides are used. Modern MEAs have a catalyst loading of about 2 mg/cm² on the anode side and about 1 mg/cm² on the cathode side. Currently, intense research and development focusses on the reduction of catalyst loadings for new MEA generations by approximately 40-60%. Iridium in particular is a critical raw material and could be a bottleneck for a multi-GW electrolysis industry [38]. The current global production capacity of Iridium is in the range of 9 tons per year [39]. The catalyst layers on both the anode and the cathode are only a few micrometers thick.

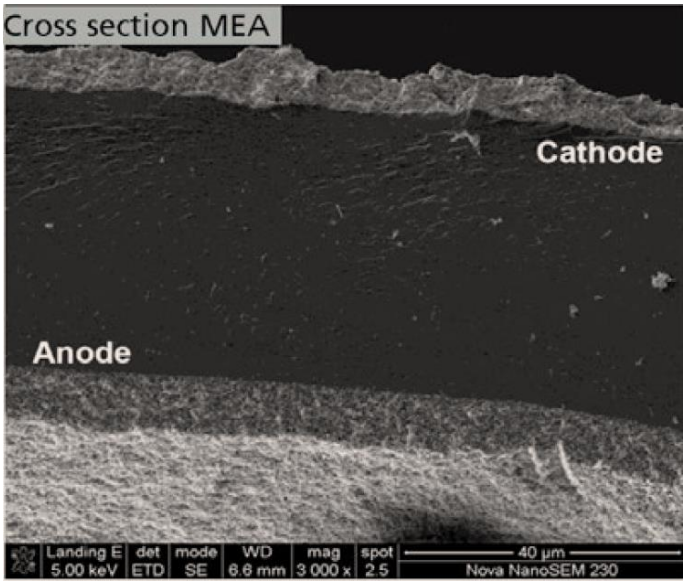

Figure 2-8: Cross-sectional view of a membrane electrode assembly for PEM electrolysis [40]

Between the MEA and the flow channels (flow field) of the bipolar plates (BBP) porous transport layers (PTL) are placed. Although these PTLs are each only a few 100 µm thick, they ensure uniform distribution of the electric current between the bipolar plate and the electrodes. High electrical as well as thermal conductivity and gas and water permeability are the characteristics of a suitable PTL. On the hydrogen side, the electrode potential is close to 0.0 V_{RHE}, so the use of carbon paper or nonwovens is possible as in

PEM fuel cells. On the oxygen side, the use of carbon is not possible since the electrochemical oxidation of carbon occurs above a potential of 0.9 V_{RHE}. Therefore, titanium is almost exclusively used. Titanium is characterized by its high conductivity and above all by its high corrosion resistance. Disadvantages are its high price, poor machinability, and the formation of titanium oxide on the surface on contact with oxygen, which acts as a passivation layer providing electrical insulation and increasing the internal cell resistance.
Also, the flow field plates or the bipolar plates in a stack must be made of corrosion-resistant materials such as titanium or coated steel. However, the latter approach is practically not used in commercial products today. On the hydrogen side, cheaper carbon composite materials can also be used, but this approach has not yet gained acceptance either, since the use of a single-layered titanium sheet as bipolar plate is more cost-effective. In most cases, flow structures are integrated in a bipolar plate (flow field) to enable water and gas transport. Titanium sheets with a thickness of up to 1 mm are used, which is preferably stamped out and the required channel and sealing structures are deep drawn or hydroformed.

2.2.2 General Stack Design

As it is the case for AEL stacks, several single cells in a PEMEL stack are connected electrically in series and hydraulically in parallel (with the bipolar plates separating adjacent cells) to increase the hydrogen production rate. The numbers of cells in today's PEMEL stacks ranges between 30-220 cells with an active area of up to 1,500 cm². Prototypes with an active cell area larger than 2,000 cm² are under development. Although the active cell area of a PEMEL stack is lower by a factor of 5 to 10, the gas production rate of a PEMEL stack has the same order of magnitude compared to an AEL stacks, due to higher current density. In general, PEM stacks have a more compact design, since the use of an ionomer as solid electrolyte and the arrangement of the electrodes on this ionomer/membrane effectively prevent mass transport limitation in a wide current density range. PEM electrolysis stacks are designed almost exclusively for operation under pressure. Typically, hydrogen is produced with 20-30 bars. Due to the high pressures inside the stack, massive end plates made of steel are applied to ensure gas tightness.

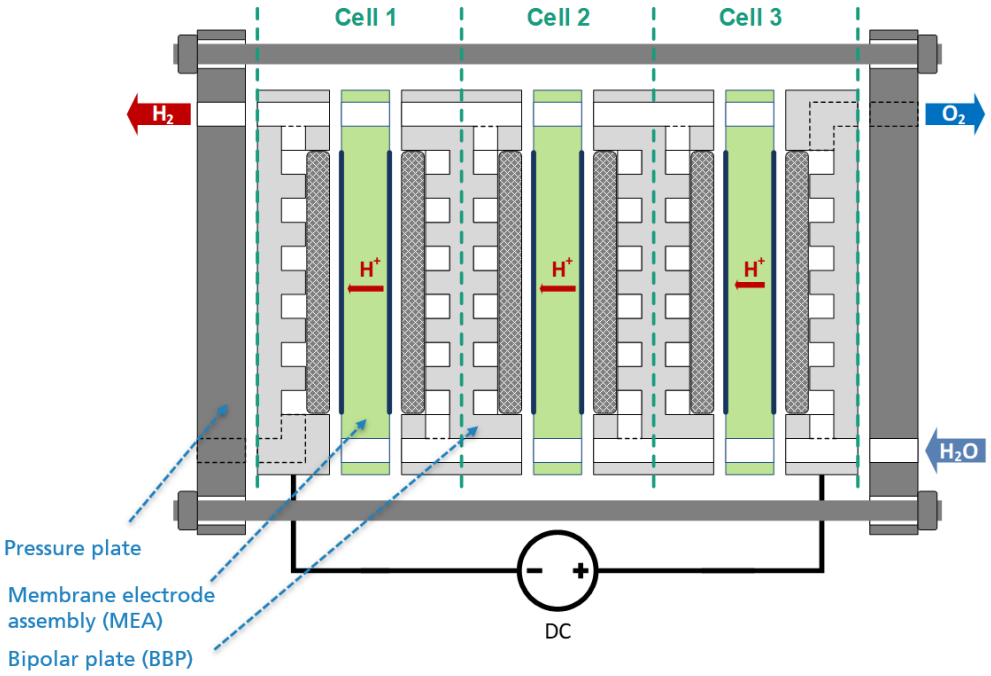

Figure 2-9: Schematic design of a PEM electrolysis stack

2.2.3 Typical Plant Layout

The basic configuration of a PEM electrolysis system is similar to that of an alkaline unit. However, the system design is simpler due to the absence of lye as the liquid electrolyte. Figure 2-10 shows a general schematic of a PEMEL system. It should be noted, however, that the system layout changes from manufacturer to manufacturer depending on their expertise and product orientation. In general, when designing a pressurized PEM electrolyzer, a distinction must be made between balanced pressure and differential pressure systems. In the first case, both sides of the electrolyzer are operated at the same pressure, controlled by an anode and cathode control valve. This principle is identical to that of alkaline electrolysis. In the second case, only the hydrogen side is operated under pressure, while the oxygen side operates at near-atmospheric conditions. This mode of operation requires a well-designed stack and high technological competence, as the membrane must withstand the differential pressure of up to several MPa. Key advantages are the use of low-cost components on the oxygen side. This concept cannot be used in alkaline electrolysis with liquid electrolytes.

As for alkaline electrolysis, DC current is supplied by a rectifier, which converts AC current to DC current. For the circulation of the reactant water, a circulation pump is used on the anode side in most cases. The heat exchanger in the circulation loop is used to dissipate heat from the system to avoid damages of the stack. Heavy metal ions, which are dissolved from the components of the stack and the system during operation are bound to the filling of the ion exchanger. In general, metal ions increase the conductivity of the water and thus reduce its quality, which leads to a faster degradation of the stack. In the gas-water separator, oxygen is separated from the water. The gas leaves the system through a demister, which removes fine water droplets from the oxygen stream. In most PEM electrolysis systems, the cathode side does not have its own water circulation. However, due to a drag current, water gets from the anode side to the cathode side. For this reason, a smaller gas-water separator is also installed on the cathode side. The water that has accumulated in the gas-water separator can be returned to the anode side via a drain valve. The gas flow is led through a heat exchanger, where

large parts of the entrained water condenses and is separated via a condensate separator.
The system is supplied with reactant water via a fresh water supply. This must first be purified to the required water quality. A feed water pump increases the water pressure to the pressure of the anode side and feeds it to the process. For cooling the anode circuit, external recoolers are usually used, which dissipate the process heat to the environment. Lower temperatures are required for cooling the hydrogen in order to condense out as much water as possible from the gas streams. In most cases, a compression refrigeration machine is used for this purpose. In order to use the hydrogen for subsequent applications or for storage, it must be dried, and entrained oxygen must be removed. Oxygen removal is performed by a deoxidizer reactor, usually based on a palladium catalyst. For fine drying, pressure swing or preferably temperature swing adsorption is used [41].

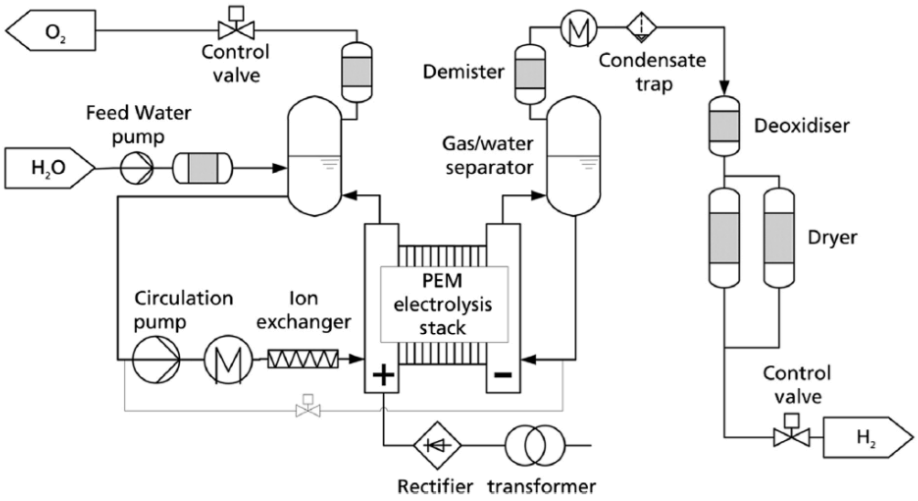

Figure 2-10: Plant layout of a PEM electrolysis system

2.2.4 Commercial Examples and Developments

PEM water electrolysis stack development has made great progress in the last several years. While PEM electrolysis stacks had hydrogen production capacities of up to 10 m³/h (input power ~50 kW) a few years ago, today a single stack can produce more than 200 m³/h (input power larger than 1 MW). The process of an increasing production capacity at stack level continues. The production capacity has been increased due to different approaches. Both the cell area and the number of cells per cell stack have been increased. As an example, Figure 2-11 shows the stack scale-up process at ITM Power. While the 200 kW stack module (consisting of three individual stacks) has round cells, the 2 MW module (also consisting of three stacks) has rectangular cells. The newly developed 5 MW module only consist of two individual stacks, with a larger cell area and an increased number of cells.

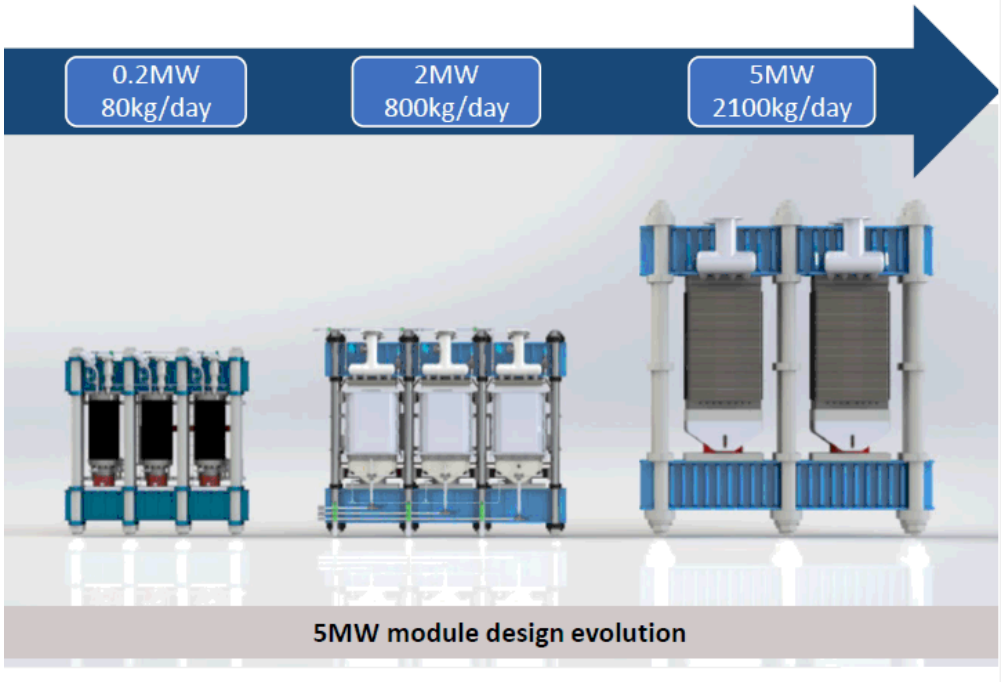

Figure 2-11: Stack scale-up development at ITM Power (courtesy of ITM POWER)

Nowadays, several manufacturers offer PEM electrolysis systems and it can be observed that new players will be entering the market in the near future. In the meantime, all available PEM electrolysis stacks follow a rectangular shaped cell design and are operated at temperatures of 55 to 70 °C with current densities varying roughly between 1.5 – 2.5 A/cm². PEM electrolyzers are particularly suitable for pressurized hydrogen operation and today's stacks typically produce hydrogen at 20 - 40 bar.
Table 2-4 lists some examples of commercially available PEM electrolysis stacks.

Table 2-4: Current PEM electrolysis stack specifications

Type	M Series	SILYZER 300 [42]	Allagash [43]	HyLYZER[19,44]	S450 [45]	HGAS [46]
Manufacture	Proton Onsite (USA)	Siemens (GER)	Giner ELX (USA)	Hydrogenics (CA, BE)	HTEC (GER)	ITM Power (GB)
Rated Stack Input Power (kW)	250	730	1,000	2,500	~125	~670
Hydrogen Production Capacity (m³/h)	52	~160	200	500	~26	~125
Cell Area (cm²)	n/a	< 5,000	1,250	1,500	450	1,000
Current Density (A/cm²)	~ 2.0	<1.5	3	2.3	n/a	3

Pressure (bars)	30 (differential)	atm. (balanced)	40 (differential)	30	30 (differential)	20 (differential)

In addition to the current available PEM electrolysis stacks, some manufacturers already introduced the next stack generation. As already depicted in Figure 2-11, ITM Power developed a 5 MW module with two single 2.5 MW stacks. Before, three stacks with a total capacity of ~2 MW (~0.7 MW per stack) have been applied. Giner ELX (acquired by Plug Power Inc.) presented a future design of an electrolysis stack with a capacity of 5 MW, which is presented in Figure 2-12. The stack has a cell area of 3,000 cm² and produces hydrogen with a current density of up to 5 A/cm² [47]. Also, in January 2021, NEL introduced a new PEM electrolysis stack. The capacity of the stack is 1.25 MW, which equals a five times higher capacity compared to the current PEM stack [48].

Figure 2-12: 5 MW PEMEL stack named "Kennebec" by Giner ELX (courtesy of Giner ELX, acquired by Plug Power Inc.)

2.3 Anion Exchange Membrane Electrolysis

Anion Exchange Membrane Electrolysis (AEMEL) combines the advantages of both alkaline and PEM electrolysis using a thin anion exchange membrane with low internal resistance, similar to the ion-exchange membrane in PEM electrolysis, utilizing the charge transfer mechanism via hydroxide ions, as in AEL, but with a less corrosive electrolyte or even pure water in the future. This approach promises to enable the use of cost-efficient and abundant catalyst and electrode materials, while allowing high power densities under differential pressure and a compact design.

However, the highly hydroxide-conductive, polymeric membranes still suffer under substantial chemical and mechanical stability problems, especially at higher temperatures, even when using highly diluted KOH as a supporting electrolyte to enhance the conductivity and enable higher current densities [49,50]. So far, the resulting short lifetime of the membrane remains the key issue to be resolved in the development of the AEMEL technology. The main degradation mechanism, known as a hydroxide (OH^-) attack on the polymer backbone of the AEM, has been a focus of research in the past several years and is therefore well understood. Operation of the stack without supporting KOH electrolyte could solve the durability problem and can lead to lifetimes > 5,000 h but results in lower efficiency [51]. Besides the research on durable and more ion conductive AEM, the electrode preparation and development of durable and highly active and PGM free catalysts is in focus [52,53].

The research on new membranes is still ongoing and the latest results clearly outperform commercially available membranes. However, none of the lab scale membranes are used in commercial products yet. Often, long-term stability data of AEM are missing as most work focuses on the initial performance after cell activation, rather than long-term operation on system level in an industrially relevant environment. [53,54]
Therefore, the AEMEL technology is still at a less-mature stage than PEMEL or AEL with only a few companies so far working on commercializing it. Available systems operate at 30 bar pressure and 50 °C, with 50 bar and higher temperatures being explored on a laboratory scale. Figure 2-13 shows the first MW-scale AEMEL system design concept released by the company Enapter. This system design follows a strategy of cost-reduction through mass-fabrication and modularization of hundreds of smaller AEMEL units and combining them to MW-scale modular systems [55]. – a typical numbering-up approach. This approach shall offer advantages of high flexibility, high reliability due to built-in redundancy, and a high utilization of installed manufacturing equipment at the production site. However, this must also increase the susceptibility and overall maintenance effort of the system and the membrane lifetime remains the most critical challenge for AEMEL technology.

Figure 2-13: "Multicore" 1MW AEMEL system based on the modularization of 440 mass-produced AEM electrolysis core units by Enapter (courtesy of Enapter)

Due to the lower technology readiness level, data on commercial AEMEL technology are scarce and a rapid large-scale deployment of AEMEL technology at a commercial multi-MW-scale in the coming years is not very likely. Although, AEMEL technology presents a high cost-reduction potential by using cheap and abundant materials. It also needs to operate at high current densities to be competitive with AEL and PEMEL, which themselves will make continuous progress in the next years. For these reasons, a cost analysis and cost outlook for AEM electrolysis will not be considered in this study.

2.4 General Description of Balance-of-Plant Components

In the following chapter, the requirements of the main balance-of-plant components are explained in more detail.

2.4.1 Transformer / Power Electronics

The process of water splitting takes place when direct current (DC) is applied to the electrolysis stacks. Due to the fact that electricity grids are operated with alternating current (AC), the electricity needs to be converted first. For the conversation of AC to DC, thyristor-based rectifiers are typically utilized. These rectifiers work at DC voltage levels of several hundred volts and provide enough current to be suitable for the most

stack sizes. Figure 2-14 shows a rectifier system used to power electrolysis stacks of up to 1 MW capacity at the test lab of Fraunhofer ISE.
The stack voltage depends on the number of cells and the nominal cell voltage at rated load and is in the range of several hundred volts. Degradation of electrolysis cells leads to higher cell voltage with increasing operation hours. To produce the rated amount of hydrogen even with degraded stacks, the stack voltage needs to be increased. Therefore, the output voltage window of the rectifiers must include the minimum voltage of the electrolysis stack at start-of-life and partial load, as well as the maximum voltage of the stack at end-of-life at full load. Regarding the EU-specific low voltage directive (2014/35/EU), the maximum DC voltage is 1,500 V. The stack current depends on the current density and the cell area. For single electrolysis stacks with large cell areas, the stack current can be up to 30,000 A (e.g. for an alkaline stack with a cell area of 30,000 cm² and current density of 1 A/cm²). In principle, several power electronic components can be connected in parallel to achieve such high currents.

Figure 2-14: Thyristor rectifier system of a 1 MW electrolysis stack test lab at Fraunhofer ISE

Advantageously, thyristor rectifiers have no output limit for minimum DC voltage, which is needed to operate the stack in partial load.
To reduce the effects of reactive power of the converters, filter circuits are applied to the systems [56]. A small part of reactive power remains. The connected AC grid needs to be stable enough to bear that reactive power, else an installation of external compensation, e.g. with STATCOMs, is needed. In relation to the maximum plant capacity, the system needs to be connected to the corresponding network level. Electrolysis plants with a single digit capacity are usually connected to mid-voltage grid (20-30 kV). A 100 MW plant would be usually connected to the high-voltage grid (110 kV) and electrolysis plants with capacities of 1 GW are connected to the transport grid (380 kV). However, the rectifiers themselves are supplied with low-voltage of around 0.4 kV. Typically, each rectifier has its own low-voltage transformer. Figure 2-15 shows a simplified power supply system for an electrolysis plant.

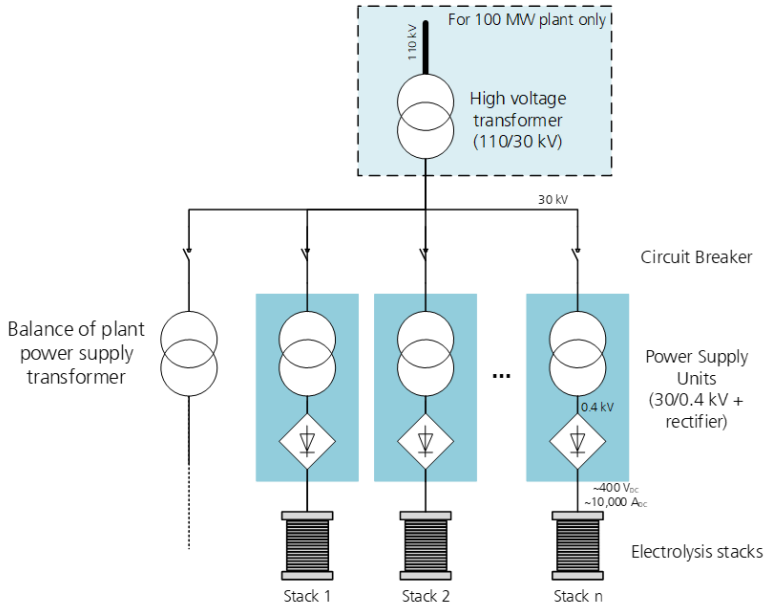

Figure 2-15: Power supply for a system with several electrolysis stacks; adapted from Energiepark Mainz (based on [57])

2.4.2 Water Purification

To produce hydrogen, water is the most important reactant. Electrolysis systems require high-purity feed water to avoid damage to the electrolysis cells. Without proper water purification, contaminants in the feed water can poison and deactivate the catalysts, which leads to strong degradation of the electrolysis cells (resulting in higher cell voltages and lower efficiency). Therefore, every electrolysis system consists of a water purification unit to ensure the required low conductivity (µS/cm) of the feed water by cleansing it to the level of fully deionized water. With the help of these systems, water of almost any quality can be purified to the required extent needed for electrolysis. Looking at potential water sources, tap water (typically is 100-1,000 µS/cm) from public grids is most common for electrolysis systems today, due to the benefits of a stable supply, general low cost, and less effort with regulatory permits. The usage of seawater (with up to 42,000 µS/cm) and wastewater is also possible, but additional pretreatment processes, for example an upstream desalination unit, add to the cost. The cost for overall water treatment is highly dependent on the water source, the transport distance and possible waste disposal. [58] Therefore, in this study the water purification system considered includes the fine purification components from standard tap water in Germany towards the feed water conductivity according to ASTM D1193-99e1 Type II.

Although, the required water conductivity for water electrolysis systems is defined by the manufacturer, for most systems, a feed water conductivity of max.1 µS/cm according to ASTM D1193-99e1 Type II and total dissolved solids <0.5 ppm is recommended. However, PEM electrolysis especially can require lower conductivities (<0.1 µS/cm).

Due to the requirements of a reverse osmosis system alone, to produce 1 Nm^3 of hydrogen, 1-2 liters of tap water are needed, which is twice the amount compared to demineralized water [59]. Furthermore, AEL systems are filled with liquid electrolyte (KOH)-solution during commissioning, for the mixing of which highly purified water is also needed.

The cost share of the water purification system in the overall cost of large-scale electrolysis systems, like the ones investigated here, typically amounts to 1-2 % with a decreasing trend towards higher system capacities.

Feed water purification systems are state-of-the-art and commercially available on a large-scale. Maintenance intervals depend on the dimensions and tap water quality. During maintenance, filters and membranes are changed. In Figure 2-16, an example of a feed water purification unit manufactured by Grünbeck Wasseraufbereitung is shown.

Figure 2-16: Example for feed water purification unit (courtesy of Grünbeck Wasseraufbereitung)

Inside a PEM electrolysis system (e.g. circulation water loop), water quality decreases because ions are dissolved from system components, such as pipes. Without countermeasures, the water quality in the circulation loop would quickly decrease and lead to the aforementioned degradation [60]. To avoid this, inside the PEM electrolysis systems, ion exchanger are installed, which keep the water quality at the required level. For alkaline electrolysis, this is not applied.

2.4.3 Hydrogen Purification

Hydrogen produced by water electrolysis processes has a high purity compared to conventional hydrogen production processes like steam-methane reforming or coal gasification. However, the hydrogen contains small amounts of oxygen, transferred from the anode side to the cathode side in the electrolysis stack. Furthermore, because the hydrogen is in contact with water, it is saturated with water when it exits the stack. Many applications require high purified hydrogen in order to avoid damage to components. For example, a small amount of oxygen in the hydrogen can deactivate the catalyst in a methanol synthesis. Also, water can condensate in hydrogen tanks or pipelines, leading to safety issues. Table 2-5 shows the maximum amount of impurities allowed for different industry standards and mobility applications.

Table 2-5: Hydrogen Purities standards [41]

	Industrial Hydrogen Qualities Levels		Hydrogen for Mobility Applications	Unit
	3.0	5.0	SAE2719	
O_2	≤50	≤2	≤5	ppm
N_2	≤500	≤3	≤100	ppm
H_2O	≤100	≤5	≤5	ppm

In order to meet the requirements on the hydrogen quality, hydrogen needs to be purified. For this reason, a purification unit is applied in electrolysis plants, removing water and oxygen.
A schematic layout of a hydrogen purification unit is shown in Figure 2-17. In the first step, small traces of oxygen, which crossed over the membrane into the hydrogen product gas stream, are removed in a deoxygenation reactor. The reactor is filled with aluminum oxide, which has a catalytic surface based on the catalyst palladium. On this catalytic surface, the traces of oxygen (ppm) react with hydrogen to water [41].
This leads to a first hydrogen loss within the purification unit. The reaction is strongly exothermic, resulting in a high temperature increase of the hydrogen. In order to cool the hydrogen, a heat exchanger is installed after the deoxygenation reactor. Due to the cooling, water condensates in the heat exchanger and is removed.

However, for some applications the water content needs to be reduced even more to avoid later condensation in pipelines [61] or storage tanks. For this purpose, an adsorption process is installed after the heat exchanger. For continuous drying, at least two columns are required. While the hydrogen coming from the deoxygenation flows through the first column (see Figure 2-17) and the water is adsorbed by the adsorption material (e.g. silica gel, molecular sieves), the other column is regenerated. To do so, the column is heated by an electric heater to desorb the water from the adsorption material. To remove the water from the column, the column is purged with a small amount of the dried product gas.

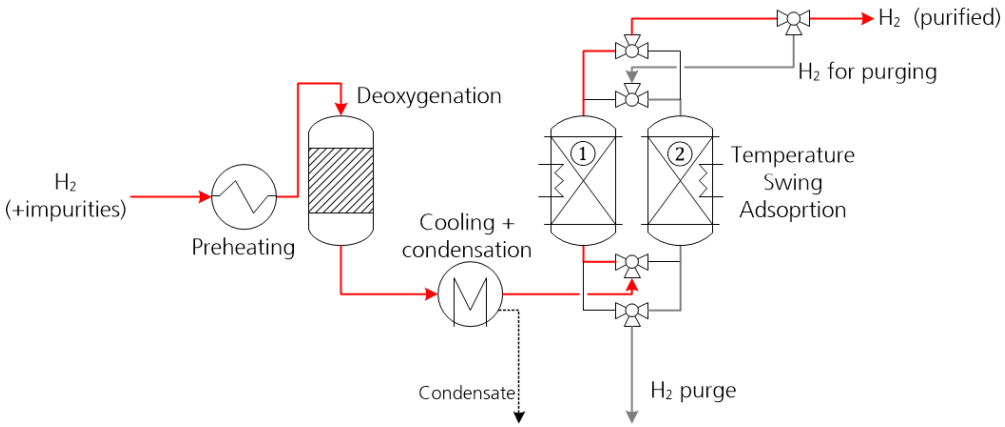

Figure 2-17: Schematic Layout of a hydrogen purification unit

Figure 2-18 shows a gas purification system manufactured by Silica Verfahrenstechnik GmbH with a capacity of 4,000 Nm³/h, which equals the hydrogen production capacity of a 20 MW electrolysis system.

Figure 2-18: Gas purification system for a capacity of 4,000 Nm³/h (~20 MW electrolysis) (courtesy of Silica Verfahrenstechnik GmbH)

2.4.4 Cooling System

Like any other process, the electrolysis of water is not an ideal process. Due to internal resistances in the cells, heat is generated inside the electrolysis stack. To avoid damage to the cells, the heat needs to be dissipated from the system. For this reason, a heat exchanger is placed in the circulation cycle (water or lye). Also, the product gases are cooled in order to condense water from the gas flows. The water is fed back to the electrolysis system to reduce water demand. Additionally, heat needs to be dissipated from the gas purification unit and the compression system. Mostly, cooling is realized with cost-effective dry coolers, which chill the coolant (water/glycol mixture) down to near ambient temperature. For cooling of the product gases, industrial cooling machines are also applied to cool the gases down to 10°C. However, industrial cooling machines consume much more electricity than dry coolers.
The dissipated heat ("waste" heat) also can be used for space heating, e.g. via district heating grids. This increases the efficiency regarding of the input power [62]. .

2.4.5 Compression

Hydrogen has a high gravimetric energy density. However, the density of hydrogen under standard conditions (0°C; 1.013 bars) is very low, resulting in a low volumetric energy density. For storage, transportation, and further processing, this is not an option from a technical and economical point of view. In relation to the applications, a final pressure of 80 to 900 bars is required.

Table 2-6: Pressure levels of different applications

Application	Pressure (bars)
Pipeline injection	60-100
Underground storage (cavern)	<200
Hydrogen Refueling Station	350-900
Ammonia production	~200

To increase the density (kg/m³) and the volumetric energy density, hydrogen needs to be compressed to higher pressure levels. The compression of hydrogen is a state-of-the-art process, which is applied in nearly all hydrogen related applications. For the compression of hydrogen in large-scale applications, reciprocal, multi-stage compressors are typically used. Each compression stage has a compression ratio of maximum ~3 in order to limit the hydrogen outlet temperature after each stage to a maximum of 135°C to meet the requirements of the API 618 [63]. Figure 2-19 shows an example picture of a large-scale hydrogen compressor. Compression systems are available in a wide range of capacities, starting from drive powers in the single-digit kW range and ending up in the two-digit MW range. The compressor stages are usually powered by an electrical motor, whose characteristics limit the flexibility regarding part load operation of single compressor units. Therefore, for large-scale plants that need to follow highly fluctuating input power, the installation of several compression units enabling more efficient part-load operation might be required.

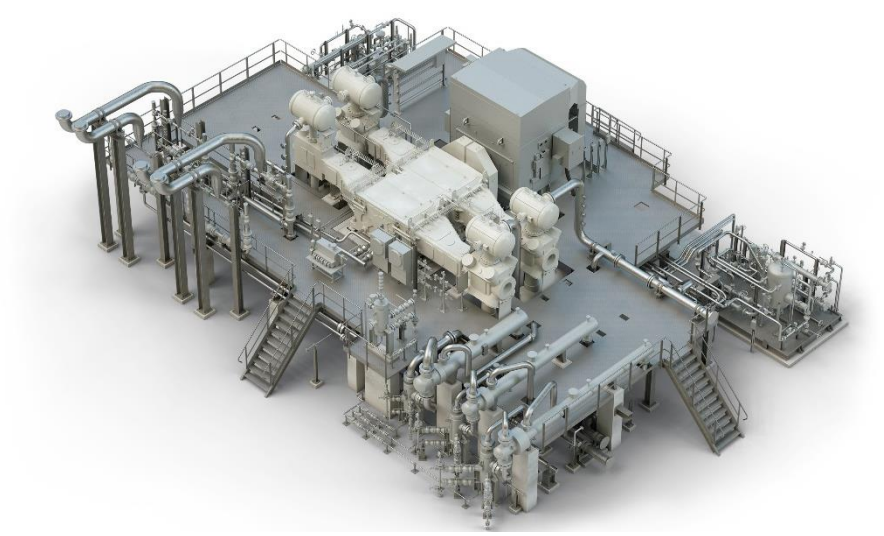

Figure 2-19: Picture of a large-scale hydrogen compressor system [64] (courtesy of Burckhardt Compression)

3
Bottom-Up Cost Analysis of Electrolysis Systems

3.1 Methodology of the Cost Analysis Approach

The cost analysis approach follows a methodology with several steps, which was developed in recent years at Fraunhofer ISE [65,66]. An overview of the applied methodology for the bottom-up cost analysis is given in the form of a flow chart diagram, shown in Figure 3-1.

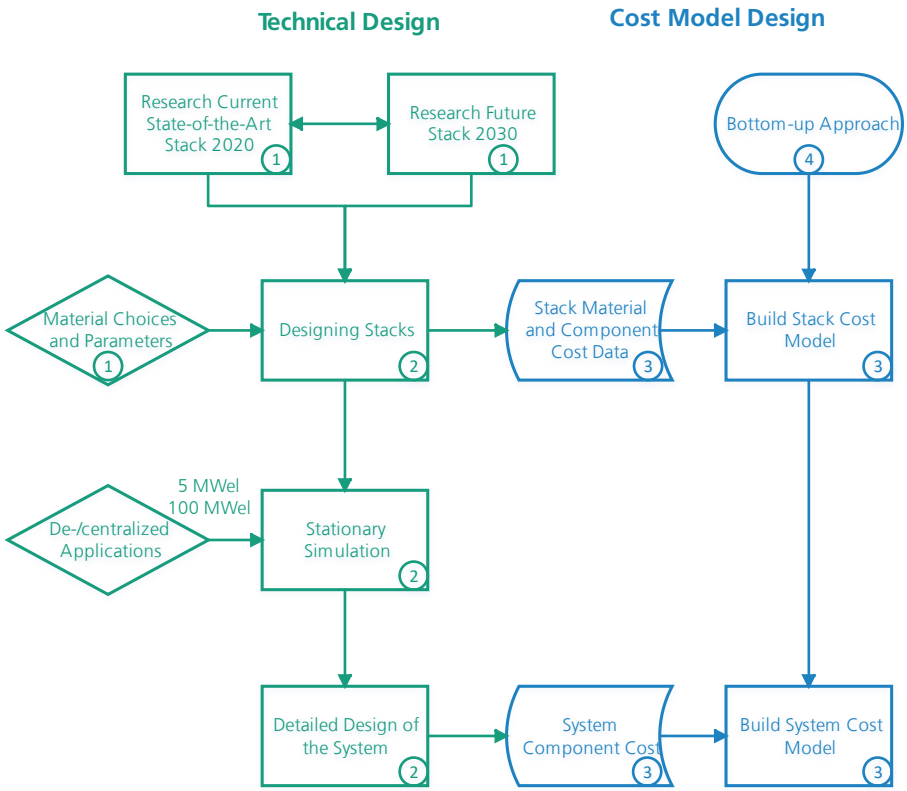

Figure 3-1: Flow-chart of the cost analysis methodology in this study

It should be taken into account that this described approach will result in investment or production costs from a general contractor's point of view, but not final selling or market prices, as the estimation of margins, system R&D surcharges, overhead surcharges, and buffer surcharges are company specific data and highly dependent on individual project requirements and the portfolio policy of the company. Other project-specific costs like greenfield development, capital costs, and insurance can vary greatly from case to case and therefore are not considered in the cost analysis as well. Furthermore, since some of the used data are sensitive stakeholder information, no company-specific cost data are presented in this study. The following descriptions explain the steps in more detail.

1. Determination of Current State-of-the-Art and Technological Outlook

In the first step, the current state-of-the-art status and respective development potential of AEL and PEMEL systems is drawn up on the basis of an extensive literature research, a survey of commercial products, development targets [26,67], internal expert knowledge, and consultations with external experts. Based on these findings, the material specifications for current stacks and a potential technology projection towards the year 2030 are derived and shown respectively in Table 3-1 and Table 3-6. In alignment with those material specifications, key performance parameters are determined and listed in Table 3-2 and Table 3-7. These parameters are in agreement with the polarization curves from different AEL and PEMEL stacks or cells shown in Figure 3-2.The assumed values are focused on drawing a realistic picture of the situation today, while maintaining the comparability towards the year 2030 scenarios. It needs to be mentioned that such a long-term forecast on further technology development is naturally subject to greater uncertainties.

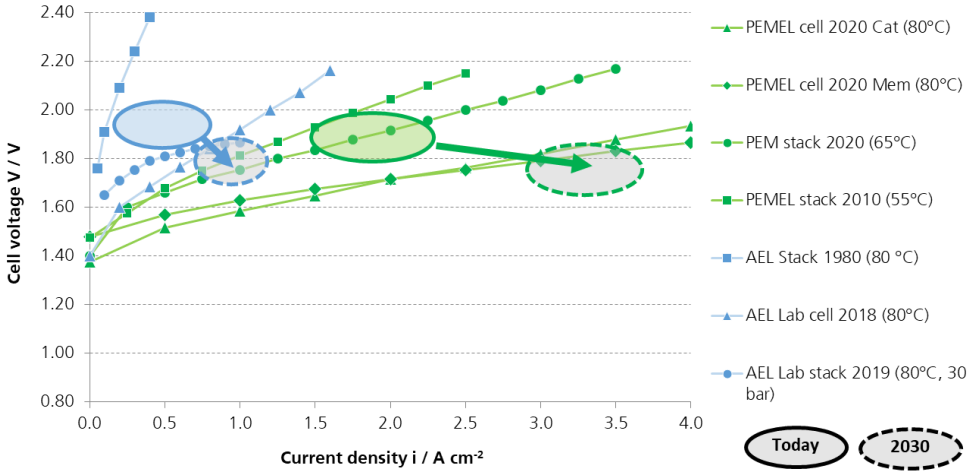

Figure 3-2: Comparison of different polarization curves of AEL and PEMEL [8]

2. Design Electrolysis Systems and Set System Boundaries

In the next step, the state-of-the-art and future performance and materials specifications are used to create realistic stack designs (cell area, number of cells, etc.), which are the centerpieces for the different electrolysis system configurations with 5 MW and 100 MW DC input power for both reference years. The two system scales are chosen as best fits to represent centralized and decentralized electrolysis plants. The differentiation between two technologies, two system sizes, and two years results in a 2x2x2 matrix of respective system arrangements and associated cost scenarios, which are shown in Table 3-3 and Table 3-8. Depending on the required number of stacks in a system and their interconnection, all relevant energy and mass flows of the stacks themselves and the balance-of-plant components are calculated by a stationary system simulation using the model toolbox H_2ProSim developed at Fraunhofer ISE. The resulting values are listed in Table 3-5 and Table 3-10, respectively. These simulation results are necessary to adequately design and size the balance-of-plant components and to determine their cost. Considering the system boundaries and the concepts of cell stacks, general system layouts are established, which include major peripheral components. To achieve comparability between AEL and PEMEL installations, identical system boundaries for the designs are chosen in terms of plant size, input parameter, and output parameter, as well as gas purities and hydrogen pressure following the ISO 14687-2 standard (pressure of 30 bar and gas purity of 99.999 %). As a result, the considered AEL systems, which

are operated at atmospheric pressure, require an additional downstream mechanical compression unit and the associated costs are added to the overall system costs.

3. Building Stack and System Cost Models

The aim of a cost model is to estimate the investment cost of a specific stack or system. The cost models developed at Fraunhofer ISE take into account the type, dimensions, and quantity of the materials and components that are given by the previous specifications. In general, these models implement compiled cost data from budget quotations for main stack components and materials, staggered by quantity, as well as target prices for system components, stakeholder information, and available literature values. For most of the components, specific cost functions are created, which depend on different quantities or capacities. Thereby, the cost models offer the possibility to analyze the cost effect of increasing production capacities or component dimensions to a certain extent.
However, some balance-of-plant components and further cost items, such as piping, instrumentation, engineering, construction, housing costs, and others are considered only by using fixed markdowns as used in chemical plant engineering and projecting. Furthermore, previously gathered cost data on system components are updated and inflation-adjusted by applying cost indices, such as the chemical plant index (CEPCI) [68]. In contrast to the stack models, the system cost models for 2030 do not include technological improvements of the system or BOP components, but solely specific material savings by intensified usage of central components.

4. Bottom-Up Analysis Approach

These cost models are detailed enough to calculate costs of the basic components on the stack level (as bipolar plates or membranes), as well as component costs on system level (as circulation pump). Therefore, the resulting cost breakdowns start at the material level of stack components and component level on the system side (bottom). The derived direct cost of materials and basic components, which are needed to build a stack with the determined capacity and performance, get accordingly aggregated towards the resulting stack cost and these stack costs get combined with the according system component cost, which finally results in the total system cost (top). This procedure provides a measure for a detailed cost structure analysis and identification of cost-reduction potentials.

3.2 Alkaline Electrolysis Cost Model

3.2.1 Cell and Stack Specifications

In Chapter 2.1.4 it was described that AEL systems at atmospheric pressure can have a cost benefit in large-scale applications over pressurized systems. Therefore, the cost model here is based on a rectangular-shaped cell and stack design for atmospheric operation.
Table 3-1 shows the main cell and stack components and materials, which are determined for this study. Specifications for 2030 are subject to assumption of some technological progress in performance-relevant areas but are justified by a literature review and interviews with AEL experts.

Table 3-1: Cell and stack material specifications for the 2020 and 2030 cost model

	Alkaline Electrolysis	
	2020	**2030**
Electrolyte	Potassium hydroxide KOH 25 %	Potassium hydroxide KOH 25 %
Separator	ZrO_2 based diaphragm (500 µm)	ZrO_2 based diaphragm (220 µm)
Cathode side Electrode substrate	Woven nickel mesh	Steel expanded metal sheet, nickel coated
Catalyst material	Mixed metal oxides (e.g. RuO_2)	Mo-doped Raney nickel (Ni-Al-Mo)
Anode side Electrode substrate	Expanded nickel sheet	Expanded stainless steel, nickel coated
Catalyst material	Nickel based (Raney Ni-Al)	Nickel based (Raney Ni-Al)
Bipolar plates	Stainless steel, Nickel coated	Stainless steel, Nickel coated
Current collector	Expanded steel plate, Nickel coated	Expanded steel plate, Nickel coated
End plates	Stainless steel	Stainless steel
Elastic elements	Woven nickel mesh	Woven nickel mesh
Sealing	PTFE	PTFE

In general, no game-changing, new cell concept and redesigned AEL stacks are expected to become commercially relevant until the year 2030. Although, incremental and continuous improvements can be expected, especially towards higher power densities by maintaining low material cost and a similar efficiency. However, a reduced cell complexity with more integrated components or fewer components overall could be realized, which is not directly taken into account here, but rather considered by general component cost reductions. As a result, the main developments towards 2030 in AEL stack design are seen on the cell component level, first and foremost the separator, electrode substrates, and catalyst materials.

In the past there was not enough demand from the electrolyzer manufacturer side to justify a further development of the separator by the suppliers. This has since changed and development activities are now ongoing. They are mostly aiming to make the separators thinner in order to lower the ohmic resistance and consequently increase the current density. This trend is considered in the specifications below. At the same time, the separators impermeability towards the product gases is of the utmost importance in terms of safety and to improve or even reach high gas purity levels.

Due to its electrical conductivity and durability in caustic environments, nickel as a substrate material for electrodes is most common today. Lab tests under industrially relevant conditions with already commercial stacks showed that stainless steel-based substrates with a thin nickel coating can present a long-term, stable, and cost-effective alternative to nickel.

High surface area electrodes, for example Raney nickel surfaces, with enhanced catalysts, such as Molybdenum on the cathode side, will be needed towards 2030 to meet the

goal of avoiding noble metals and provide sufficiently high efficiencies. Continuous processes for the application of such Raney-nickel coatings on the substrate exist and are scalable as a condition for increasing production capacities [53,69–71]. Compared to today's stacks, some of the cell materials that will be potentially used for a 2030 stack design have only been proven in laboratory tests so far. However, such a stack could thus be available till 2030 if R&D work is carried out accordingly.
In accordance with the cell component and material selection, the stack has been designed in terms of meeting the typical input stack capacities of 2.5 MW and 10 MW in 2020 and 2030, respectively. The resulting stack parameters are listed in Table 3-2.

Table 3-2: Technical stack parameters for the cost model 2020 and 2030 at rated load

	2020	**2030**
Rated Stack Input Power (DC)	2.5 MW	10 MW
Cell Area	20,000 cm²	30,000 cm²
Number of Cells per Stack	116	200
Rated Current Density	0.6 A/cm²	1 A/cm²
Rated Cell Voltage (BoL)	1.8 V	1.7 V
Stack Current	12,000 A	30,000 A
Stack Voltage (BoL)	208 V	340 V
Faradaic Efficiency	99 %	99 %
Pressure Cathode	1 bar	1 bar
Pressure Anode	1 bar	1 bar
Temperature	80°C	80°C
Voltage Efficiency	82 %	87 %
H_2 Production Stack	51.8 kg/h	223.9 kg/h
	576 Nm³/h	2,485 Nm³/h
Specific Energy Consumption	48.3 kWh/kg	45.6 kWh/kg
	4.35 kWh/Nm³	4.1 kWh/Nm³

The parameters for 2020 represent a general design, rather than a specific commercial setup. The parameter projections towards 2030 of Table 3-2 are oriented on recent research activities and development trends in next generation alkaline cell components, expert knowledge, and target developments, aligned with the potential of the material choices determined in Table 3-1.

3.2.2 Stack Cost Breakdown

The data from Table 3-1 and Table 3-2 are used as framework conditions for the stack cost model. The alkaline stack cost model determines the direct costs depending on the required quantity and dimensions of the materials and components specified in Table 3-1 of Chapter 3.2.1.
For example, a rectangular 23,000 cm² cell design with an active electrode area of 20,000 cm² and in filter press construction was used for the 2.5 MW stacks of 2020. The

10 MW cell stack in 2030 corresponds to the cell stack described above but the slightly modified design results in the following deviations:

- The active electrode area is increasing by 50% and the required number of cells is almost doubled.
- The separator, electrode substrates, and catalyst material are changed.

For the base material of the electrode substrates, current collector, and elastic elements reliable, staggered price offers from suppliers are available, which are extrapolated to the large-scale cell geometries. For the separators, staggered, indicative price offers from potential manufacturers are used. To reflect the costs of bipolar plates, end plates, and sealings, price offers for the stainless-steel base plates and sealing material are used and additional manufacturing costs are added in consultation with manufacturing experts. Additional cost for nickel coatings as corrosion protection are significantly dependent, on the size and geometrical complexity of the substrate. Here, a simplified approach is applied by combining the general material, labor, and equipment costs, depending on the dimensions of the part. As expected, it is very difficult to determine reliable manufacturing costs for the catalyst coating because this is sensitive data from the AEL companies and heavily depends on the catalyst material, the preparation, and the coating processes involved. Consequently, literature data is extrapolated here. The cost for the electrolyte is assumed by an estimation of to internal volume of the stack for simplicity. In addition to the displayed main components, there are also other relevant stack components, such as threaded rods, construction frame materials, and fittings. Most of them are assumed to be made from stainless steel and are summarized as Balance-of-Stack (BoS) components. Also, cell and stack assembly costs are considered, based on common labor costs in the metal and electrical industries in Germany and own empirical values adapted from PEMEL technology.

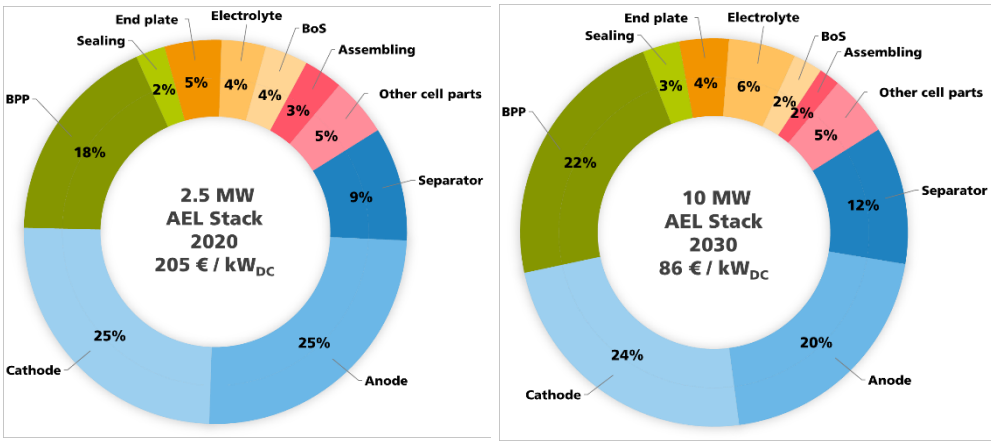

Figure 3-3: Cost breakdowns of state-of-the-art 2.5 MW (2020) and an assumed 10 MW (2030) alkaline electrolysis stacks

With the help of the developed bottom-up stack cost model, two cost breakdowns have been created: A 2.5 MW single stack design of 2020 and a second, upscaled 10 MW stack design for 2030, including the previously described technological development. These results are illustrated in the Figure 3-3. Half of the stack costs in the 2.5 MW stack 2020 scenario and 44% of the 10 MW 2030 scenario stack costs are associated only to the electrodes. High effort in manufacturing and catalyst coating of the electrodes is the main reason. In the future, cathode and anode costs will almost be equal because both half sides need a highly active, and therefore, costly catalyst coating to reach the required performances. Furthermore, the costs for the base substrates are comparably low in relation to the costs of the applied catalyst coatings and, in consequence, do not show a significant influence on the costs. In general, the cost share of the electrodes is shrinking towards 2030, which underlines the effect on catalyst development and the associated manufacturing processes. The bipolar plates also have a significant share of

18% (2.5 MW, 2020) to 22% (10 MW, 2030). Although, they are made from already cost-effective materials, like stainless steel, and thinly coated with nickel, the geometry of the plates can be complex and therefore costly. Due to the fact, that other components offer a higher cost-reduction potential towards 2030, the share of the BPP on stack costs is rising slightly. The separator is a crucial component, concerning the performance of the stack, but only contributes 9% (2.5 MW, 2020) to 12% (10 MW, 2030) to the total cost. Under the term "other cell parts" the elastic element and current collector are combined.
In general, the cost shares of the respective components do not change significantly between both illustrated cost breakdowns, which is plausible considering that the general design of the stack is similar.

3.2.3 System Layout and Dimensioning of Balance of Plant Components

With the specifications from the stack design and the characteristic values derived from it, the process technology and periphery of the system layouts were conceptualized and roughly dimensioned for the 5 MW and the 100 MW AEL plants using the model-based system simulation H_2ProSim developed at Fraunhofer ISE. Thereby, the arrangement of stacks and balance-of-plant components, as well as their dimensions needed to be considered. As the different rated stack powers in 2020 and 2030 have an influence on the system layout, it is necessary to develop different systems for both base years.
The 100 MW system is divided across several electrolysis arrays. In 2020, for the 100 MW scenario, four electrolysis stacks are interconnected to one 10 MW array and as a result, 10 arrays are needed in total. Table 3-3 gives an overview about the number of stack arrays, the rated stack capacity of each array, and the total number of stacks. Due to comparability reasons, the 5 MW plant in 2030 is designed as a short stack from an assumed 10 MW standard stack size.

Table 3-3: AEL System arrangement

	2020		2030	
Plant Capacity	5 MW	100 MW	5 MW	100 MW
Single Stack Capacity	2.5 MW		5 MW (short stack)	10 MW
Arrays	1	10	1	5
Array Capacity	5 MW	10 MW	5 MW	20 MW
Total Number of Stacks	2	40	1	10
Power Electronics	Stack Level			
Gas Water Separator	Array Level			
Gas Cooling	Array Level			
KOH Circulation Loop	Array Level			
Input Water Purification	Central			
Gas Purification	Central			
Compression Unit	Central			

For the 5 MW system, the stack design results in two stacks (4) (one array) with a nominal output of 2.5 MW each. The schematic system layout is depicted in Figure 3-4.

The stacks are connected in parallel on the fluidic side, as it is mostly realized today in existing plants. Both stacks are connected to the central circulation circuit of KOH and the gas/liquid (KOH) separators on the hydrogen and oxygen side (7, 8). KOH separated from the product gases in the separators is fed back into the KOH circulation circuit via a pump (6) and cooled before entering the stacks by a heat exchanger (5). Thereby the KOH is mixed again to prevent the build-up of a concentration gradient between the half-cells of the stacks. The educt water for the reaction and for the gas scrubber (11) on the hydrogen side is supplied via a water purification plant (1). The stacks both operate at almost the same atmospheric pressure. Furthermore, the system incorporates a deoxygenation reactor (14) and a water condenser (15) to separate the liquid water.
A compression unit (13) including a H_2 buffer (12) is needed to compress the hydrogen to 30 bar and thereby increase the efficiency of downstream purification processes and enable a comparability with the PEMEL systems. For the year 2020, four compressors with 650 kW each are assumed for the 100 MW system and one single compressor with 130 kW for the 5 MW system (in 2030: 5MW 1x 140 kW, 100 MW: 4x 700 kW). All are assumed to be four-stage compressor systems, elevating the pressure from 1 to 30 bar. Although it is possible to use only one compressor for a 100 MW system, four compressors are considered here to take limited part-load performance of such a mechanical compressor into account.
Electrically, each cell stack has a rectifier unit (3) and a medium-voltage transformer (2). For the dissipation of the waste heat from the stacks and the gas purification system, a central cooling water supply (18) based on dry coolers and compression refrigeration (17) is also required.
The number of downstream components, such as gas scrubber, compressor and buffer tank, deoxidizer, and dryer show the rather high effort for the purification and compression of hydrogen to 30 bar.
The produced oxygen is cooled down to condense the water in the gas stream and is subsequently vented. Further gas purification is not required here.

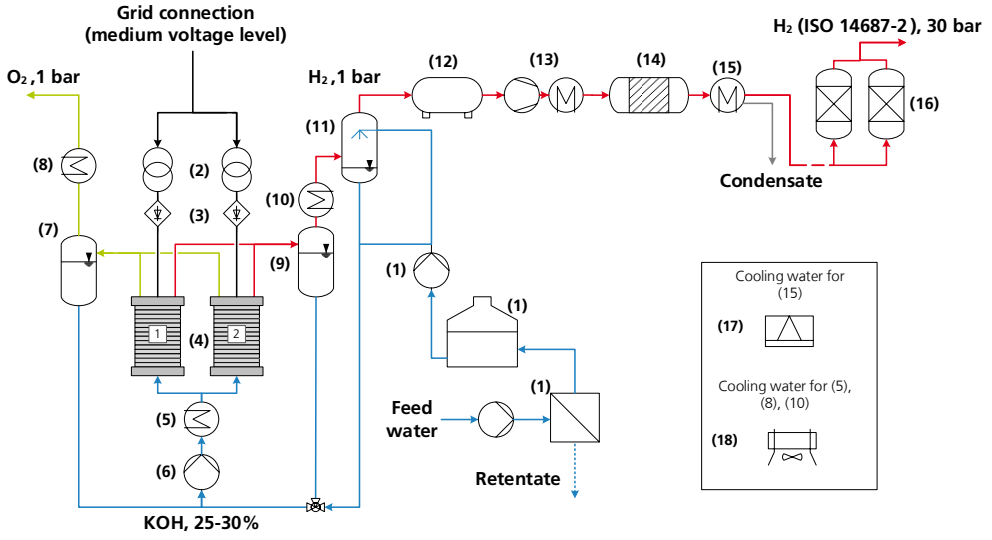

Figure 3-4: Schematic system layout for the state-of-the-art (2020) 5 MW alkaline electrolysis plant

A large-scale 100 MW system (2020), as depicted in Figure 3-5, differs from the 5 MW system mainly in the number of stacks and their arrangement. Four 2.5 MW stacks are combined to an array using one circulation circuit of KOH, common gas/liquid (KOH) separators at the hydrogen and oxygen side (7, 8), and a gas scrubber (11). The educt water for the reaction and for the gas scrubber (11) of the 10 arrays is supplied via a centralized water purification plant (1). In the same way, downstream hydrogen purification facilities are centralized and fed by all arrays.

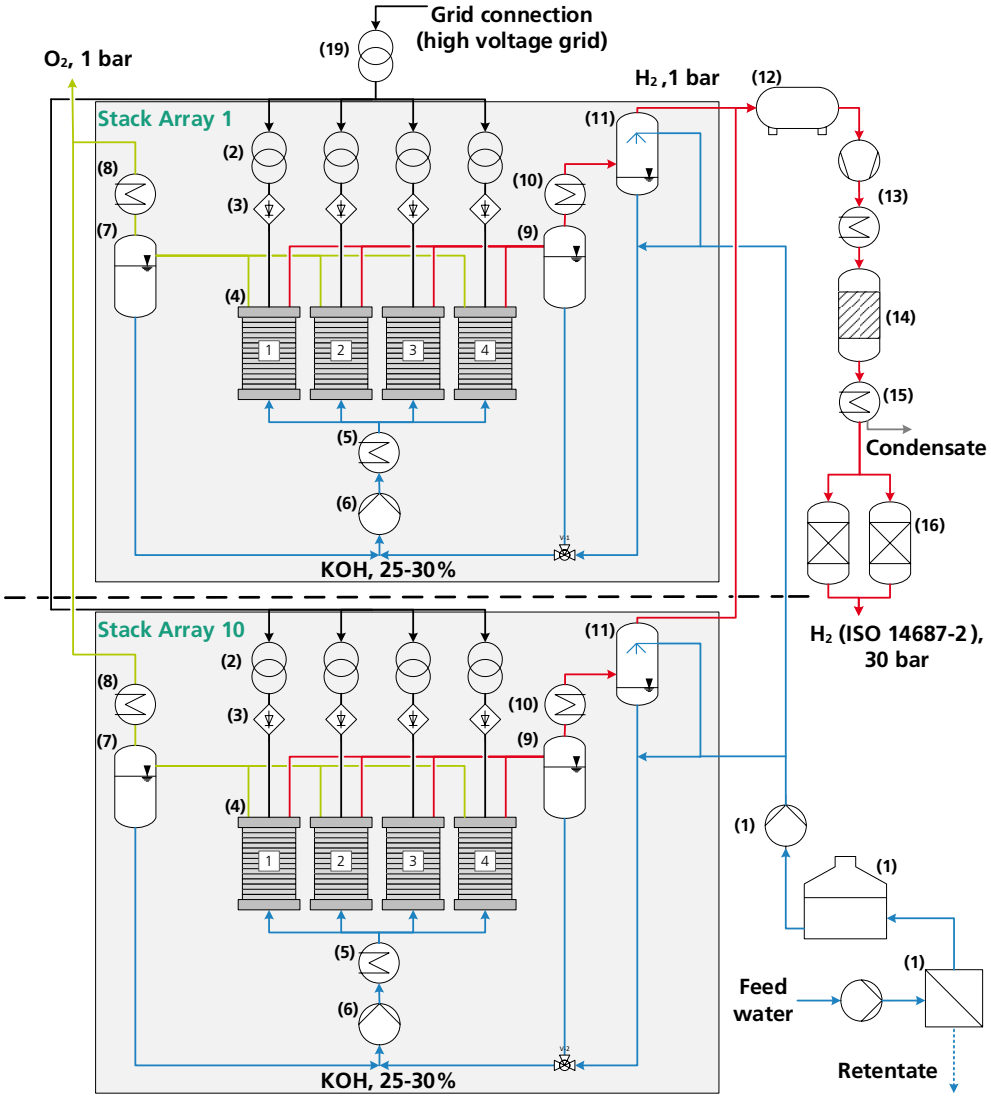

Figure 3-5. Schematic system layout for the state-of-the-art (2020) 100MW alkaline electrolysis plant

Electrically, each cell stack has its own rectifier (3) and an integrated, medium-voltage transformer (2). To meet the power requirements of the plant, a connection to a high-voltage grid and therefore the installation of an additional high to medium-voltage transformer (19) is required. For the dissipation of the waste heat, each array is connected to a cooling water supply (18) based on dry coolers in addition to the whole plant sharing a compression refrigeration (17) as part of the gas purification.

Table 3-4: List of components for 5MW and 100 MW AEL 2020 System

No.	Component description	No.	Component description
1	Water purification plant including feed pump and reservoir	**11**	Hydrogen scrubber
2	Medium-voltage transformer	**12**	Hydrogen buffer
3	Rectifier	**13**	2-stage compressor with intermediate cooling

4	Electrolysis stacks	**14**	Deoxidizer
5	Heat exchanger for KOH cooling	**15**	Condensing heat exchanger and separator
6	KOH recirculating pump	**16**	Gas dryer
7	Anode: gas/water separator	**17**	Compression chiller
8	Anode: heat exchanger for O_2 cooling	**18**	Dry cooler
9	Cathode: Gas/water separator	**19**	High-voltage-transformer
10	Cathode: heat exchanger for H_2 cooling		

As part of the system design, a stationary simulation of energy and mass flows of all system components is executed using the model H_2ProSim developed at Fraunhofer ISE [Ref]. The main results of the stationary simulation are shown in Table 3-5. The stack efficiency is calculated based on the stack specifications, the IV-characteristic, and the Faraday efficiency. On the system side, the various main components were analyzed and the electrical consumption of the components at rated load is determined. Electrical efficiencies of 96% in 2020 and 98% in 2030 are assumed for the rectifiers. Almost all energy is consumed by the electrolysis stacks. Also, the plant's final hydrogen production rate and the specific energy consumption are given for purified hydrogen at a pressure of 30 bar. It should be noted that the specific energy consumption for 100 MW plants is higher compared to the 5 MW plants, due to the additional high voltage transformer required, which causes an additional efficiency loss in the scenarios.

Table 3-5: Results of stationary simulation of energy and mass flows at rated load (BoL: Begin of life)

	Unit	2020		2030	
Case		5 MW	100 MW	5 MW	100 MW
Total power consumption system	MW_{AC}	5.5	110.4	5.5	110.1
Stack power consumption	MW_{DC}	5.0	100.2	5.1	102.0
Power losses rectifier and transformers	MW	0.3	6.4	0.2	4.3
Power consumption circulation pump	kW	5	98	4	72
Power consumption process cooling	kW	45	892	39	772
Power consumption gas purification	kW	10	207	11	223
Power consumption compression	kW	130	2602	140	2804
Number of compressors		1	2	1	2
Water demand	kg/h	958	19152	1032	20638
Hydrogen production rate system	kg/h	103	2069	111	2229
Specific Energy Demand System	kWh_{AC}/kg	52.8	53.4	48.9	49.4

3.2.4 System Cost Results

For an overview of the total costs at the system level, a system cost model for components and peripherals is developed, which includes the results of the respective stack cost model (see chapter 3.2.2), according to the set scenarios. The system layouts and the simulation results are considered in the system model.
The resulting specific system costs are illustrated in Figure 3-6. The largest cost share here is not the stack, but the combined balance-of-plant components. However, the three main cost drivers on AEL system level are the stacks, the power electronics, and the compression unit. The results show a strong decrease in the total specific system costs with increasing system size, adding a cost reduction towards 2030 of around 25-30% compared to 2020.

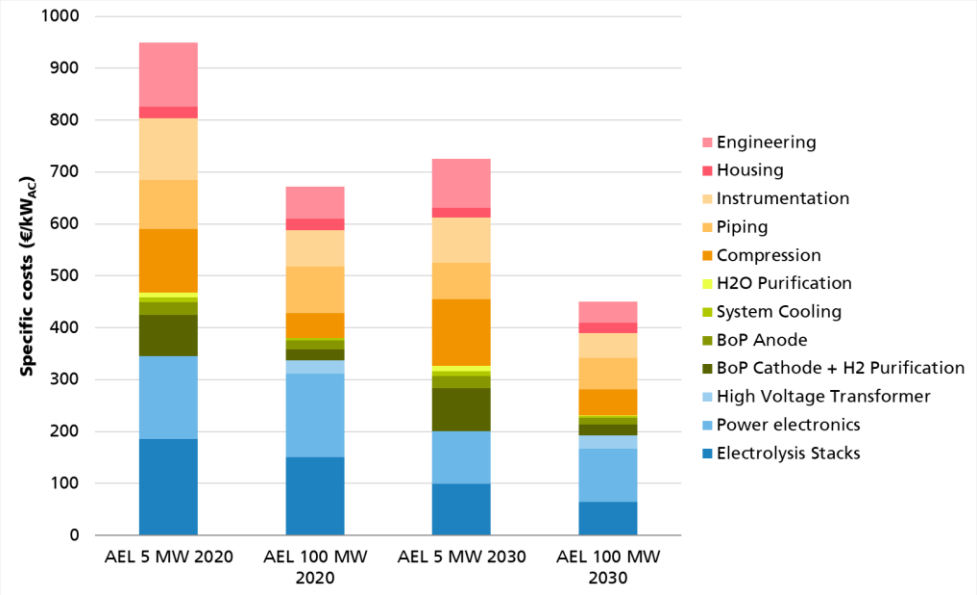

Figure 3-6: Specific costs of 5 MW and 100 MW next generation AEL systems (including mechanical compressors) for the design scenarios 2020 and 2030

The reason for the cost-reductions is the equipment savings by scaling-up and numbering-up of the required balance-of-plant components, such as compression unit, instrumentation, and minimizing the overall engineering effort per installed capacity. The cost shares, shown in Figure 3-7, support this trend. It needs to be mentioned that the specific costs of power electronics and piping are almost constant with increasing system capacity but decrease towards the year 2030 and the required high-voltage transformer is added to the total costs in the 100 MW plants.

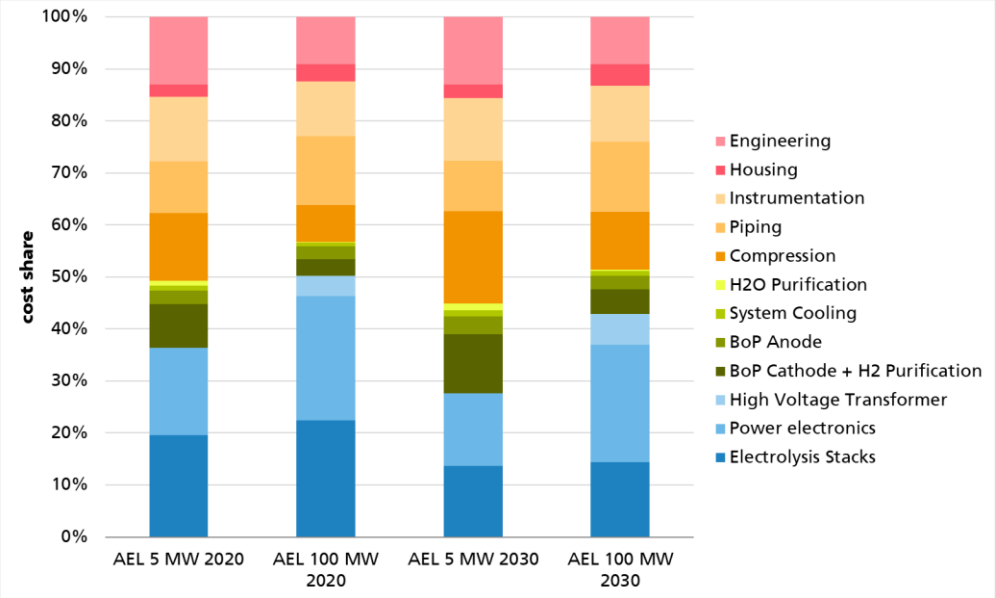

Figure 3-7: Cost breakdowns of 5 MW and 100 MW next generation AEL systems (including mechanical compressors) for the design scenarios 2020 and 2030

3.3 PEM Electrolysis Cost Model

3.3.1 Cell and Stack Specifications

The methodology used for the cost analysis of PEM water electrolysis systems is the same as that used for the AEL systems. Table 3-6 shows the selected main cell and stack components and the respective materials, which are considered for the PEM electrolysis stack cost model in this study. As for the alkaline electrolysis stack, the specifications for 2030 are subject to the assumption of some technological progress.

Table 3-6: Main cell specifications for 2020 and 2030 PEM electrolysis stacks

	PEM Electrolysis	
	2020	**2030**
Electrolyte	solid polymer electrolyte	solid polymer electrolyte
Membrane	PFSA based membrane	Hydrocarbon based membrane
Cathode side Catalyst loading	1.0 mg/cm²	0.4 mg/cm²
Catalyst material	Platinum	Platinum
Anode side Catalyst loading	2.0 mg/cm²	0.8 mg/cm²
Catalyst material	Iridium oxide	Iridium oxide
Bipolar plates	Structured titanium plates Grade 2 Thickness: 1mm	Structured titanium plates Grade 2 Thickness: 1mm

Bipolar plate coating (anode side)	1 µm Ta	1 µm Ta
Porous transport layer	Carbon fiber (cathode) Titanium fiber (anode)	Carbon fiber (cathode) Titanium fiber (anode)
End plates (Pressure plates)	Stainless steel 1.4301 / AISI 304	Stainless steel 1.4301 / AISI 304

Fundamental new stack concepts are not expected until 2030. The largest challenge will be to increase the current density and reduce the cell voltage in combination with a considerable reduction of the PGM loading in the catalyst layer. For the state-of-the-art electrolysis stack in 2020, a standard PFSA-based membrane with typical catalyst loadings of 1 mg/cm² on the cathode side and 2 mg/cm² on the anode side is considered. For the further PEM electrolysis stack in 2030, a hydrocarbon-based membrane with reduced catalyst loadings of 0.4 mg/cm² platinum on the cathode side and 0.8 mg/cm² iridium on the anode side is assumed. Hydrocarbon-based membranes are currently under development at the lab scale and promise higher current densities and a lower gas-crossover compared to PFSA membranes. However, long-term stability of hydro-carbon based membranes still needs to be improved. [39]
The specific stack parameters for 2020 and 2030 are listed in Table 3-7, respectively. For 2020, the chosen cell stack has a DC input power of 1 MW. As shown in Chapter 2.2.4, PEM electrolysis stacks are currently scaled up to higher hydrogen production capacities. Due to this upscaling, we assume a feasible PEM electrolysis stack in 2030 with a DC input power of 5 MW. The upscaling is based on larger cell areas and increased number of electrolysis cells. Also, it is expected that the rated current density will increase from 2 A/cm² in 2020 to 3 A/cm² in 2030. At the same time, cell voltage at rated load decreases from 1.9 V in 2020 to 1.7 V in 2030 due to thinner membranes and more active electrocatalysts, resulting in a higher efficiency of the electrolysis stack.
The hydrogen operating pressure is assumed to be 30 bars in both the 2020 and 2030 cost scenarios. From a technical point of view, higher operation pressures were already realized numerous times, but BoP costs for higher pressures increase disproportionately. Also, it is expected that membranes will be thinner in order to reduce the internal cell resistance. In combination with a differential pressure between the anode and cathode sides, gas crossover will be increased. Another point is the use of standard components for balance-of-plants components, like flanges. These are available for specific pressure classes [73] and a higher-pressure class leads to a high cost increase for balance-of-plant components.
The defined representative electrolysis stacks have a hydrogen production rate of 19.5 kg/h and 109.5 kg/h in 2020 and 2030, respectively. The specific energy demand on the stack level equals 51 kWh/kg in 2020 and 45.7 kWh/kg in 2030.
The data from Table 3-6 and Table 3-7 are used as framework conditions for the stack cost model. The specifications represent a general design, rather than a specific commercially available setup. The parameter projections towards 2030 of Table 3-7 are oriented by recent research activities and development trends in next generation PEM electrolysis components, as mentioned in Chapter 2.2, expert knowledge, and target developments.

Table 3-7: PEM electrolysis stack specifications at rated load

	2020	**2030**
Rated stack input power (DC)	1.01 MW	5.05 MW
Cell area	1,000 cm²	3,000 cm²
Number of cells per stack	265	330

Current density	2 A/cm²	3 A/cm²
Cell voltage (BoL)	1.9 V	1.7 V
Stack current	2,000 A	9,000 A
Stack voltage (BoL)	503 V	560 V
Faradaic efficiency	99 %	99 %
Pressure cathode	30 bars	30 bars
Pressure anode	1 bar	1 bar
Temperature	60°C	70°C
Voltage efficiency (BoL)	78 %	87 %
H_2 production rate (stack)	19.7 kg/h	110.6 kg/h
	219.5 Nm³/h	1230 Nm³/h
Specific energy consumption	51.0 kWh/kg	45.7 kWh/kg
	4.58 kWh/Nm³	4.1 kWh/Nm³

3.3.2 Stack Cost Breakdown

The stack cost breakdown takes into account the data in Table 3-6 and Table 3-7, which specify the materials and dimensions as well as performance data. The 1 MW PEM electrolysis stack in 2020 for example, has an active cell area of 1,000 cm². Based on the methodology explained in Chapter 3.1, the stack costs and the cost breakdowns have been determined for both years. In Figure 3-8 on the left, the stack cost breakdown for the 1 MW stack in 2020 and on the right side the stack cost breakdown for the 5 MW electrolysis stack in 2030 is depicted.

For the membrane electrode assembly, current cost projections (2020) for different quantities from several manufacturers are available, which cover the considered range. Based on this data and the fact that these are sensitive manufacture data, specific cost functions have been derived. For 2030, we expected hydrocarbon-based membranes. However, future cost data for hydrocarbon-based membranes in 2030 are not available. Therefore, cost assumptions based on state-of-the-art MEAs, taking the reduction of catalyst and improved membrane production into account, have been derived.
To reflect the costs of bipolar plates, price offers for titanium grade 2 sheets are available. In addition, we assumed costs for structuring the flow fields. For anode and cathode PTL, target price offers for different quantities from different manufacturers are available. For the end plates, price offers for the stainless-steel base plates are used and additional manufacturing costs are added in consultation with inhouse manufacturing experts.
In addition to the displayed main components, there are other relevant stack components, such as threaded rods, frame parts, and fittings. Most of them are assumed to be made from stainless steel and are summarized as balance-of-stack (BoS) components. Cell and stack assembly costs are considered, based on common labor costs in the metal and electrical industries in Germany and on own empirical values.

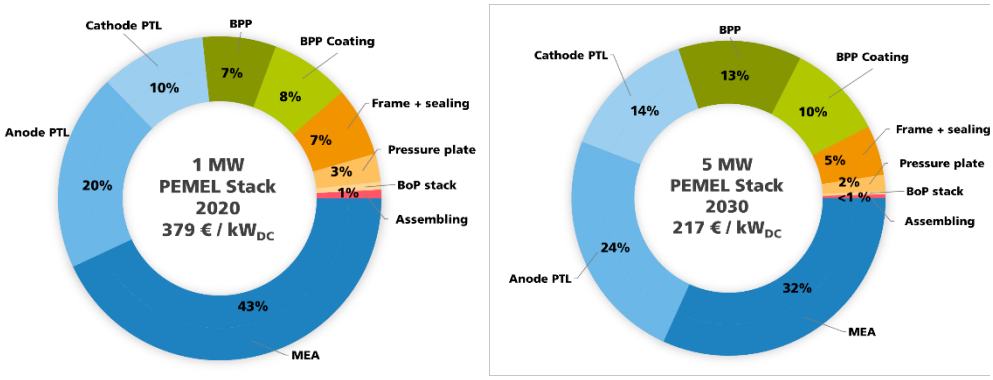

Figure 3-8: Cost breakdowns of state of the art 1 MW electrolysis stack (2020) and future 5 MW electrolysis stack (2030)

In the 2020 scenario (1 MW stack), the membrane electrode assembly (MEA) accounts for 43% of the total stack costs, followed by the single side coated bipolar plate and anode PTL. In 2030, the share of the MEA on the total stack costs is reduced to 32%, considering further development and associated cost reduction. For both scenarios, cost share for the porous transport layers on the anode and cathode sides increases because no further technology and cost improvement is expected.
The cost share for the bipolar plates increases from 8% in 2020 to 13% in 2030, due to additional manufacturing costs, which arise from the hydroforming process in order to integrate flow channels into the bipolar plate.

3.3.3 System Layout and Dimensioning of Balance of Plant Components

Based on the specifications of the stack design and parameters, system layouts for a 5 MW and 100 MW electrolysis plant have been derived. The rated stack capacity in 2020 and 2030 influences the system layout; and therefore, it was necessary to develop different system layouts for both base years and both target capacities.
The larger system with an electrolysis power of 100 MW is divided in several stack arrays. In 2020, ten stacks with a capacity of 1 MW each are arranged in one 10 MW array. In 2030, four stacks with a capacity of 5 MW each are interconnected to 20 MW arrays.
The system development includes the arrangement and the dimensions of the system components. Table 3-8 gives an overview of the number of stack arrays, the rated stack capacity of each array, and the total number of stacks.

Table 3-8: System arrangement

	2020		2030	
Plant Electrolysis Capacity	5 MW	100 MW	5 MW	100 MW
Single Stack Capacity	1 MW		5 MW	
Arrays	1	10	1	5
Array Capacity	5 MW	10 MW	5 MW	20 MW
Total Number of Stacks	5	100	1	20
Power Electronics	Stack level			
Gas Water Separator	Array level			
Gas Cooling	Array level			

Water Circulation Loop	Array level
Input Water Purification	Central
Gas Purification	Central

According to the stack design in 2020, the 5 MW system consists of five 1 MW cell stacks, producing hydrogen at a pressure of 30 bar and oxygen close to ambient pressure. An additional compression unit is not necessary to meet the requirements of the ISO 14687-2 (H_2-pressure of 30 bar). The electrolysis stacks are connected in parallel, as depicted in Figure 3-9. All five stacks are supplied with water by one single-anode water circulation system, including circulation pump (7), heat exchanger for heat management (8), ion exchanger to keep water quality at a high level (9), and the anode gas water separator (5). On the cathode side (= hydrogen side), all stacks are connected to one gas water separator (10), where hydrogen is separated from water, which is transferred from the anode to the cathode side (electroosmotic drag). In order to purify the hydrogen, a gas purification system consisting of a deoxygenation reactor, a condenser, and a temperature switch adsorption (12,13,14) is applied. Cooling of anode water circulation is done by a dry cooler. To reduce the dew point of hydrogen down to -70 °C, a cooling machine is expected. Table 3-9 lists all numbered components from the schematic layout.

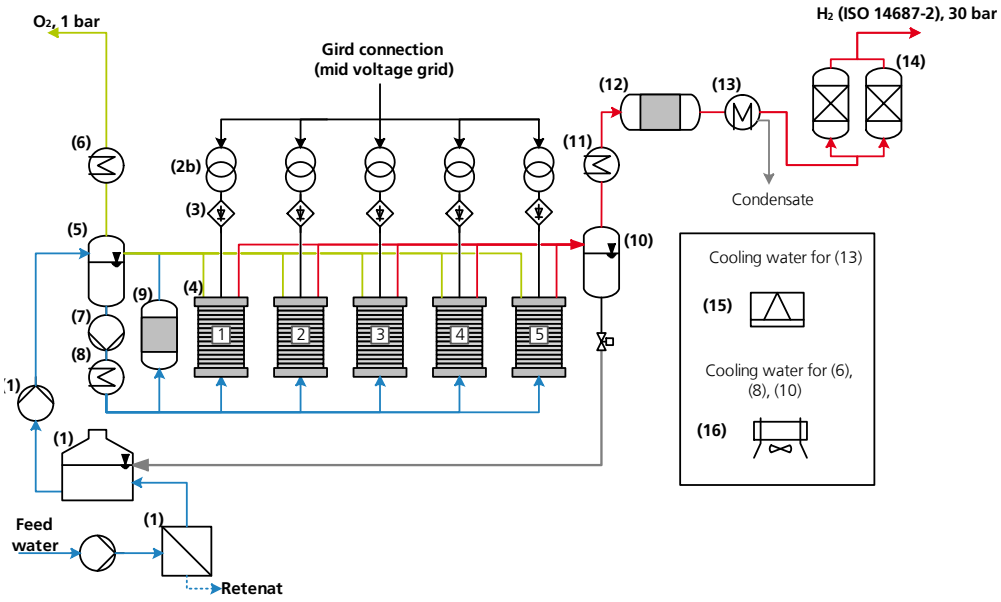

Figure 3-9: Schematic layout of the 5 MW PEM electrolysis plant for 2020 with five 1 MW stacks

The large-scale 100 MW PEM electrolysis system, based on 1 MW (2020) stacks, is depicted in Figure 3-10. The system consists of 10 stack arrays. Each stack array consists of 10 PEM electrolysis stacks connected in parallel with the system BoP. The plant has a central water purification unit (1), which supplies all stack arrays. Also, all arrays are connected to one gas purification subsystem, one gas chiller (13), and one cooling water generation unit (15,16).

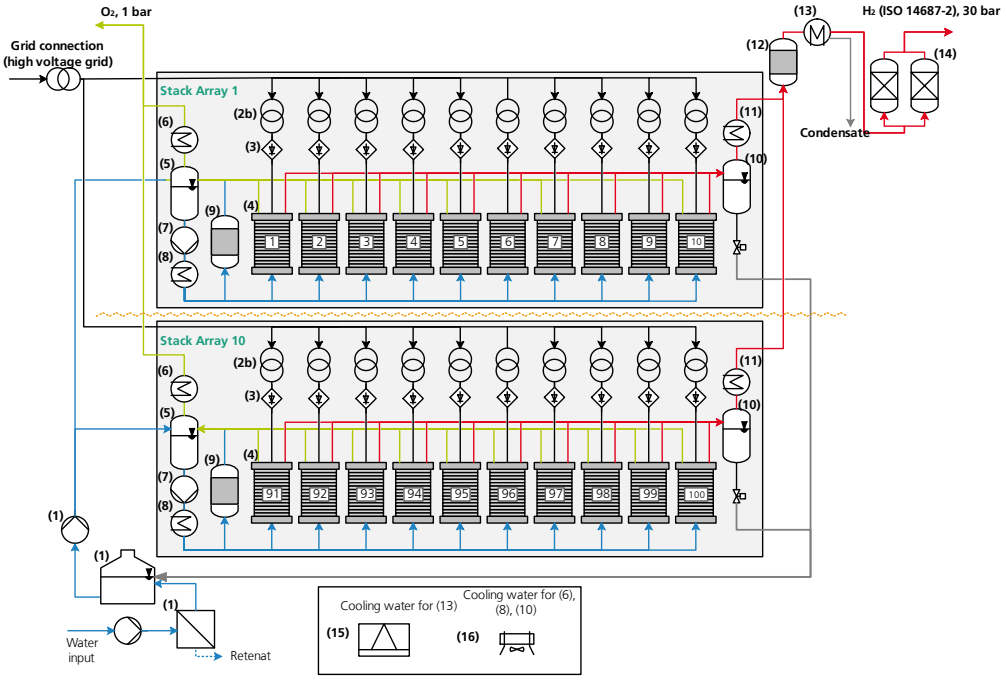

Figure 3-10: Schematic layout of the 100 MW PEM electrolysis plant for 2020

Due to the high power demand of the plant, an electrical connection to the high-voltage grid is required. This results in an additional high-voltage transformer (2a), which supplies the low-voltage transformer (2b) and the rectifier (3). Each electrolysis stack is connected to an individual rectifier.

Table 3-9: Component list for the 5 MW PEM electrolysis system (2020 layout)

No.	Component description	No.	Component description
1	Water purification plant including feed pump and reservoir	**9**	Ion exchanger
2	Transformer	**10**	Cathode: Gas water separator
3	Rectifier	**11**	Cathode: Heat exchanger for H_2 cooling
4	PEM electrolysis stack	**12**	Deoxidizer
5	Anode: Gas water separator	**13**	Condensing heat exchanger
6	Anode: Heat exchanger for O_2 cooling	**14**	Dryer
7	Water circulation pump	**15**	Compression chiller
8	Heat exchanger	**16**	Dry cooler

As part of the system dimensioning, a stationary simulation of energy and mass flows of all systems was executed. The results for the PEM electrolysis systems are shown in Table 3-10. The results are based on the stack specifications, such as the Faraday efficiency and resulting Vi characteristics. On the system side, the various main components were analyzed and the electrical consumption of the components at full load was determined. Electrical efficiencies of 96% in 2020 and 98% in 2030 are assumed for the rectifiers.

Almost all energy is consumed by the electrolysis stacks. Also, the plant's final hydrogen production rate and the specific energy consumption are given for purified hydrogen at a pressure of 30 bars. It should be noted that the specific energy consumption for both 100 MW plants is higher in comparison to the 5 MW plants, due to the additional requirement of a high-voltage transformer with an assumed efficiency of 99% in both scenarios.

Table 3-10: Resulting energy and mass flows of the systems at rated load (BoL)

	Unit	2020		2030	
Case		5 MW	100 MW	5 MW	100 MW
Total power consumption system	MW_{AC}	5.4	108.5	5.3	106.1
Stack power consumption	MW_{DC}	5.0	100.7	5.0	101.0
Power losses rectifier and transformers	MW	0.3	6.4	0.2	4.2
Power consumption circulation pump	kW	7	134	4	79
Power consumption process cooling	kW	56	1118	34	685
Power consumption gas purification	kW	10	197	11	221
Power consumption compression	kW	0	0	0	0
Deionized water demand	kg/h	896	17930	1005	20095
Hydrogen production rate system	kg/h	98	1969	110	2207
Specific energy demand system	kWh_{AC}/kg	54.5	55.1	47.6	48.1

3.3.4 System Cost Results

To determine the system costs, a cost model for the system components and peripherals was used as already explained in the AEL section. The stack costs for the set scenarios, the system layouts, and the simulation results of Chapter 3.3.3 were considered in the system model.

As it can be seen in Figure 3-11 and Figure 3-12, the stack is the dominant component for a PEM electrolysis system but has a share of less than 40%. The larger the system, the smaller the specific costs for peripheral components (gas purification and BoP) become. This can be explained by optimized and centralized balance-of-plant (BoP) components (gas and water treatment, cooling, etc.) and is a general trend for all larger electrolysis systems. The power supply is the second major cost contributor with around 20% of the total costs. For the 100 MW electrolysis plant, cost share of power supply increases because costs do not decrease by the same magnitude as for the electrolysis stack and other components.

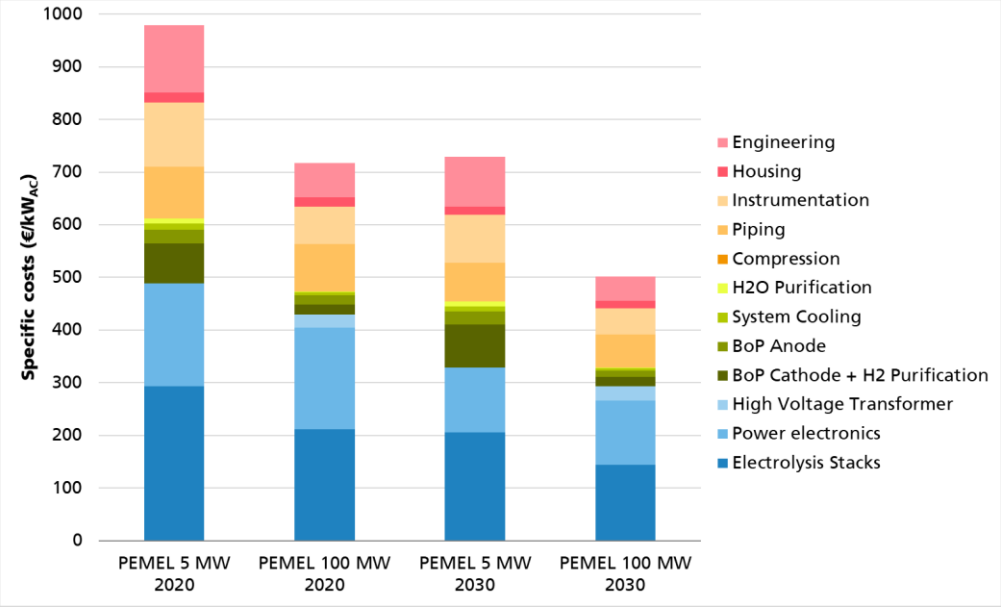

Figure 3-11: Total PEM electrolysis system cost for all analyzed scenarios. Mechanical compressors are not required.

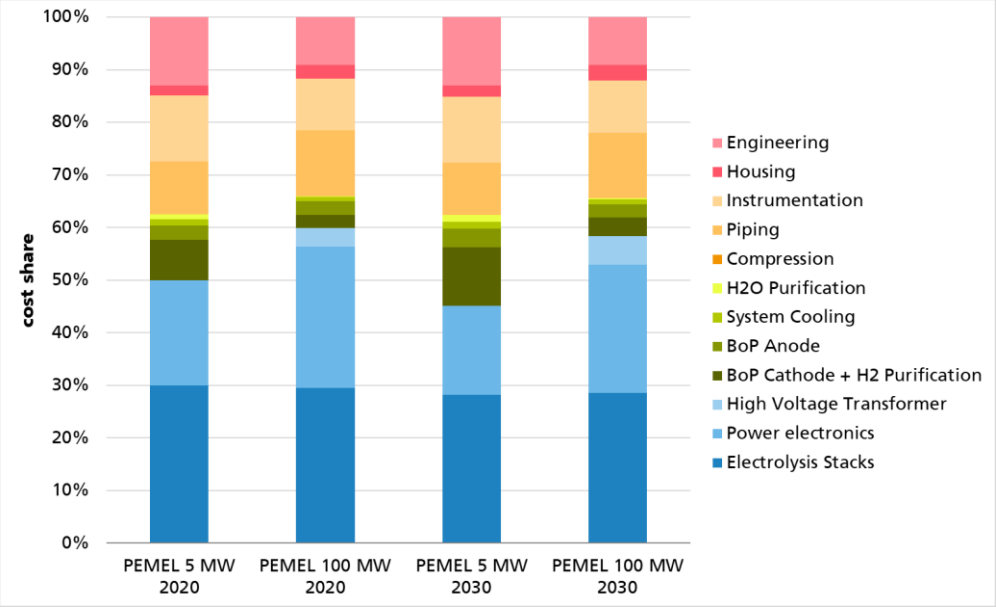

Figure 3-12: Cost breakdowns of 5 MW and 100 MW PEMEL systems for the design scenarios 2020 and 2030. Mechanical compressors are not required.

3.4 Maintenance Costs

The operating costs of electrolysis plants are generally dominated by the electricity purchase costs, which are also referred to as variable operating costs. In addition, there are ongoing costs for maintenance and replacement, which are often summarized as fixed operating costs. The data for annual maintenance costs gathered by a manufacturer survey in 2018 [8] have been updated towards 2020 and amount to:

- 20 ±5 €/kW_{AC}*a for AEL systems
- 15 ± 5 €/kW_{AC}*a for PEM systems

Regular replacements of the stacks and other BoP components are not included as the replacement intervals are highly dependent on the operational management, the application, and practically no reliable data exist to date. Although, AEL technology is more mature, the maintenance requirements due to the caustic electrolyte are higher and therefore the costs are as well. For the near future, it can be expected that the specific maintenance costs for both technologies will decrease. However, it is likely that PEM systems will keep a cost benefit in maintenance compared to AEL.
Regular maintenance of the plant components is essential to avoid unplanned idle time and unexpected failure of hydrogen production plants.
For PEM water electrolysis, low water conductivity is very important for a long lifetime of the electrolysis stacks. Impurities in the water can lead to a faster degradation of the electrolysis cells. Next to the upstream water purification, an additional ion exchanger is installed within the water loop of an electrolysis system to absorb dissolved ions from pipes etc. as described in chapter 2.4.2. The ion exchanger is filled with resin beads, which need to be replaced regularly, otherwise the absorption capacity will decrease. In relation to the specific system, maintenance of the ion exchanger is required several times a year.
For both electrolysis technologies, regular maintenance of safety-relevant parts is mandatory. Hydrogen production plants need to be equipped with a gas warning system, which is connected to the general safety system of the plant. In the case of a certain amount of hydrogen (and oxygen) the plants need to be shut down to prevent the generation of an explosive atmosphere. Gas warning equipment needs regular maintenance, which includes a visual inspection for mechanical damage, a functionality test, and the calibration of sensors. In relation to the application, maintenance intervals of 4-12 month are required. Also, safety valves need a regular visual inspection and functionality test.
In case a compressor is part of the system, as it is the case for most alkaline electrolysis systems and some PEM electrolysis systems with a higher final pressure, additional maintenance is required. The main part of compressor maintenance is the regular exchange of piston rings. Typically, the maintenance interval for piston rings is one year.
A larger maintenance issue is the replacement of electrolysis stacks. Degradation of electrolysis cells results in higher cell voltages which lead to a decreased efficiency. At some point, it is more economical to replace a degraded electrolysis stack with a low efficiency with a new stack with a high efficiency. The lifetime of a stack depends on the selected electrolysis technology and the manufacturer. Typically, after 10 years, a replacement of the stack is necessary. Alkaline electrolysis stacks normally have a higher lifetime of around 60,000 to 80,000 hours. The lifetime of PEM-electrolysis stacks is around 40,000-70,000 hours. The replacement of electrolysis stacks could result in a longer downtime compared to standard maintenance procedures.

4
Cost-Reduction Potential

Based on own cost model data from the previous chapter, cost-reduction potentials are investigated and evaluated in more detail in this chapter considering four different aspects for cost reduction:

- by scaling-up (sizing-up) of components
- by technological advancements on stack level
- by increasing production volumes (numbering-up)
- by improvements in production technologies (e.g. automatization)

In this discussion sizing-up and numbering-up should be explicitly distinguished from one another. Sometimes both aspects are used under the general term of scaling-up. Sizing-up stands for an increase in component dimensions, for example in cell area and number of stacked cells, or in energy and mass flows, such as the hydrogen volume flow of a compressor. Numbering-up in this context means the process of increasing production volume, which can lead to an economies-of-scale effect, for example by mass production of stack components. Both aspects can independently result in costs savings. A third approach to reduce costs is the technological advancement at the stack level from the year 2020 towards 2030, which is considered in this study only by improvements in the electrochemical performance of the stack, as explained earlier in Section 3.1. Moreover, a brief analysis of potential improvements of production technologies for stack and system components and their impact on costs is made.
The cost-reduction potential is focused on the main cost drivers of each analyzed electrolysis technology.

4.1 Sizing-Up and Technological Cost-Reduction Potential

4.1.1 Next Generation AEL Stacks

The impact of increasing the stack size from 2.5 MW to 10 MW on the total specific stack costs is depicted in Figure 4-1. It should be mentioned that currently, a 10 MW single stack in 2020 is not state-of-the-art and is only cost-wise calculated here to give a comparable impression of the influence by sizing-up. On the other side, a 2.5 MW single stack in 2030 is assumed to only be a short-stack design of the determined 10 MW standard size, which may be available as a next-generation design in the future.

The 10 MW stack 2020 is upscaled in terms of the electrode area (30,000 cm²) and the number of stacked cells (310) compared to the 2.5 MW stack, but no improved efficiency and current density is assumed. Both parameters have already been realized in AEL stacks, but such stacks have so far been operated with lower power densities, so that no 10 MW stack is currently available.

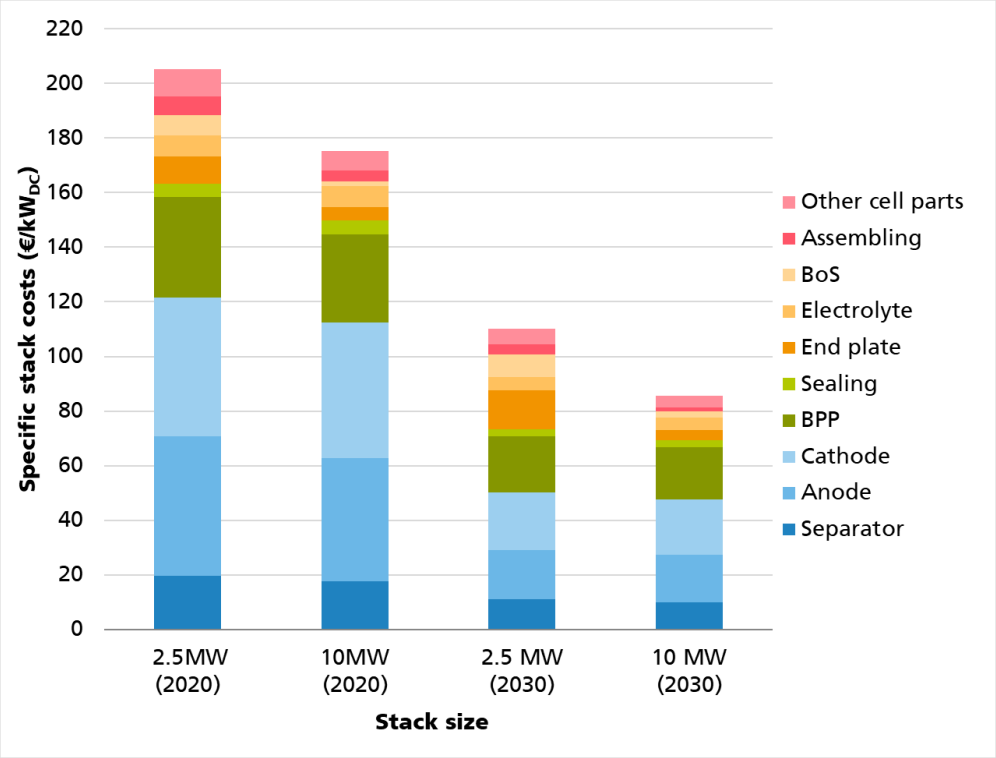

Figure 4-1: Comparison of specific next generation alkaline electrolysis stack costs for 2.5 MW and 10 MW stack sizes.

The specific costs of a single state-of-the-art 2.5 MW stack are calculated to 205 €/kW, compared to 175 €/kW for a 10 MW stack. This corresponds to a potential cost reduction of 15% by quadrupling the stack capacity. This is mainly caused by the fact that an increased number of cells leads to specific cost benefits in cell material and manufacturing costs of the cell components. Moreover, in the 10 MW stack, more cells share the same stack components, such as end plates and balance-of-stack components, which supports the reduction of the specific cost. Additionally, this also decreases the assembling effort per MW. Sizing-up the stack only shows a moderate potential for cost reduction, which can partially be explained by keeping a similar stack design. In general, the limitations of the cost model should be kept in mind, which will be discussed later in Section 4.3.2.

With a drop of 50% in specific stack costs from 2020 to 2030, the cost reduction by technological development is significantly higher than by only sizing-up the stack size. This cost leverage is, for example, based on the use of advanced, thinner diaphragms and more active electrodes, which improve the power density at assumed, similar costs. In case the operating point of the stack is shifted due to a higher available power density, other design parameters can be adapted accordingly, which can enable further cost reductions. Another factor is the assumed progress in more cost-efficient manufacturing processes (e.g. APS) of highly integrated diaphragm-electrode assemblies and associated catalyst coatings (cathode: NiAlMo and anode: NiAl). Although improved electrocatalytic performance reduces the cell overvoltage, the better kinetic of the electrodes allows larger current densities. However, single stack dimensions cannot increase much further in 2030 due to technical limits in manufacturing cell components and efficient component handling. Therefore, technological improvements seem to be crucial for further stack cost reduction.

4.1.2 Next Generation PEMEL Stacks

A similar consideration of the cost reduction potential for PEM electrolysis leads to somewhat different results, as can be seen in Figure 4-2.

Considering the cost-reduction potential through the sizing up of the cell area, significantly better values are achieved for 2020 (- 23%) as well as for 2030 (- 32%) than for the AEL stacks. Although, all components contribute to the cost reduction, the costs for bipolar plate coating, frames, and sealings show a significantly sharp decrease. These components are mostly manufactured in a highly automated manner. Due to the automated processes applied, by sizing-up the coating area for example or increasing the unit quantities, the specific costs per unit can be significantly lowered. [74]

However, the cost-reduction potential due to technological progress from 2020 to 2030 is lower compared to the AEL technology. The main reasons for this are the expensive cell components MEA and PTL of the anode. Despite technological progress, these remain comparatively expensive in manufacturing and the positive effects of a scale-up in the cell area are rather moderate. Furthermore, the power density for PEM electrolysis increases only from 3.8 W/cm² (2020) to 5.1 W/cm² (2030). This corresponds to an increase of 34%, while an increase in power density of 57% is assumed for alkaline electrolysis (from 1.08 W/cm2 to 1.7 W/cm²). At this point, it can be discussed whether the progress for PEM technology has been estimated as too conservative. However, the target values for PEM electrolysis in 2030 are considered ambitious enough by the authors, so there is no need to change the assumptions.

In summary, the actual PEM stack will remain the more expensive component compared to the AEL stack, although the cost level here will also decrease by approximately 43% overall by 2030 (comparing the 1 MW stack in 2020 with the 5 MW stack in 2030).

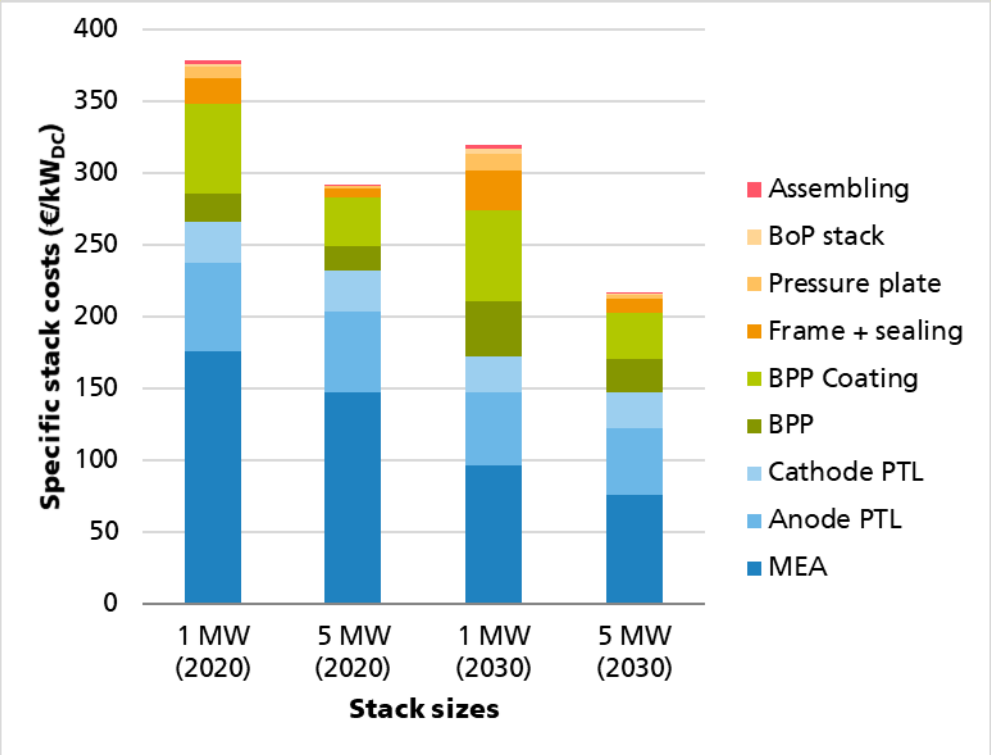

Figure 4-2: Comparison of specific stack costs for state-of-the-art and next generation PEM electrolysis technology with a rated power of 2.5 MW and 10 MW.

This cost disadvantage will be compensated at the system level by the fact that PEM electrolysis operates under pressure and at least no first compression stage is necessary.

4.1.3 Balance of Plant Components

Compression Unit (AEL only)

The compression unit contributes to about 15% of the 5 MW AEL system cost, as shown in Figure 3-7, but offers strong cost reductions by sizing-up to larger capacities. This is underlined by the fact that specific compression costs from a 5 MW to a 100 MW system is more than halved and the share on the overall costs is reduced to less than 10% (100 MW).
Therefore, a single compressor unit is more cost-effective than several smaller compressors according to previous studies. [75] This relationship is also shown in Figure 4-3. However, for the 100 MW systems, not a single large compressor, but two smaller compressors in parallel are assumed (see Chapter 3.2.3) to have a reasonable trade-off between part-load operation capability, providing a minimum of redundancy in case of malfunctions and low costs. Although one, single, large compressor would represent the economic optimum and is technically feasible, it is not a preferred scenario in terms of plant operation.

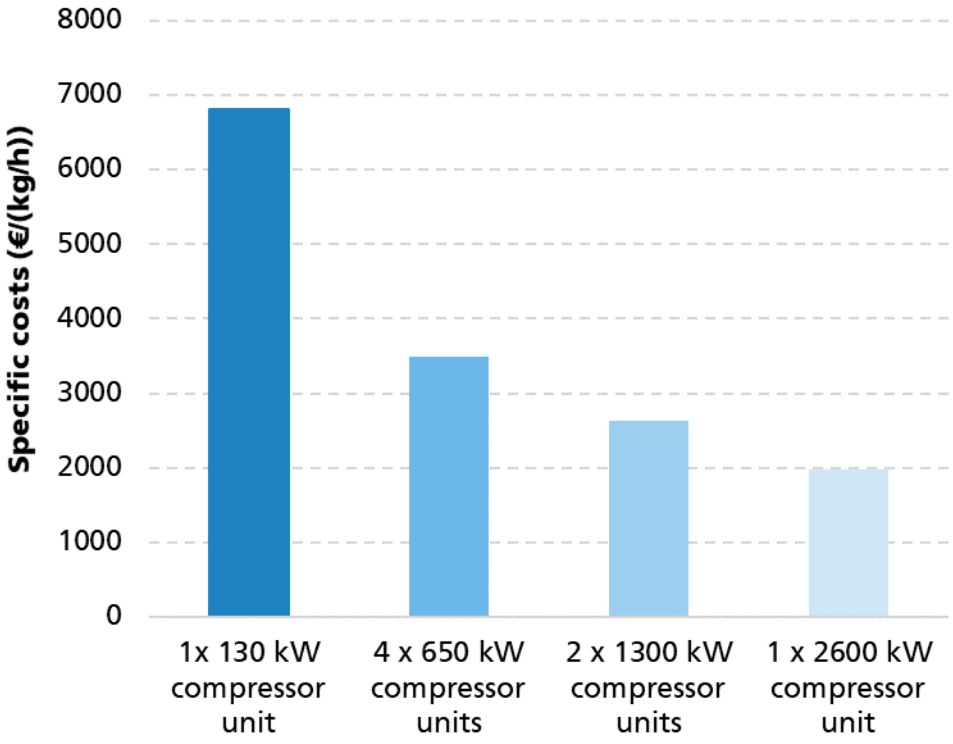

Figure 4-3: Comparison of specific costs per pressurized kg of hydrogen

A rough comparison of the total system costs between a pressurized AEL system without a compressor unit and the cost model results for the atmospheric systems shows a larger cost benefit for the atmospheric system with increasing scale:

- at 5 MW scale 4 % lower cost
- at 100 MW scale 13 % lower cost

Due to increased material demand and requirements for pressurized systems, around 20% [32,33] need to added to the overall costs from atmospheric systems without a compressor unit. If operational costs for the compressor unit are neglected, even for 5 MW systems, mechanical compression can reach a parity in investment costs with pressurized systems.

Table 4-1: Cost comparison of AEL systems with mechanical compression and pressurized AEL system

	Unit	2020	
Total system cost		5 MW	100 MW
Atmospheric system with compressor unit	k€	4.970	68.840
Pressurized system with added cost surcharge of 20 % [32,33]	k€	5.160	78.000
Cost benefit of atmospheric system	%	4	13

It is noteworthy, that additional costs for redundancies in the compression unit due to a required high availability (typically > 95 %) are not considered here. For example, two units with a 100% capacity rating or three units with a 50% capacity rating can be installed for this purpose, but this is also highly project-depending [76] and should not be elaborated here in more detail.

From a technological development point of view, it can be stated that compressors for process gases are already widely used in industry. However, many manufacturers are continuously developing or adapting their conventional (reciprocal and centrifugal) compressors for usage with hydrogen. Thereby, reciprocal compressors are currently the most mature and efficient solution in the targeted capacity class. It can be assumed that the cost reductions by improved performance and reliability of these hydrogen compressors of the MW-class will increase in the coming years and more systems will be built.
On the other hand, if pressurized systems can reach cost parity with atmospheric systems, they can represent the most cost-effective alkaline solution in terms of the investment cost. Other promising compression technologies, such as external electrochemical compressors, are on the verge to enter the hydrogen refueling station market with several small-scale pilot plants in operation. They are able to combine hydrogen purification and compression in one unit. [77] How far such an electrochemical compressor can offer cost advantages for large-scale electrolysis plants in the future still needs to be calculated in detail and discussed.

Power Electronics

The developed cost models show that the power electronics, which include state-of- the-art thyristor rectifiers and medium-voltage transformers, contribute a major part to the total cost of an electrolysis system, as shown in Figure 3-6 and Figure 3-11. With the parameter used in this cost model, cost reductions for power electronics are only marginal by sizing-up the systems from 5 to 100 MW independently of the electrolysis technology. The reduction of around 25% in specific cost of the power electronics towards 2030 are based on the improved energy efficiency of the stacks enabling the usage of less but higher-capacity power electronics in the whole systems setup. Looking at the cost shares in Figure 3-7 and Figure 3-12, the cost-reduction potential by sizing-up is limited compared to other system components.

From a technological perspective on the rectifiers, thyristor-based units provide established solutions for smaller stack sizes so far but utilizing classic, low-voltage inverters from the wind and solar industries could present a cost advantage in the future. They do not weaken the AC grid with reactive power. On the contrary, they can stabilize it by controlling their power factor. The downside of low-voltage inverters is that the minimum DC voltage is limited to the input AC- peak voltage, which makes additional DC-DC converters necessary.
Another approach is to lift the DC voltage of the rectifier to the upper limit of the low voltage directive (up to 1.5 kV) by connecting stacks in series, and thereby, enable the usage of more suitable components with higher-rated power and bring the cost down. A similar process was started in the utility-scale PV sector, which led to a successful cost decrease [78]. However, research on potential risks for the operation of the stacks (e.g. series resistances and leakage currents) still needs to be done.
Furthermore, for large-scale electrolysis systems with high currents (e.g. in AEL), no established solution yet exists. It remains to be seen which converter technology is the most suitable solution.
In general, the power inverter market is expected to grow by 5% per year in the future, pushed by rising installation numbers in renewables and electric vehicles with new suppliers entering the market [79]. According to expert estimations, considering the dynamic of the power inverter market and a future demand for tailored electrolysis solutions, further cost reductions of about 25% towards 2030 can be expected.

Gas Purification Unit

As depicted in Figure 3-7 and Figure 3-12, the costs for gas purification can have a high share of the total plant costs in the lower power range of electrolysis systems. In our cost analysis for the 5 MW plants, the gas purification unit contributes to up to 10% of the total plant costs. However, with increasing capacity, the share in the plant costs is significantly reduced. Sizing-up the components of the gas purification unit (such as deoxidizer, heat exchangers, and columns for temperature swing adsorption), respective to the system capacity, offers a huge cost advantage, which is shown in the specific hydrogen purification costs of Figure 4-4. One reason for this can be similar cost expenditures for designing and acceptance testing of the pressurized gas purification components, independent of their dimensions. Furthermore, these components are relatively easy to scale in size, resulting in the fact that many stack arrays can be connected to one gas purification unit (see Figure 3-5 and Figure 3-10), and substantially reduce the specific costs in relation to the installed stack capacity.

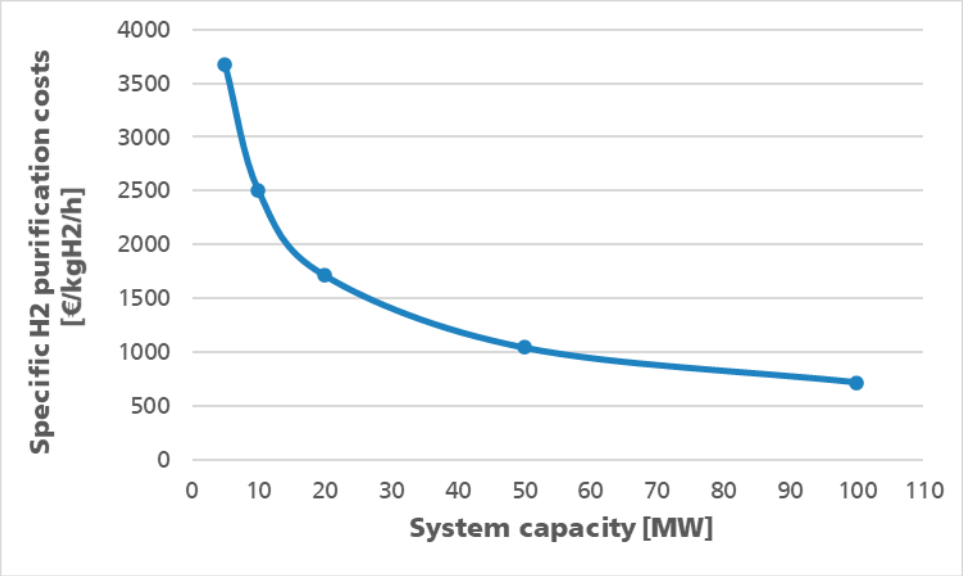

Figure 4-4: Specific costs for hydrogen purification depending on system capacity

Assembly and System Integration

Looking at system assembly costs (see Figure 3-7 and Figure 3-12: piping, instrumentation, enclosures), small-scale (e.g., 1 MW) modular containerized solutions that are fully pre-assembled at the manufacturer's facility can offer cost advantages to the customer over final assembly at the plant site. However, depending on the specific project requirements, there is also a threshold in system size, at which a cost advantage from containerized solutions no longer exists. An evaluation of already realized electrolysis projects makes it already clear that for power classes above 5 MW, pre-installed containers are no longer used. This is mainly due to the fact that central subsystems, such as gas purification or water treatment, have significantly lower specific costs than several small systems integrated in containers. Ultimately, the size of the stacks above a certain performance class is also no longer suitable for integration in a standard container. In terms of ease of maintenance, installations in adapted factory buildings also show clear advantages.

Some manufacturers assume that non-containerized systems have a cost advantage of about 4% compared to containerized solutions. This advantage must improve significantly as the size of the electrolysis plant increases. For future, large systems, there is also the option that the electrolysis blocks are assembled on site, as a transport of a whole electrolysis block from the actual manufacturer to the installation site would be too costly.

4.2 Numbering-Up and Production Technologies

The trend towards GW-scale production capacities is already shown in Figure 1-2. This is, for example, supported by the recent announcements of the companies NEL and ThyssenKrupp, which plan to timely increase their production of AEL systems to 1 GW/year [1,2] and ITM Power, who claimed to have completed their gigafactory for PEMEL systems [80]. These GW-scale manufacturing capacities require well-developed supply chains for many different stack components and system parts. The availability of reliable cost data for the required, large quantities of material or components at such a large scale is very limited and prone to high uncertainties. Consequently, the analysis of the cost impact by numbering-up is limited to a maximum stack production capacity of

100 MW (40 units) here. This represents a current, custom-made production rather than a future GW-scale production scenario.
However, to investigate the potential influence of modularization in the production (scaling by numbers), the specific stack costs dependent of the stack production capacity have been analyzed. The produced number of stacks are based on the respective stack designs of 2020, described in sections 3.2.1 and 3.3.1. Apart from this, the numbering-up approach analyzed here, is independent from the previously build system scenarios.
The scaling-up in production numbers is often connected to the implementation and development of production technologies. Cost-effective manufacturing processes can be essential to achieve cost reductions, and hence, a greater market penetration. Therefore, a qualitative approach is followed to evaluate potential production technologies (e.g. forming and coating) and their impact on cost.

4.2.1 Next Generation AEL Stacks

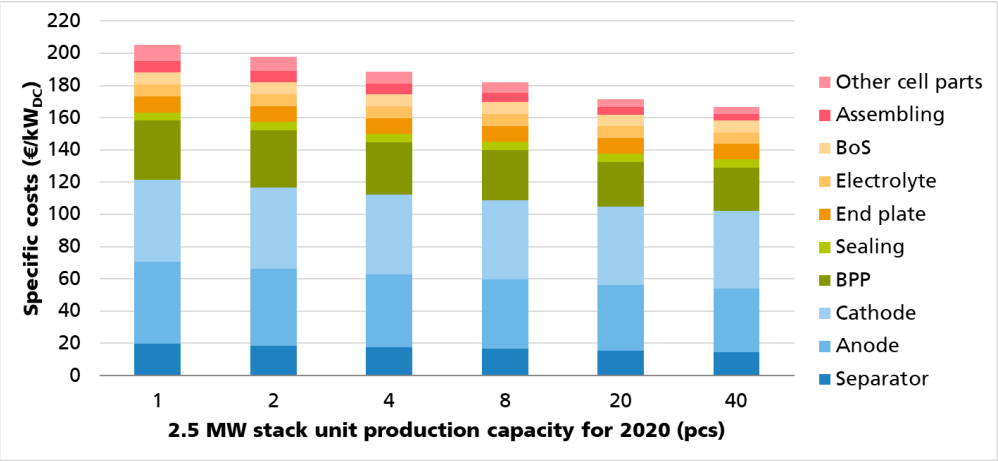

Figure 4-5: Specific alkaline electrolysis stack costs in relation to the total stack production capacity for the 2020 scenario

The results are shown in Figure 4-5 for the year 2020. As expected for a classic economies-of-scale-effect, cost reductions from a single stack production (2.5 MW) towards a production of 40x 2.5 MW stacks (100 MW) are shown for all main components with a logarithmically flattening trend. In total, the cost models show a maximum of about a 20% decrease in specific stack cost from a single unit production towards 40 units. These results do not consider a potential shift to more cost-efficient manufacturing processes by exceeding a certain production volume threshold of the respective stack components or base materials, but only the reduced material cost by increased purchasing quantities. The flattening trend can be explained by the fact that with an increasing amount of materials needed (e.g. electrode material), the cost data also shows marginal reductions for a further increase in purchasing quantities.

However, the implementation of new production technologies can lead to significant cost-reduction steps. Together with the efforts of the AEL manufacturers in building new and larger factories, manual production and assembly of stack components are also replaced by more automated manufacturing processes. [30] Typically, the processes for electrode production, such as pretreatment of the base materials, coating, and catalyst activation, are thus far mostly based on manual batch processes. In the future, a high degree of automation in production lines for even large-sized components, such as alkaline electrodes, will be essential to achieve the required production numbers in the GW-scale in addition to lowering the cost by reducing processing time and labor costs.

Furthermore, catalyst coating processes like vacuum plasma spraying (VPS) for NiAl or NiAlMo on electrode substrates are still typically performed as batch process. Further development of this plasma spraying technology is the atmospheric plasma spray (APS) deposition technique, which is estimated to reduce the cost by one third compared to VPS. Additionally, APS can be integrated as a continuous process within a fully automated assembly line. So far, this process is only used and proven at the lab-scale, but a scale-up to m² sized electrode substrates is part of current research activities. [29,81]

4.2.2 Next Generation PEMEL Stacks

The results for scaling up production capacity for PEM electrolysis stacks are shown in Figure 4-6. For all stack components, the specific costs decrease with higher production capacity. A strong decrease in stack costs can especially be observed at lower production capacities, such as for one to five units. The cost models show a maximum of nearly 40% lowering of specific stack costs by increasing the production from 1 (1 MW) to 100 stacks (100 MW). In particular, costs for the membrane electrode assembly decreases with higher production volume, due to lower specific costs for higher quantities. But specific costs for the porous transport layers do not decrease much due to de facto quantity independent costs, which can be explained by the production technology currently in use. Also, for bipolar plates, the specific costs do not decrease much with higher quantities, due to the chosen cell design and production processes assumed in this scenario. However, the bipolar plate coating shows a high cost-reduction potential, especially in the area of small quantities.
As already mentioned for the alkaline electrolysis, these results do not consider a potential shift to more cost-efficient manufacturing processes by exceeding a certain production volume threshold of the respective stack components or base materials, but only the reduced material cost by increased purchasing quantities.

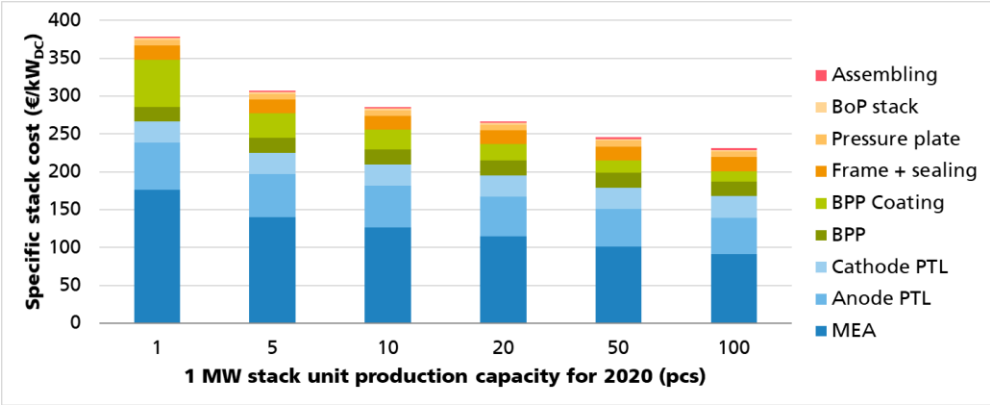

Figure 4-6: Specific electrolysis costs for 1 MW electrolysis stacks in 2020 in relation to the total manufactured stack capacity

Improved production technologies and automation of component production is required, not only to reduce production costs, but also to significantly increase production capacity. To achieve announced expansion targets for electrolysis installations, numbering up and scaling up requires additional production facilities for electrolyzers. Current production facilities are mostly built-up according to the workshop principle without any automation. To realize GW-scale electrolysis installation, larger facilities are required with at least a semi-automation production of stacks. For example, ITM Power is currently building a new production facility for PEM electrolysis. Their previous production facility had an annual production capacity of max. 100 MW without any automation. Also, testing of the produced stacks was only possible up to a power input of 0.5 MW. The new production facility in Sheffield/UK will have an annual

production capacity of more than 1 GW and will be run semi-automated. Also, a test bench with a 5 MW power supply will be installed. [80]

4.3 Discussion of the Results

Comparing the cost results for alkaline and PEM electrolysis systems (see Figure 3-6 and Figure 3-11), it can be observed that the specific costs for alkaline electrolysis are lower compared to PEM electrolysis systems in all analyzed cases. However, the differences are rather marginal and mostly result from lower stack costs for AEL compared to PEM, which is also likely to not notably change in the near future. On the other hand, this cost benefit is almost negated by the additional compression units for the AEL systems to achieve the required output pressure of 30 bar. The cost advantage for AEL systems would increase significantly if compression were not required, especially for small-scale systems, where the compression unit has a significant contribution to the costs. Furthermore, specific costs for power electronics for the PEM systems are higher compared to the AEL systems. As depicted in the 100 MW system layouts of Figure 3-5 and Figure 3-10, each stack is powered by a corresponding rectifier. However, AEL stacks have a higher production capacity in these scenarios, resulting in a lower number of stacks compared to the PEM systems, and thus, fewer rectifiers of higher performance class to empower the AEL stacks are required.

4.3.1 Comparison with other Studies

In addition to the cost analysis in this study, other cost analyses available in literature should be compared and discussed here (see Figure 4-7). It is noteworthy that a direct comparison of the published cost values is often impossible or at least difficult, due to large differences in the given system boundaries, underlying assumptions, and the data sources used. Assumed parameters like production numbers, system capacities, system design, and even the publication date can influence the results drastically, and therefore, need to be considered while comparing the results with each other.

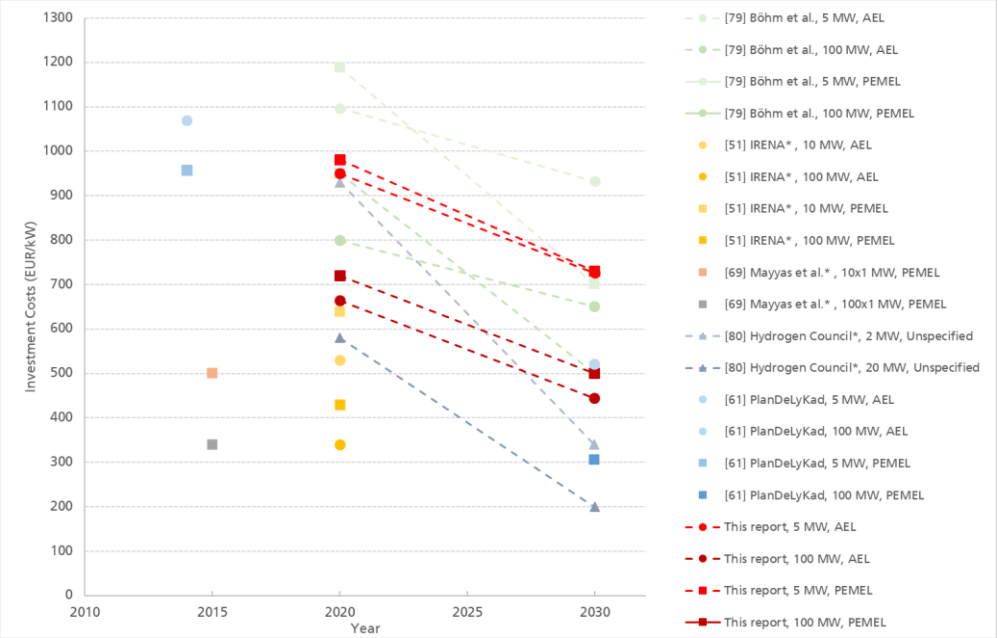

Figure 4-7: Investment costs from available literature depending on year considered, technology and production capacity [1]

One of the first studies to compare the investment costs for alkaline and PEM electrolysis systems in a bottom-up approach was the PlanDeLyKad report [66] from 2014, in which the authors of this study were responsible for the PEM cost model. The study compared the cost structures for both a 5 MW alkaline and a 5 MW PEM electrolysis system with state-of-the-art technology from 2015 and 100 MW systems of both technologies for the year 2030, which takes a certain amount of technical progress into account. Table 4-2 summarized the main findings on the specific investment costs of this study as is depicted in Figure 4-7.

As can be seen from the calculated values, alkaline electrolysis (including a mechanical compression stage), in particular, was estimated much more conservatively for the year 2015, since a mature system with a low power density was assumed. For the year 2030, significant progress in alkaline electrolysis was then already used as a basis for the calculations. However, from today's perspective, even better performance values can be expected in the future, so that the costs for alkaline electrolysis should fall below 500 €/kW by 2030 as predicted in this study.

On the other hand, the investment costs for the PEM electrolysis system in 2030 were estimated to be significantly lower. This can essentially be explained by the fact that in the PlanDeLyKad study, PEM stacks with a nominal capacity of 10 MW were assumed, which from today's perspective is no longer realistic for 2030 as long as no robust alternative to the current membrane materials is available.

[1] Values converted to €/kW by an exchange rate of 0.88 €/USD

Table 4-2: Summary of the calculated investment costs for AEL and PEMEL systems according to the study PlanDeLyKad [66]

Type of System (technology year)	Total costs (€/kW)	Including
AEL – 5 MW (2015)	1070	stack, transformer, rectifier, control and process visualization, KOH management, gas analytics, ambient air monitoring, water treatment, hydrogen purification, fittings and pipes, spare parts, assembly supervision and commissioning, scrubbers, H2 compressor and copper cables
AEL – 100 MW (2030)	520	
AEL – 5 MW (2015)	937	stack, water treatment, transformer, deoxygenation reactor, rectifier, heat exchanger (condenser), condensation separators, cooling water, air cooler, circulation pump, gas-water separator for the anode and cathode, demineralization cartridge, fittings and pipes and a 20% surcharge to cover research costs and accrue a profit
AEL – 100 MW (2030)	305	

In 2020, IRENA published a report on green hydrogen cost reduction, which distinguishes between different types of water electrolysis technologies, including alkaline and PEM electrolysis [55]. The results show current cost breakdowns for 1 MW systems at the cell, stack, and system levels, as well as estimated current specific costs for 100 MW AEL and PEMEL systems. Due to different minimum analyzed system sizes (IRENA: 1 MW, this study: 5 MW) and another cost analysis approach, the resulting system cost shares given in the IRENA report are not directly comparable with this study. However, some general similarities and distinctions in the results can be discussed. For both technologies, the cost shares of the BOP components (~15-25%) are lower, and consequently, the stack cost shares are higher in the IRENA report than here.
At the stack level, the AEL stack cost breakdown in the IRENA study identifies the diaphragm electrode assembly as the most cost intensive component (~50 - 60%), which aligns with the results of the 2.5 MW stack for the year 2020 in Figure 3-3. The cost breakdown of the 1MW PEMEL stack, however, shows a 53% share for the BPP's and 24% for the MEA. These values differ considerably from the results inFigure 3-8: Cost breakdowns of state of the art 1 MW electrolysis stack (2020) and future 5 MW electrolysis stack (2030)
(BPP: 7%, MEA: 43%) and can probably be attributed to the fact that milled BPP are assumed, although they are no longer state of the art.[1]
Furthermore, the report gives estimated current specific costs of ~380 USD/kW (~340 €/kW) for a 100 MW AEL and of ~490 USD/kW (~430 €/kW) for a 100 MW PEMEL system based on the cost shares and cost exponents from Böhm et al. [82]. These results are more optimistic and approximately in the range of the estimated specific costs for the 100 MW systems in 2020 of this study, if additional costs such as instrumentation, housing, piping, engineering, and in the case of the AEL, system compression are neglected.

For the estimation of future cost development trajectories, Böhm, Zauner et al. [82] adapted existing investment cost data for AEL and PEMEL by applying calculated learning curves of the most relevant system components, depending on the year of installation till 2050. The resulting future investment costs shown include direct capital costs of

[1] Similar results were found in the European FP7 project NEXPEL, see https://cordis.europa.eu/project/id/245262

system components and expected replacements, as well as construction and commissioning of plants using overhead factors.
In general, technological development due to an expected strong increase in installed capacities was identified as the most significant driver for a reduction in investment costs, which agrees with the results from this study. However, the cost-reduction potential from 2020 to 2030 is evaluated to be 40% for PEMEL systems compared to 15% for AEL systems with a capacity of 5 MW (this study ~25% for 5 MW systems for both technologies). The findings of Böhm et al. support the trend that capacity scaling effects on the specific system costs are declining relatively fast with increasing system sizes. For an increase from a 5 MW system to a 100 MW system, the specific costs decrease by overall ~30% for AEL and by ~20% for PEM in 2020. These results are in a similar range with the values calculated in Section 3.2.4 for AEL (~29%) and slightly lower than the results of Section 3.3.4. for PEM (~26%).

Mayyas et al. [74] developed a bottom-up cost analysis for 1 MW PEM electrolysis systems with the focus on manufacturing costs and the impact of increasing annual production rates (10 to 50,000 PEMEL systems per year are considered). Thus, the analysis goes far beyond the limits (100 MW) of this study in terms of production capacity, and the base year for the cost values in USD is the year 2015.
Considering an inflation rate of 2%/year, specific costs of ~550 €/kW (561 USD/kW) and of ~370 €/kW (380 USD/kW) are determined for an annual production rate of 10 systems (10x 1 MW = 10 MW) and of 100 systems (100x 1 MW = 100 MW), respectively. The BOP components dominate the total system costs with a share of 60 – 70% (in this study ~70%, see Section 3.3.4), followed by the stack with 30 – 40% (in this study ~30%, see Section 3.3.4). Within the BOP components, power supply and electronics represent the main cost share, similar to this study. On the stack level, the MEA (share of ~30 – 40%) and the PTLs (share of ~20%) are identified as the main cost drivers for the 1 MW PEM electrolysis stack, which is in line with this study. However, the absolute specific costs in [74] rather correspond to the 2030 values in Figure 3-11 of this study, and again, it becomes clear that a direct comparison is difficult to make because Mayyas et al., for example, assumed a change from manual to semi-automated manufacturing processes at a threshold of 100 systems per year, which leads to a significant decrease in total system costs.

Further, the Hydrogen Insights Report published by the Hydrogen Council in 2021 [83] predicts investment costs for electrolysis systems. System costs of 660 - 1,050 USD/kW (~580 – 930 €/kW) are estimated in 2020. Therefore, the range depends on the different electrolysis system capacities from 2 – 20 MW and the technology is not specified further. Also, the system costs exclude installation and building costs. Based on assumed learning rates of 12%, these costs would drop down to 230 - 380 USD/kW (200 - 330 €/kW) in 2030. However, the report mentioned that a 12% learning rate could be too conservative, if compared to the development of other technologies between 2010 and 2020, like wind (19%), solar PV (35%), and batteries (39%)[1]. With a learning rate of 20%, electrolysis costs might be reduced to 130 - 190 USD/kW (115 - 170 €/kW) in 2030, which is far below the results of this study.

In summary, it can be stated that all studies predict a significant cost reduction within the next 10 years until the end of the decade, although even today's systems cannot be realized at the stated costs for 2020. This is mainly due to the small order volume and the associated high costs for single unit production. The next large projects will show

[1] At this point, however, it must be noted that the learning curves of electrolyzers (chemical plant installation) cannot be compared with learning curves of solar cells and battery cells, which are manufactured in highly automated production processes.

which cost structures are achievable. However, no uncomfortable surprises are expected, due to the scale-up experience with other energy technologies.
Although all cost projections are within a certain corridor, the individual figures can differ greatly, which can mostly be well justified by the different boundary conditions and assumptions. When evaluating such cost data, a precise distinction must be made between the methods chosen. Bottom-up calculations, as used in this study, allow more robust statements, although many uncertainties remain in the assumptions, as described in the next section. Projections or predictions of future electrolysis capacities and linkage to generalized learning curves, on the other hand, do not take into account technological or production-specific features of the different processes.

4.3.2 Limitations of the Bottom-up Cost Model

In general, cost data for electrolysis systems are not yet transparent or easily available, due to reasons of confidentiality and potential competitive advantages in a small market with only a few manufacturers and systems deployed in the investigated multi-MW capacity range until today.
Following a bottom-up cost calculation, the data quality can be a limiting factor and has a direct influence on the derived results because data inaccuracies could be propagated from bottom (material cost) to the top (total system cost) of the cost model. The developed costs models in this study are based on well-founded manufacturer data, expert information, and own estimations for equipment costs, operating costs, labor costs, and material costs for limited manufacturing volumes. However, they can quickly lose their relevance due to the dynamic developments on the electrolysis market.
Looking at high manufacturing volumes, e.g., in GW scale in particular, reliable cost data is very scarce and difficult to validate. This is especially the case for cost estimates of complex production processes involved in the manufacturing of the components, like the MEA, because it is mostly sensitive IP of the manufacturers that is required.
For the 2030 scenarios, several key performance and material parameters needed to be assumed for the electrolysis stacks. Although, these assumptions are verified by experts, they are merely an educated outlook of potential future developments.
For the balance-of-plant components, no technological progress or experience rates in system components towards 2030 are included in the models, because these are mainly standard components, applied in many other applications since decades (e.g., transformers, pumps). This approach does only consider a potential trend to specifically tailored and highly-integrated BOP components for electrolysis in the future, and therefore, might limit the estimated cost-reduction potential of the BOP components. However, some research studies approached this issue by adaption of experience and learning rates [55,82].
Furthermore, the bottom-up approach here does not include certain overhead (rent, insurance etc.) and markup costs of installed electrolysis system because these are highly manufacturer and project dependent. Also, the final installation costs can vary with the location of the plant. Adding markup surcharges and installation costs can result in nearly double the final installed system cost [74].
However, determining final costs for electrolysis systems from a customer view is not the scope here, but rather to evaluate the cost-reduction potentials starting from concrete cost data.

4.3.3 Hydrogen Production Costs

To evaluate an electrolysis system in terms of economic viability, it is important to not only consider the fixed costs (investment costs of an installed system + maintenance costs), but particularly also the electricity costs (variable costs) and the annual full load hours, as well. In Figure 4-8 the hydrogen production costs are shown in relation to the annual full load hours.

Electricity costs of 50 €/MWh represent an optimistic average for production via a mix of onshore wind and photovoltaic plants and were taken as a basis for the hydrogen cost calculation here. In order not to distort the impact of decreasing fixed costs on the hydrogen production costs, the same electricity costs are assumed for 2030. Although, from a global perspective levelized cost of energy (LCOE) are predicted to further decline in the future. [83,84] This is mostly caused by ongoing cost reductions of renewables, especially in regions with optimal conditions, such as the Middle East & North Africa (MENA), Chile, South Africa, and Australia. Therefore, such locations are also favorable for cost-efficient hydrogen production.

Furthermore, the given efficiencies from Section 3.2.1 and 3.3.1 for the 100 MW systems in 2020 and 2030, as well as the system cost results from Section 3.2.4 and 3.3.4, are taken for the calculation in Figure 4-8. As shown in the figure, the hydrogen production costs decrease strongly with rising annual full load hours. For annual full load hours up to 3,000 hours, the capital expenditure (CAPEX) of an electrolysis system dominates the total hydrogen production costs, because they are spread over a shorter period of operation time and therefore smaller amounts of generated hydrogen.

However, lower hydrogen production costs can be obtained with high full load hours. Here, the electricity cost and overall system efficiencies become the main cost drivers. In consequence, a substantial cost reduction for hydrogen production from electrolysis can also be achieved by decreasing electricity prices and increasing full load hours of the electrolysis system.

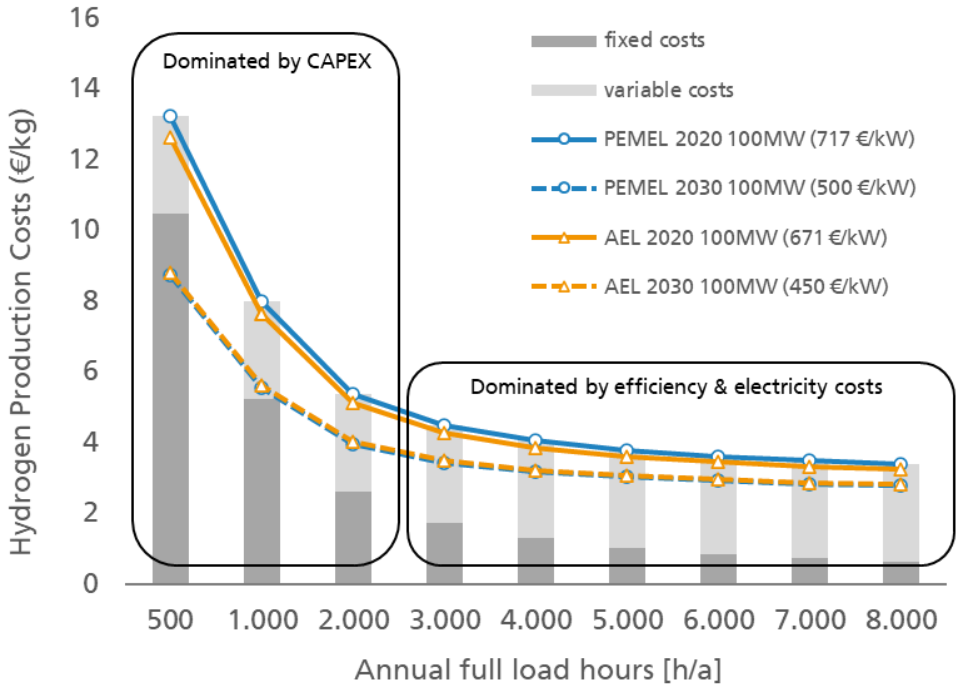

Figure 4-8: Hydrogen production cost depending on annual full load hours (LCOE= 50 €/MWh, specific energy demands from Table 3-5 and Table 3-10)

5 Conclusion and Outlook

Due to the large-scale market ramp-up of the technology that is just beginning, available electrolysis systems are neither standardized products nor designed and manufactured in a multi-MW performance class, but rather custom-made with associated, highly specific manufacturing costs. But the general trend of growing numbers and larger capacities of future electrolysis installations over the coming years, as shown in Figure 1-2, is consistent with efforts manufacturers are currently taking to upscale their electrolysis cell and system designs. At the same time, manufacturing capacities, as shown in Sections 2.1.4 and 2.2.4, are being rapidly expanded. The cost findings in this study justify these development efforts by highlighting the cost benefits due to scaling-up of system sizes and economies-of-scale effects.

Several approaches are analyzed to bring costs for hydrogen production by low-temperature electrolysis down. Technological development by improving cell, stack and overall system designs, reaching higher power densities, is one of them. Thereby, the development of more compact electrolysis block concepts with improved MEA's is in focus of PEMEL activities; while for AEL stacks, an incremental improvement of the diaphragm-electrode assembly is a key factor. The minimization of specific energy consumption and the extension of service life for the central electrochemical components and catalytic coatings, for PEMEL especially, are important issues, as well. Pressurized AEL systems can become more cost-efficient compared to atmospheric AEL system, especially in smaller capacity classes < 5MW or if the investment surcharges for higher-grade materials and components can be decreased. However, probably every further development to optimize design or setup presents a trade-off to reach specific requirements. These need to be considered and evaluated in the context of specific project requirements and targeted hydrogen application. For example, a higher power density due to improved components and materials is likely to have a shortening effect on stack lifetime, which in the end, is reflected in stack replacement costs.
Another approach is increasing production volumes and using the resulting learning effects to reduce costs. However, there are still major challenges in the development of the corresponding production processes suitable for series production. Furthermore, a cost reduction can also be sought through modularization and up-scaling of electrolysis systems. The minimization of maintenance and repair costs and the operational automation, including remote control, still only play a minor role.

Based on the developed cost models in this study, significant cost decreases for alkaline and PEM electrolysis systems have been determined. Large-scale 100 MW alkaline electrolysis system costs can be reduced from 663 €/kW in 2020 to 444 €/kW in 2030. Small-scale 5 MW alkaline plants show potential cost reductions from 949 €/kW in 2020 to 726 €/kW in 2030. A focus was set on analyzing stack cost-reduction potential and it was estimated, that for 100 MW large-scale AEL plants in 2030 stack costs of only 65 €/kW are reachable. It is worth mentioning that in this scenario, the stack costs undercut the power supply in the total system costs.

Similar cost-reduction trends are derived for PEM electrolysis plants. Large-scale 100 MW PEM electrolysis plants can cost 720 €/kW in 2020 and 500 €/kW in 2030. Costs for small-scale 5 MW PEM systems can decline from 980 €/kW in 2020 to 730 €/kW in 2030. The PEMEL stack costs can be decreased to 150 €/kW in large-scale 100 MW plants of 2030. For both technologies, estimations suggest that a numbering-up in manufacturing volume of the stacks results in less cost-reduction potential than scaling them up in size. In the developed cost models, a system size of 5 MW presents a threshold, where technological improvements seem crucial for further, significant cost reductions.

Cost reduction for balance-of-plant components can be observed for electrolysis systems with higher capacities, due to scaling-up in size and by centralizing the components in large-scale plants, resulting in higher utilization per installed stack power. However, it is expected that technology improvement is limited, since such components have already been used for decades in the construction of chemical plants, which is underlined by lower cost-reduction potential towards 2030 compared to the stacks for both technologies. However, this does not apply to the power electronics. The cost impact of the power electronics on the total system costs is significant and shows a steadily increasing trend in the cost share towards 2030 as the stack becomes less expensive. Measures to bring the cost of the power electronics down seem to be crucial. Different technical options are discussed qualitatively in Section 4.1.3, but are not considered in the cost scenarios.

Based on a more conservative development path for PEMEL systems, the results show slightly lower costs for alkaline electrolysis systems compared to PEM electrolysis systems can be reached. Even so, it is already clear today that both technologies will be used on a large scale. Each technology has its own challenges, from critical materials to performance, durability, and maturity; there is no clear winner across all applications, which leaves the door open for competition and innovation driving costs down.

Today, mass production of electrolysis systems is in its early beginnings and first multi-MW systems are realized, but it is still a long way towards market integration. Standardization and increased automation of manufacturing processes is crucial to reach cost and production volume targets. This is especially the case for PEM electrolysis stacks, where more different designs and concepts for MEAs, bipolar plates, or PTLs exist.
As an outlook, a further investigation of the cost-reduction potential of manufacturing processes seems like a logical step.

So far cost-reduction efforts are mainly focused on the stack, but also the cost structures of power supply and electronics needs to be analyzed further. Finding cost-efficient solutions, customized to the requirements of an electrolysis systems is essential to bring the total cost down.

Once the first MW-scale installations are commissioned and GW-scale factories start producing, there will be a chance to get better insights in current costs and manufacturing processes, which could lead to improved cost-reduction estimates.

6 References

[1] European Commission, Pariser Übereinkommen, 2019. https://ec.europa.eu/clima/policies/international/negotiations/paris_de (accessed 15 May 2019).

[2] Hydrogen Council, How hydrogen empowers the energy transition, 2017.

[3] Hydrogen Council, Hydrogen scaling up: A sustainable pathway for the global energy transition, 2017.

[4] International Energy Agency - IEA, The Future of Hydrogen: Seizing today's opportunities, Paris, 2019.

[5] World Energy Council, International Hydrogen Strategies: A study commissioned by and in cooperation with the World Energy Council Germany, 2020.

[6] T. Smolinka, N. Wiebe, P. Sterchele, A. Palzer, F. Lehner, M. Jansen, S. Kiemel, R. Miehe, S. Wahren, F. Zimmermann, Studie IndWEDe: Industrialisierung der Wasserelektrolyse in Deutschland: Chancen und Herausforderungen für nachhaltigen Wasserstoff für Verkehr, Strom und Wärme, Berlin, 2018.

[7] IEA, Hydrogen Projects Database, 2020. https://www.iea.org/reports/hydrogen-projects-database (accessed 27 May 2021).

[8] T. Smolinka (Ed.), Grundlagen der Wasserelektrolyse zur Wasserstofferzeugung, Vulkan-Verlag, 2020.

[9] W.J.F. Gannon, M.E.A. Warwick, C.W. Dunnill, Woven Stainless-Steel Mesh as a Gas Separation Membrane for Alkaline Water-Splitting Electrolysis, Membranes (Basel) 10 (2020). https://doi.org/10.3390/membranes10050109.

[10] A. Manabe, M. Kashiwase, T. Hashimoto, T. Hayashida, A. Kato, K. Hirao, I. Shimomura, I. Nagashima, Basic study of alkaline water electrolysis, Electrochimica Acta 100 (2013) 249–256. https://doi.org/10.1016/j.electacta.2012.12.105.

[11] D. Pletcher, X. Li, Prospects for alkaline zero gap water electrolysers for hydrogen production, International Journal of Hydrogen Energy 36 (2011) 15089–15104. https://doi.org/10.1016/j.ijhydene.2011.08.080.

[12] D. Pletcher, X. Li, S. Wang, A comparison of cathodes for zero gap alkaline water electrolysers for hydrogen production, International Journal of Hydrogen Energy 37 (2012).

[13] A. Nielsen, 2nd Generation Alkaline Electrolysis - final report, 2013.

[14] Y. Nakajima, N. Fujimoto, S. Hasegawa, T. Usui, Advanced Alkaline Water Electrolyzer for Renewable Hydrogen Production, ECS Trans. 80 (2017) 835–841. https://doi.org/10.1149/08010.0835ecst.

[15] McPhy, McPhy 2018 Full-Year Results.

[16] N. Tenhumberg, K. Büker, Ecological and Economic Evaluation of Hydrogen Production by Different Water Electrolysis Technologies, Chemie Ingenieur Technik 92 (2020) 1586–1595. https://doi.org/10.1002/cite.202000090.

[17] NEL Hydrogen, The world's most efficient and reliable electrolysers, 2019.

[18] Green Hydrogen Systems, HyProvide A-Series: Produce your own hydrogen from renewable energy sources at the lowest cost possible, 2021.

[19] D. Thomas, Power to hydrogen to power solution: PEM Water electrolysis, 2020.

[20] McPhy, McPhy Portfolio McLyzer, 2020.

[21] C. Braatz, McPhy - Elektrolyseanlagen für Multi-MW Anwendungen, 2019.

[22] Asahi Kasei, The Role of "Power-to-Gas" in the coming Green Society and Asahi Kasei's Activity in Europe ADEMA Presentation, 2017.

[23] Asahi Kasei Corporation Executive Officer Masami Takenaka Ph.D., Asahi Kasei's Activities on green hydrogen, 2020.

[24] Asahi Kasei, Press Release - Asahi Kasei's electrolysis system starts world's largest-scale hydrogen supply operation at the Fukushima Hydrogen Energy Research Field in Namie, 2020.

[25] A. Zschocke, Alkalische Wasserelektrolyse von thyssenkrupp: Fortschrittliche Technologie für Power-to-X-Anwendungen, 2019.
[26] Hydrogen Europe, Strategic Research and Innovation Agenda - Final Draft, 2020.
[27] F. Razmjooei, T. Liu, D.A. Azevedo, E. Hadjixenophontos, R. Reissner, G. Schiller, S.A. Ansar, K.A. Friedrich, Improving plasma sprayed Raney-type nickel-molybdenum electrodes towards high-performance hydrogen evolution in alkaline medium, Sci. Rep. 10 (2020) 10948. https://doi.org/10.1038/s41598-020-67954-y.
[28] NEL Hydrogen, Capital Markets Day Presentation, 2021.
[29] L. Bertuccioli, A. Chan, D. Hart, F. Lehner, B. Madden, E. Standen, Study on development of water electrolysis in the EU - final report, 2014.
[30] T. Smolinka, M. Günther, J. Garche, NOW-Studie Stand und Entwicklungspotenzial der Wasserelektrolyse zur Herstellung von Wasserstoff aus regenerativen Energien: Kurzfassung des Abschlussberichts, 2011.
[31] NEL Hydrogen CEO Jon André Løkke, NEL ASA - update February 2016, 2016.
[32] W. Grot, Perfluorierte Ionenaustauscher-Membrane von hoher chemischer und thermischer Stabilität, Chemie Ingenieur Technik 44 (1972) 167–169. https://doi.org/10.1002/cite.330440408.
[33] L. NUTTALL, Conceptual design of large scale water electrolysis plant using solid polymer electrolyte technology, International Journal of Hydrogen Energy 2 (1977) 395–403. https://doi.org/10.1016/0360-3199(77)90046-5.
[34] T. Takahashi, Water Electrolysis, in: Solar-Hydrogen Energy Systems, Elsevier, 1979, pp. 35–58.
[35] F. Pantò, S. Siracusano, N. Briguglio, A.S. Aricò, Durability of a recombination catalyst-based membrane-electrode assembly for electrolysis operation at high current density, Applied Energy 279 (2020) 115809. https://doi.org/10.1016/j.apenergy.2020.115809.
[36] C. Klose, P. Trinke, T. Böhm, B. Bensmann, S. Vierrath, R. Hanke-Rauschenbach, S. Thiele, Membrane Interlayer with Pt Recombination Particles for Reduction of the Anodic Hydrogen Content in PEM Water Electrolysis, J. Electrochem. Soc. 165 (2018) F1271-F1277. https://doi.org/10.1149/2.1241814jes.
[37] C. Klose, T. Saatkamp, A. Münchinger, L. Bohn, G. Titvinidze, M. Breitwieser, K.-D. Kreuer, S. Vierrath, All-Hydrocarbon MEA for PEM Water Electrolysis Combining Low Hydrogen Crossover and High Efficiency, Adv. Energy Mater. 10 (2020). https://doi.org/10.1002/aenm.201903995.
[38] C. Minke, M. Suermann, B. Bensmann, R. Hanke-Rauschenbach, Is iridium demand a potential bottleneck in the realization of large-scale PEM water electrolysis?, International Journal of Hydrogen Energy (2021). https://doi.org/10.1016/j.ijhydene.2021.04.174.
[39] P.C.K. Vesborg, T.F. Jaramillo, Addressing the terawatt challenge: scalability in the supply of chemical elements for renewable energy, RSC Adv. 2 (2012) 7933. https://doi.org/10.1039/c2ra20839c.
[40] Huaneng Su, Bernard Jan Bladergroen, Sivakumar Pasupathi, Vladimir Linkov, Shan Ji, Performance Investigation of Membrane Electrode Assemblies for Hydrogen Production by Solid Polymer Electrolyte Water Electrolysis, International Journal of Electrochemical Science (2012) 4223–4234.
[41] P. Häussinger, R. Lohmüller, A.M. Watson, Hydrogen, Wiley-VCH Verlag GmbH & Co. KGaA, Weinheim, 2007.
[42] Karl-Josef Kuhn, Electrolysis / eFuels: Pathways to synthetic eFuels, 2020.
[43] Giner ELX, Electrolyzer Stacks, 2021. https://www.ginerelx.com/electrolyzer-stacks (accessed 1 July 2021).
[44] Denis Thomas, Renewable Hydrogen: the missing link between the power, gas, industry and transport sectors, 2018.
[45] HTEC Systems, H-TEC Series-ME: ME 450/1400 product data sheet.
[46] Simon Bourne, Scaling PEM Electrolysis to 100 MW, Hannover Messe, 2017.
[47] Monjid Hamdan, Advanced Electrochemical Hydrogen Compressor, Boston Convention and Exhibition Center, Boston, 2018.
[48] NEL Hydrogen, Capital Markets Days Presentation, 2021.

[49] H.A. Miller, K. Bouzek, J. Hnat, S. Loos, C.I. Bernäcker, T. Weißgärber, L. Röntzsch, J. Meier-Haack, Green hydrogen from anion exchange membrane water electrolysis: a review of recent developments in critical materials and operating conditions, Sustainable Energy Fuels 4 (2020) 2114–2133. https://doi.org/10.1039/C9SE01240K.
[50] D. Li, A.R. Motz, C. Bae, C. Fujimoto, G. Yang, F.-Y. Zhang, K.E. Ayers, Y.S. Kim, Durability of anion exchange membrane water electrolyzers, Energy Environ. Sci. 14 (2021) 3393–3419. https://doi.org/10.1039/d0ee04086j.
[51] D. Henkensmeier, M. Najibah, C. Harms, J. Žitka, J. Hnát, K. Bouzek, 2021. Overview: State-of-the Art Commercial Membranes for Anion Exchange Membrane Water Electrolysis. Journal of Electrochemical Energy Conversion and Storage 18, 024001. https://doi.org/10.1115/1.4047963.
[52] G.C. Anderson, B.S. Pivovar, S.M. Alia, Establishing Performance Baselines for the Oxygen Evolution Reaction in Alkaline Electrolytes, J. Electrochem. Soc. 167 (2020) 44503. https://doi.org/10.1149/1945-7111/ab7090.
[53] F. Razmjooei, A. Farooqui, R. Reissner, A.S. Gago, S.A. Ansar, K.A. Friedrich, Elucidating the Performance Limitations of Alkaline Electrolyte Membrane Electrolysis: Dominance of Anion Concentration in Membrane Electrode Assembly, ChemElectroChem 7 (2020) 3951–3960. https://doi.org/10.1002/celc.202000605.
[54] IRENA, Green Hydrogen Cost Reduction: Scaling up Electrolysers to Meet the 1.5ºC Climate Goal, Abu Dhabi, 2020.
[55] Enapter, Enapter AEM Multicore Brochure, 2021.
[56] Hans van 't Noordende, Peter Ripson, Baseline design and total installed costs of a GW green hydrogen plant: State-of-the-art design and total installed capital costs, 2020.
[57] Martin Kopp, David Coleman, Georg Derscheid, Matthias Werne, Birgit Scheppat, Energiepark Mainz: Elektrolyse-Wasserstoff als Energiespeicher und -vektor (Final report), 2018.
[58] S.G. Simoes, J. Catarino, A. Picado, T.F. Lopes, S. Di Berardino, F. Amorim, F. Gírio, C M Rangel, T.P. de Leão, Assessing water availability and use for electrolysis in hydrogen production, Unpublished, 2021.
[59] Element Energy, Hydrogen supply chain evidence base, 2018.
[60] G. Papakonstantinou, G. Algara-Siller, D. Teschner, T. Vidaković-Koch, R. Schlögl, K. Sundmacher, Degradation study of a proton exchange membrane water electrolyzer under dynamic operation conditions, Applied Energy 280 (2020) 115911. https://doi.org/10.1016/j.apenergy.2020.115911.
[61] B. Bensmann, R. Hanke-Rauschenbach, G. Müller-Syring, M. Henel, K. Sundmacher, Optimal configuration and pressure levels of electrolyzer plants in context of power-to-gas applications, Applied Energy 167 (2016) 107–124. https://doi.org/10.1016/j.apenergy.2016.01.038.
[62] M.H. Nikolas Knetsch, Waste Heat Utilisation of Power to Gas Plants for Localand Disctrict Heating, Düsseldorf, 2018.
[63] American Petroleum Institute, API Standard 618: Reciprocating Compressors for Petroleum, Chemical, and Gas Industry Services, 2007.
[64] Burkhardt Compression, Compressor Solutions for Power-To-Gas Applications: Oil-free Hydrogen compressor systems, 2021.
[65] Christoph Noack, Dr. Fabian Burggraf, Seyed Schwan Hosseiny, Philipp Lettenmeier, Svenja Kolb, Dr. Stefan Belz, Dr. Josef Kallo, Prof. K. Andreas Friedrich, Dr. Thomas Pregger, Karl Kiên Cao, Dr. Dominik Heide, Dr. Tobias Naegler, Frieder Borggrefe, Dr. Ulrich Bünger, Jan Michalski, Tetyana Raksha, Christopher Voglstätter, Dr. Tom Smolinka, Fritz Crotogino, Sabine Donadei, Peter-Laszlo Horvath, Dr. Gregor-Sönke Schneider, Studie über die Planung einer Demonstrationsanlage zur Wasserstoff-Kraftstoffgewinnung durch Elektrolyse mit Zwischenspeicherung in Salzkavernen unter Druck, 2014.
[66] Thomas Gabor, Tom Smolinka, Public report with condensed findings and conclusions from organised international workshop on PEM electrolysis, 2013.
[67] FCH2JU, Addendum to the Multi-Annual Work Plan 2014-2020, 2018.

[68] Lozowski, Chemical Engineering April 2021: An Inside Look at Expanders, Chemical Engeneering 128 (2021).
[69] B. Zayat, D. Mitra, S.R. Narayanan, Inexpensive and Efficient Alkaline Water Electrolyzer with Robust Steel-Based Electrodes, J. Electrochem. Soc. 167 (2020) 114513. https://doi.org/10.1149/1945-7111/aba792.
[70] C.I. Bernäcker, T. Rauscher, T. Büttner, B. Kieback, L. Röntzsch, A Powder Metallurgy Route to Produce Raney-Nickel Electrodes for Alkaline Water Electrolysis, J. Electrochem. Soc. 166 (2019) F357-F363. https://doi.org/10.1149/2.0851904jes.
[71] A.N. Colli, H.H. Girault, A. Battistel, Non-Precious Electrodes for Practical Alkaline Water Electrolysis, Materials (Basel) 12 (2019). https://doi.org/10.3390/ma12081336.
[72] ISO 2944:2000, Fluid power systems and components — Nominal pressures 23.100.01.
[73] Ahmad Mayyas, Mark Ruth, Bryan Pivovar, Guido Bender, Keith Wipke, Manufacturing Cost Analysis for Proton Exchange Membrane Water Electrolyzers, 2019.
[74] E.R. Morgan, J.F. Manwell, J.G. McGowan, Opportunities for economies of scale with alkaline electrolyzers, International Journal of Hydrogen Energy 38 (2013) 15903–15909. https://doi.org/10.1016/j.ijhydene.2013.08.116.
[75] Peter Adam, Ralf Bode, Markus Groissboeck, Readying pipeline compressor stations for 100% hydrogen, 2021. https://www.turbomachinerymag.com/view/readying-pipeline-compressor-stations-for-100-hydrogen (accessed 21 June 2021).
[76] Bouwman, Peter, H2 Compression and Purification.
[77] Greentechmedia, The Global PV Inverter and MLPE Landscape: Q1 2017, 2017.
[78] Yole Développement, Status of the Power Electronics Industry, 2020.
[79] thyssenkrupp Uhde Chlorine Engineers, Press Release - thyssenkrupp expands production capacities for water electrolysis to gigawatt scale, 19.06.20.
[80] ITM Power, ITM Power Facilities. https://www.itm-power.com/facilities (accessed 7 June 2021).
[81] Günter Schiller, Entwicklungsarbeiten zur alkalischen Wasserelektrolyse beim DLR Stuttgart, 2013.
[82] H. Böhm, A. Zauner, D.C. Rosenfeld, R. Tichler, Projecting cost development for future large-scale power-to-gas implementations by scaling effects, Applied Energy 264 (2020) 114780. https://doi.org/10.1016/j.apenergy.2020.114780.
[83] Hydrogen Council, McKinsy&Company, Hydrogen Insights: A perspective on hydrogen investment, market development and cost competitiveness, 2021.
[84] Christoph Kost, Shivenes Shammugam, Verena Jülch, Huyen-Tran Nguyen, Thomas Schlegl, Levelized Cost of Electricity- Renewable Energy Technologies.

7
Appendix A

EUR/kW$_{AC}$	PEM Electrolysis				Alkaline Electrolysis			
Year	**2020**		**2030**		**2020**		**2030**	
Capacity (MW$_{AC}$)	**5**	**100**	**5**	**100**	**5**	**100**	**5**	**100**
Electrolysis Stacks	294	212	205	143	185	149	99	64
Power electronics	195	193	123	122	160	159	102	101
High Voltage Transformer	0	25	0	27	0	25	0	26
BoP Cathode + H_2 Purification	76	18	82	18	80	22	83	21
BoP Anode	26	18	25	12	24	16	24	12
H_2O Purification	9	1	10	1	9	1	9	1
System Cooling	12	6	10	5	10	4	9	4
Compression	0	0	0	0	123	47	128	49
Piping	98	90	73	63	95	88	70	60
Instrumentation	122	71	91	49	118	70	88	48
Housing	19	19	15	15	22	22	19	19
Engineering	128	65	95	46	124	60	95	40
SUMME	**978**	**718**	**729**	**502**	**949**	**663**	**726**	**444**

Hydrogen Data

Energy	
LHV	3 kWh / Nm³ 10.8 MJ / Nm³
HHV	3.54 kWh / Nm³ 12.75 MJ / Nm³
Volume (1 kg H2)	
STP	11.126 Nm³
20°C, 200 bar	5.563 x 10^{-2} m³
Density	
0.0899 kg / Nm³	

Basic Unit Conversions

Energy		
From	**To**	**Factor**
kWh	BTU	3,412
MJ	BTU	947.9
toe	BTU	39.7 x 10^{6}
Volume		
Nm³	scf	35.31
Pressure		
bar	MPA	0.1
MPA	psi	145
bar	psi	14.5

Pressure [MPa]

0.1013	5	10	15	20	25	30	35	40	50	60	70	80	90	100
Compressibility Factor														
1	1.03	1.06	1.09	1.13	1.16	1.20	1.23	1.27	1.34	1.41	1.48	1.56	1.63	1.70